Coordinated Arrival and Departure Management for Dependent Runway Operations

Master Thesis

J.L.C. Derks

Technische Universiteit Delft

knowledge & development centre
Mainport Schiphol

TU Delft

Coordinated Arrival and Departure Management for Dependent Runway Operations

Msc Thesis

by

J.L.C. Derks

to obtain the degree of Master of Science in Aerospace Engineering
at the Delft University of Technology,

Student number:	4277856	
Project duration:	November 1, 2019 – November 20, 2020	
Thesis committee:	Prof. dr. ir. J.M. (Jacco) Hoekstra	TU Delft, chair
	Dr. ir. J. (Joost) Ellerbroek	TU Delft, supervisor
	F. (Ferdinand) Dijkstra	KDC mainport Schiphol, daily supervisor
	P.C. (Paul) Roling	TU Delft, examiner

TU Delft

Preface

When I started looking for a graduation project to finish my MSc Aerospace Engineering degree in October 2019, the number of projects in my department, Air Transport Operations, were scarce. Since I developed my interest in Air Traffic Management during my master internship at Royal Schiphol Group, I decided to look for a project within the Air Traffic Management department. That is how I started my research into coordinated Arrival and Departure Management in the College of Excellence program, which is part of the Knowledge and Development Centre mainport Schiphol. Now my graduation project has almost come to an end; I would like to look back at this unforgettable period.

Right from the start I received a warm welcome at the Centre of Excellence at LVNL from my daily supervisor Ferdinand Dijkstra and my fellow CoE'ers. On my first day, Ferdinand told me I was allowed to ask him anything anytime. Almost a year later, I can say he lived up to his promise. I could not have delivered the same work without the endless dedication and enthusiasm of Ferdinand to answer all my questions and provide me with the correct data. Furthermore, I will never forget my visit to the Air Traffic Control Tower at Schiphol he fixed for me.

Also my academic supervisors Jacco Hoekstra and Joost Ellerbroek were of generous support. I want to express my gratitude to for their feedback, supportive criticism, knowledge and help throughout the past year. I have appreciated the quick responses to my, not always the most thoughtful, questions regarding BlueSky. In addition to the academic guidance, I would like to thank Jacco again for helping me to find a borrow-laptop from the TU when my own crashed.

I can also look back on pleasant cooperation with my fellow CoE'ers. Sharing their thoughts on my subject at the coffee machine at LVNL has really helped me forward. I loved our daily conversations and jokes while enjoying diner in the canteen. I hope we can meet again sometime when life returns to normal.

Even when we were unexpectedly forced to work from home, the support from the CoE and TU Delft continued unabated. The coffee moments with my fellow CoEs decreased to once a week but always remained useful. My roommates became my new colleges, and also to them; I would like to express my appreciation for the many encouraging words that I received and the pleasant moments we had while working at home.

I would also like to give recognition to my (old) roommates I used to live with in Delft. Without them, I do not think I would be nearing my graduation at this moment. Most of the best moments during my student life I shared with them. But also, during the most challenging part of my life, they gave me a listening ear, much distraction, and the motivation to carry on.

Last, I would like to show my gratitude to my family. Marloes, Ivonne and Peter, each of you have been an example to me. Mama, thank you for continuously reminding me that everything will be okay. Papa, losing you right at the start of my master degree was extremely painful and added an extra dimension. I would have wanted you here to see me graduate.

With these final words, I would like to conclude my seven years of being a student at the Delft University of Technology. It has been a real blast, and I do not regret anything. I am looking forward to starting a new chapter in my life as an engineer and TU Delft alumni.

Thank you all.

Jeanette Derks
Rotterdam, October 2020

Executive Summary

At many airports, the arrival and departure demand often outpaces the available airport capacity. Therefore, the flow of arriving and departing aircraft needs to be controlled to ensure safe and efficient operations. Many airports have been implementing systems that provide electronic assistance for air traffic control in planning and sequencing the flow of arriving and departing aircraft. Those systems are called the Arrival Manager and the Departure Manager.

At the moment the two systems do not take each other's traffic situation into account. Arriving and departing aircraft are accepted to enter the same airspace, even though no information exchange exists between the two. The lack in information exchange is not problematic for airports operating independent arrival and departure runways, arriving aircraft paths do not hinder departing aircraft paths. However, for dependent runways, when aircraft arrivals hinder departing aircraft, and vice versa, the lack of information exchange between the two systems, ATC will not be able to fit as many departures into the arrival stream as is planned by the Departure Manager. This can cause severe (surface-) congestion problems at airports that rely on dependent runways.

This study focused on the interaction between arriving and departing aircraft for dependent arrival and departure runway combinations and the magnitude of the resulting arrival and departure capacity interference. With this knowledge, this research developed and assessed strategies for coordination between Arrival Management and Departure Management. First, the uncoordinated Arrival and Departure Manager (ADMAN) was developed in BlueSky Open Air Traffic Simulator to represent the current management of arrivals and departures; the AMAN and DMAN schedule inbound and outbound independently from one another. Second, the coordinated ADMAN was developed in BlueSky Open Air Traffic Simulator as well. The coordinated ADMAN includes three different coordination modules between the AMAN and DMAN that aims to increase the operational efficiency of dependent arrival and departure runway combinations. Each of the implemented coordination modules checks the number of departure slots that are available in the scheduled arrival stream and intervene if necessary, taking into account different assumptions.

To obtain insight into the future magnitude of arrival and departure capacity interference and to demonstrate the for a coordination mechanism between the management of arrivals and departures, fast-time simulations were performed with the uncoordinated ADMAN. This experiment used an arrival and departure runway combination with a missed approach dependency to assess future arrival and departure capacity interference. To express the severeness of arrival and departure capacity interference, capacity was used as Key Performance Area (KPA). The results showed that if the arrival load would increase, due to RECAT and TBS, the arrival and departure capacity interference worsens. These results demonstrated the need for coordination mechanism between the management of arriving and departing aircraft.

A second experiment was set-up to assess the performance of the different coordination modules implemented in the uncoordinated ADMAN. The three coordination modules were evaluated in terms of capacity, delay, coordination module interventions and ATCO workload by performing fast-time simulations. Like the first experiment, the second experiment used an arrival and departure runway combination with a missed approach dependency to test the modules for different levels of arrival load during morning and evening arrival peaks. The results showed that the departure capacity could be increased, and departure delay could be decreased, when the AMAN meters the arriving aircraft as a function of the departure ground situation.

As this research set the start for coordinated arrival and departure management for dependent runway operations, other concepts could be developed to mitigate the effect of arrival and departure capacity interference. Furthermore, to improve the realism of both the uncoordinated ADMAN and coordinated ADMAN, it is recommended to upgrade the Air Traffic Control module.

Acronyms

AAA Amsterdam Advanced ATC.

AAFI Actual Arrival Free Interval.

AAH Active Advisory Horizon.

AAI Actual Arrival Interval.

AAR Airport Acceptance Rate.

AAS Amsterdam Airport Schiphol.

ACC Area Control Centre.

ADMAN Arrival and Departure MANagement.

ADR Airport Departure Rate.

AFI Arrival Free Interval.

AMAN Arrival Manager.

APP APProach control.

ASAP Advanced Schiphol Arrival Manager.

ATA Actual Time of Arrival.

ATC Air Traffic Control.

ATCO Air Traffic Controller.

ATM Air Traffic Management.

ATS Air Traffic Services.

ATSR Air Traffic Services Route.

CAS Calibrated Airspeed.

CDA Continuous Descent Approach.

CFMU Central Flow Management Unit.

CoE Centre of Excellence.

CTA ConTrol Area.

CTOT Calculated Take-Off Time.

CTR ConTRol zone.

CWP Controller Working Position.

DADC Declared Airport Departure Capacity.

DLIV Dynamic Landing Interval.

DMAN Departure Manager.

DME Distance Measuring Equipment.

EAT Expected Arrival Time.

EDIT Estimated De-Icing Time.

EFT Estimated Flying Time.

EH Eligibility Horizon.

ELRP Estimated Line-up and Roll to Airborne Period.

ERWP Expected Runway Waiting Period.

ESWP Expected Stand Waiting Period.

ETA Estimated Time of Arrival.

ETO Estimated Time Over.

ETOT Earliest Take-Off Time.

EXOP Estimated Outbound Taxi Time.

FAF Final Approach Fix.

FCFS First Come First Served.

FH Freeze Horizon.

FIR Flight Information Region.

FMS Flight Management System.

FPDS Flight Plan Data Source.

GS Ground Speed.

HMI Human Machine Interface.

IADT Inter Arrival Departure Time.

IAF InitialApproach Fixe.

IAT Inter Arrival Time.

IDAT Inter Departure Arrival Time.

IDF Initial Departure Fix.

IDT Inter Departure Time.

IFR Instrument Flight Rules.

KDC Knowledge and Development Centre.

KLM Royal Dutch Airlines.

KPA Key Performance Indicator.

LAS Last Assigned Slot.

LOS Level Of Service.

LVNL Air Traffic Control the Netherlands.

MIP Mixed Integer Programming.

MLR Main Landing Runway.

NMOC Network Manager Operations Centre.

NNHS Nieuw Normen- en Handhavingstelsel.

OPL Outbound Planner.

PDS Pre-Departure Sequencer.

RNAV Area Navigation.

ROT Runway Occupancy Time.

RTA Required Time of Arrival.

RWY RunWaY threshold.

SAFI Scheduled Arrival Free Interval.

SAI Scheduled Arrival Interval.

SARA Speed And Route Advisor.

SESAR Single European Sky ATM Research.

SID Standard Instrument Departure.

STA Scheduled Time of Arrival.

STAR Standard Arrival Route.

TAS True AirSpeed.

TBS Time Based Separation.

TMA Terminal Manoeuvring Area.

TOBT Target Off-Block Time.

TP Trajectory Predictor.

TRACON Terminal Radar Approach CONtrol.

TSAT Target Start-up Approval Time.

TTOT Target Take-Off Time.

TU Delft Delft University of Technology.

TWR ToWeR control.

UDP Uniform Daylight Period.

UTA Upper conTrol Area.

VOR VHF Omnidirectional Radio Range.

VTT Variable Taxi Time.

WTC Wake Turbulence Category.

Contents

1 Introduction

1.1. Motivation

The demand for commercial air transportation has experienced a compelling increase in the past 20 years. Despite the efforts in the development of new Air Traffic Control (ATC) technologies, the increase in capacity has shown to be disproportionate to the increase in demand. [5] As the runway is the transition point between airspace and surface operations, well-coordinated runway management is fundamental for the operational efficiency of airports and their surrounding national and international airspace [18].

Efficient runway management becomes even more crucial at airports where a dependency exists between arrival and departure capacity due to converging, diverging, or intersecting runways. The foreseen increase in air traffic movements in combination with eased separation minima between aircraft is expected to emphasize current runway dependencies further. As the number of arriving aircraft in the vicinity of an airport will increase, the number of departure slots will decrease as a result. If no coordination between arrival and departure management will be implemented soon, airports that rely on dependent runways in their daily operation await serious (surface-) congestion problems. [11]

Currently, ATC dictates the nominal flow of arriving and departing aircraft independently. No formal procedures or advisory tools exist for the optimization and de-conflicting of the arrival and departure flow for dependent runway configurations. Moreover, Arrival and Departure Management systems do not take each other's traffic situation into account. Arriving and departing aircraft are accepted to enter the same airspace, even though no formal communication or information exchange exists between the management of the two. Arrivals and departures for dependent runways are tactically de-conflicted by ATC once entering terminal airspace. [19]

It is clear that systematic strategies are needed for the coordination between arrivals and departures. The conventional representation where airports consider their capacity by two separate variables, one for the arrival and one for the departure of aircraft, is not durable for airports that rely on dependent arrival and departure runways. Instead, these airports should see themselves as a single system resource since the arrival and departure streams of aircraft interact with one another. [12]. Therefore, this research will focus on this interaction between arriving and departing aircraft for dependent arrival and departure runway combinations. Subsequently, the resulting knowledge will be used to develop and assessed strategies for coordination between the management of arrivals and departures.

1.2. Research Objective

The main research objective of this research is:

> "to identify and assess strategies that aim to increase the throughput of runway configurations that experience interference between arrival and departure capacity due to the use of intersecting or converging runways by developing and testing multiple strategies for coordinated Arrival and

Departure Management which optimizes the combined sequencing and/or metering task of an AMAN and DMAN"

1.3. Research Questions

The objective is translated into the following main research question:

> "How can the throughput of runway configurations with a dependency between arrival and departure runways be increased by coordinated Arrival and Departure Management, which optimizes the combined sequencing and/or metering task of an AMAN and DMAN?

To answer this research question, several sub-questions have been formulated to direct the thought process as well as to develop reasonable work packages for conducting the research. Therefore, the following sub-questions are formulated:

1. What is the relation between arrival and departure capacity for dependent arrival and departure runways?
   (a) Which relevant factors can be identified that cause or contribute to the interference of arrival and departure capacity of a runway configuration?
      i. Which types of runway dependencies exist?
      ii. How can interaction between arriving and departing aircraft on dependent arrival and departure runways be quantified?
   (b) What are the conventional procedures for ATC to deal with dependent arrival and departure runways?
      i. Which runway separation procedures are followed currently?
      ii. To what extent is there situational awareness between the different ATC units and what communication mechanisms are currently available?
   (c) To what extend are runway configurations affected by dependent arrival and departure runways now and in the future?
2. What are the advantages and opportunities of coordinated Arrival and Departure Management?
   (a) How is the management of arrivals and departures currently organized at airports?
      i. What is the objective of an Arrival and Departure Manager?
      ii. What does the system architecture of the Arrival and Departure Manager look like?
      iii. What are the inputs and outputs of an Arrival and Departure Manager?
      iv. Which logic's are applied in an Arrival and Departure Manager?
      v. Who are the stakeholders in the operation of an Arrival and Departure Manager and what are their respective roles and tasks?
   (b) What are potential strategies for coordinated Arrival and Departure Management and what are their effects?
      i. What is the objective and goal of coordinated Arrival and Departure Management?
      ii. What requirements can be established for coordinated Arrival and Departure Management?
      iii. Which factors, logic, tactics, and policies are involved in potential strategies?
      iv. What advantages and disadvantages can be identified for the strategies?
      v. Which activities and interactions among stakeholders are affected by potential strategies?
      vi. How are new responsibilities delegated among stakeholders?
3. What is the operational potential of the identified strategies for coordinated Arrival and Departure Management?
4. Which strategies for the coordinated Arrival and Departure Management can be recommended for further investigation?

1.4. Relevance

This thesis will give insight into current, and future arrival and departure capacity interference and will indicate the operational potential of the strategies for coordinated Arrival and Departure Management. These results can be used to decide whether or not a particular strategy is worth further investigation and/or to guide airports in their design of ATM systems for dependent runway usage. Since this research is exploratory, these outcomes are hard to predict. However, once having found and implemented a successful strategy, airport throughput is expected to benefit. These outcomes will have a positive contribution to the everlasting challenge of balancing air transportation capacity and demand.

1.5. Research Structure

The research is divided into six work packages to arrange a structured, transparent and traceable research, see Figure 1.1. In work package 1, the foundation of the research will be developed by formulating the research problem, scope and relevant scenarios. This is done by listing and processing relevant information regarding Arrival and Departure Management. Data will be collected and analyzed such that any operational conditions that are affected by the use of dependent runways will be identified. After that, in work package 2, strategies will be conceptualized by assessing relevant literature and inquiring various stakeholders and operational experts for their thoughts on coordinated Arrival and Departure Management. Executing work package 1 and 2 will give answer sub-question 1 and 2.

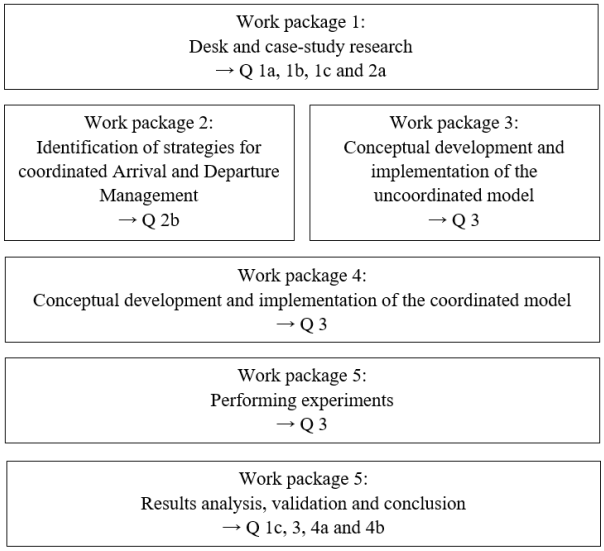

Figure 1.1: Work packages

In work package 3, the conceptual model of the baseline model, called the uncoordinated model, will be developed and implemented in software using the knowledge and insights gained from work package 1. In work package 4, the strategies for automated coupled Arrival and Departure Management will be developed and implemented in software, which is called the coordinated model. For this, the same steps as described in work package 3 will have to be executed. work packages 3 and 4 aim to answer sub-question 2.

The experiments will be performed in work package 5 by simulating the uncoordinated and coordinated models for the same set of operational conditions. In work package 6, the performance of the models will be analyzed by studying the difference between the simulation results. Finally, conclusions and recommendations on the performance of the strategies for automated coupled Arrival and Departure Management will be given to answer the main research question.

1.6. Research Background

This research is initiated by a collaboration between Delft University of Technology (TU Delft) and the Centre of Excellence (CoE). The CoE program is part of the Knowledge and Development Centre (KDC) mainport

Schiphol and allows graduate students to finish their thesis in close collaboration with the aviation industry through the KDC partners: Air Traffic Control the Netherlands (LVNL), Royal Dutch Airlines (KLM), Amsterdam Airport Schiphol (AAS) and others. Through this collaboration, a wide range of diverse topics from the KDC Research agenda will be addressed. During this project, academic support will be provided by TU Delft, and KDC will contribute with technical and financial resources. This will automatically imply that during this project, the focus will be given to AAS by using the airport in (potential) experimental set-ups. Because of this, research on AAS concerning runway management is added to the scope of this report in Chapter 4. [26]

I

Preliminary Study

- Start preliminary study -

The preliminary study was already graded for AE4020

2

Basic Concepts

Well-coordinated runway management is fundamental for the operational efficiency of airports and surrounding national- and international airspace. Managing runways involves many different factors, constraints, and competing interests of various stakeholders. [18] The active arrival and departure runways and their respective arrival and departure acceptance rates need to be chosen, and the aircraft are required to be balanced efficiently across specific runways by ATC operating policies and systems. Understanding the operational complexity and current decision-making processes within runway management is fundamental before pursuing any improvement in Arrival and Departure Management. Therefore, basic concepts concerning runway management will be clarified first in this chapter.

2.1. Air Traffic Management

A structured design of airspace and its control is the fundamental of any air traffic movement. The current Air Traffic Management (ATM) system provides services to guarantee efficient and safe air traffic flows. It includes all procedures, airborne and ground-based systems assisting an aircraft from departure to crossing airspace and eventually landing at its destination. [22] This section provides a background into ATM emphasizing airspace structure, air traffic control, and air navigational routes.

2.1.1. Airspace Structure

The Earths airspace is divided into Flight Information Regions (FIRs). Each FIR is controlled by a different authority. The managing authority is responsible for providing air traffic services to all aircraft that enter their FIR. Large countries may control more than one FIR, while small countries usually have responsibility for one FIR. Each FIR is subdivided into sectors, each with varying dimensions and classifications. Each classification has its own flight rules and limitations where pilots and air traffic controllers must adhere to. Roughly there are three types of airspaces [21]:

1. Controlled airspace: separation is provided by ATC.
2. Uncontrolled airspace: aircraft themselves are responsible for separation, no ATC services are provided.
3. Special use airspace: airspace that is used by o.a. the military, or no-fly zones.

Controlled airspace is subdivided into smaller areas. The structure of controlled airspace is complex and based on how air traffic service is provided. A distinction can be made between the following [20]:

- Upper Control Area (UTA): also called the upper airspace, refers to the airspace above Flight Level 245 (FL245). It is used by transition, en-route civil air traffic, and by military air traffic flying to and from exercise areas.
- Control Area (CTA): refers to the airspace between FL95 and FL245 and is also called the lower airspace. The CTA is used by civil and military air traffic that is descending or ascending to or from airports.
- Terminal Manoeuvring Area (TMA): the vertical and horizontal airspace that is surrounding an airport (vertically ranging from 500m to 3km). Its primary function is to protect climbing and approaching aircraft from other air traffic. In the TMA only Instrument Flight Rules (IFR) traffic is allowed. Therefore it is inaccessible for general aviation and military air traffic.

- Control Zone (CTR): the vertical and horizontal airspace that is directly surrounding an airport. Its purpose is to protect aircraft that are in the initial climb or final approach phase of the flight.

2.1.2. Air Traffic Control

Air Traffic Controllers (ATCOs) are responsible for ensuring sufficient separation between aircraft whilst handling air traffic in a smooth and orderly manner [20]. ATC is subdivided into various control units. Each control unit is responsible for providing Air Traffic Services (ATS) to its part of airspace. The Area Control Centre (ACC) is responsible for maintaining 5 NM horizontal radar separation and 1000 ft vertical separation between aircraft in the Control Area (CTA) and Upper Control Area (UTA). Approach Control (APP) is responsible for the approach control service in the Terminal Manoeuvring Area (TMA) and Control Zone (CTR). APP uses wake turbulence radar separation minima when an aircraft maintains the same height or height less than 1000 ft behind a second aircraft. Tower Control (TWR) provides ATS in the TMA and CTR. A supervisor is in charge of each control unit. Figure 2.1 shows which ATC unit is in charge during which phase of the flight.

2.1.3. Air Navigational Routes

To make the work of ATCOs less complicated, a structure of air routes exists to limit the movement of aircraft. The routes are derived from geographical points, which may or may not coincide with the location of a radio navigation aid. The trajectory of aircraft is more predictable as it moves from one navigational aid to another using a predefined path. Several different air navigational routes exist at different levels and functions:

- Air Traffic Services Routes (ATSRs): Air Traffic Services Routes are the highways of the sky. These routes are nationally, but connect national airspace to the wider international air route network, connecting national airports with every international airport. [3]
- Standard Instrument Departures (SIDs): fixed departure routes are defined between the runways thresholds and initial departure fixes at the edge of the TMA. Aircraft operators must follow instrument departure procedures to reach one of the major airways in the upper airspace. A SID procedure includes specific altitudes, speed restrictions, and checkpoints. They are designed to ensure a safe and efficient flow by separating inbound and outbound air traffic and reducing communication between the ATCOs and pilots. Moreover, they are used to avoid obstacles and reduce the noise load on the ground. One runway often has several different SIDs. [3]
- Standard Arrival Routes (STARs): standard arrival routes are defined to connect the airways to the beginning of an approach procedure. For the same reason as SIDs, STARs are designed to separate inbound and outbound air traffic, to reduce communication between the ATCOs and pilots and to reduce environmental impact. The approach procedure of an aircraft starts when it reaches one of the Initial Approach Fixes (IAFs), which are located at the edge of the TMA. [3]
- Holding stacks: international legislation requires each STAR to have a holding stack. Holding stacks are used when airport capacity is lacking behind the demand of approaching aircraft due to bad weather or a high traffic load. Aircraft that are put in the holding stacks, circle in the same pattern at different altitudes until they are allowed to enter the TMA and start their approach. When an aircraft is cleared to leave the holding stack, the other aircraft decent one level until cleared to leave themselves. This way, the first come first served criteria is maintained in the holding stacks. [1]

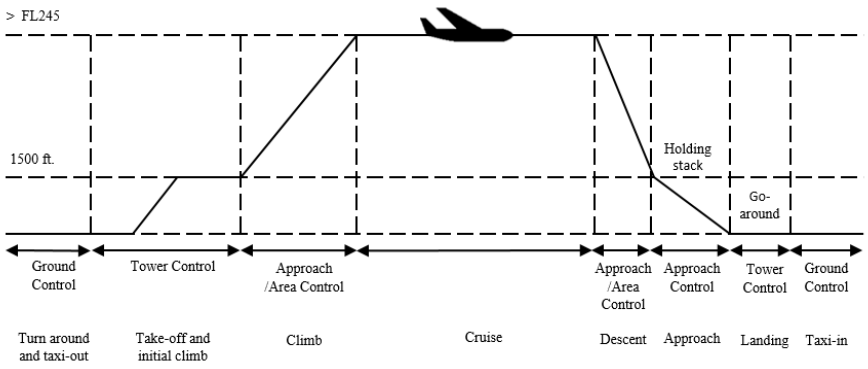

Figure 2.1: Aircraft in system

2.2. Airport Capacity

Airport capacity depends on many factors deriving from airspace, airside and landside domains. The performance depends primarily on the performance of the static design of the airport (infrastructure, airspace), the support systems, and the procedures that are being followed by humans. Airspace and landside performance both coincide with airside performance, as factors like runway and gate capacity influence both the performance of airspace and landside since it serves as a gate between the two. Delays, pressure from external parties, or an expected increase in air traffic demand can trigger an airport capacity assessment to give insight in (potential) bottlenecks. To make use of latent capacity or to increase existing capacity, an airport operator can choose to do a capacity enhancement. Depending on environmental and budgetary constraints, roughly three options for capacity enhancement can be distinguished: (1) infrastructural and airspace enhancements, (2) ATM system enhancements, and (3) human performance improvements.

2.3. Runway Capacity

The capacity if a runway can have different values at different times depending on the circumstances surrounding the operation [22]. Hence, runway capacity can be seen as a probabilistic quantity, a random variable. Neufville [22] described four definitions of runway capacity. Neufville [22] defined the declared capacity is as the number of aircraft movements per hour that an airport can accommodate at a reasonable Level of Service (LOS). For airports, the declared capacity is the most relevant definition as this capacity is communicated with the slot coordinator [17]. There is a limitation on the number of aircraft that can arrive or depart on a single runway or runway configuration. This depends on several factors such as separation regulations, presence of independent- and dependent runways, aircraft fleet mix, airborne constraints, taxiway constraints, meteorological influences and experience of ATCOs [22].

2.3.1. Separation Regulations

Aircraft separation regulation is coordinated by the International Civil Aviation Organization (ICAO) to ensure the safe operation of aircraft. One might think that separation regulation is primarily meant for reducing the risk of airborne collisions and runway incursions. However, aircraft in the vicinity create a potential safety hazard before the risk of collision or incursion due to wake turbulence [14]. ICAO defined Wake Turbulence Categories (WTCs) based on an aircraft Mean Take Off Weight (MTOW) to incorporate safety hazards due to wake vortices. Using the redefined WTCs in RECAT-EU, new separation minima have been established between combinations of leading and following aircraft of certain aircraft WTCs. Two types of separation exist (1) distance-based separation applicable for arrivals and (2) departures and time-based separation solely applicable for departures. When no wake turbulence distance-based separation minima is prescribed, Minimum Radar Separation (MRS) holds. [23]

Table 2.1: RECAT-EU WT distance-based separation minima on approach and departure [23]

Leader / Follower	A	B	C	D	E	F
A	3 NM	4 NM	5 NM	5 NM	6 NM	8 NM
B		3 NM	4 NM	4 NM	5 NM	7 NM
C		(*)	3 NM	3 NM	4 NM	6 NM
D						5 NM
E						4 NM
F						3 NM

(*) means minimum radar separation (MRS), set at 2.5 NM, is applicable as per current ICAO doc 4444 provisions.

2.3.2. Independent Arrival and Departure Runways

When the physical spacing between runways is sufficient, independent operations between arrival runways and departure runways are allowed. This implicates that the arrival at a runway does not intervene in a departure at another runway. During independent runway operations, the separation between successive arrivals and departures is solely dependent on the regulations regarding Inter-Arrival Time (IAT) and Inter-Departure Time (IDT). The fundamental methodology to derive the IAT and IDT was described by Stamatopoulos et al. [25].

Table 2.2: RECAT-EU WT time-based separation minima on departure [23]

Leader / Follower	A	B	C	D	E	F
A		100 s	120 s	140 s	160 s	180 s
B				100 s	120 s	140 s
C				80 s	100 s	120 s
D						120 s
E						100 s
F						80 s

Inter-Arrival Time

The radar and wake turbulence separation and runway occupancy time (ROT) is relevant for determining the required Inter-Arrival Time (IAT) between two consecutive arrivals on a single runway. The first regulation states that the radar and wake turbulence separation requirements (μ_1) should be maintained continuously between two arrivals at a common approach path (D_A). Secondly, an arrival is cleared for landing at the runway threshold when the proceeding arrival has left the runway. The time separation imposed by this regulation is denoted as μ_2. The time separation (μ) that should be maintained by ATCO between the following aircraft at the entry of the common path and the leading aircraft, such that the minimum IAT is achieved at touch down of the leading aircraft, is presented by Equation 2.1. The derivation of both μ_1 and μ_2 is presented below.

$$\mu = max(\mu_1, \mu_2) \tag{2.1}$$

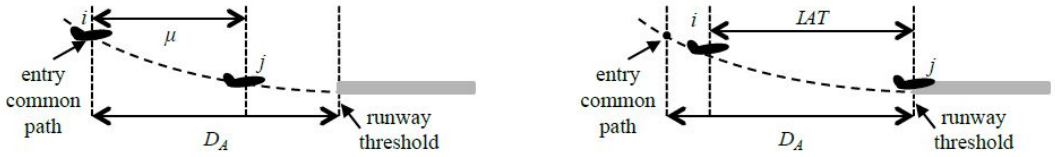

Figure 2.2: Time separation between a following aircraft i and leading aircraft j, at the entry at the common path of following aircraft i and at touch down of leading aircraft j [27]

The required radar and wake turbulence separation should be maintained starting from the entry of the common path until the arrival has reached the runway threshold. Since different aircraft types have different approach speeds, the following aircraft may run in on or separate from the leading aircraft with time. When closing, the average ground speed of the leading aircraft is lower than the average ground speed of the following aircraft ($V_{A,j} < V_{A,i}$). Vice versa, when opening, the average ground speed of the leading aircraft is equal or higher than the average ground speed of the following aircraft ($V_{A,j} \geq V_{A,i}$). For closing and opening, different equations hold for the calculation of the required separations μ_1. For closing and opening respectively Equation 2.2 and 2.3 hold, with S_{ij} being the required distance-based separation between an aircraft pair.

$$\mu_{1,closing} = \frac{D_A}{V_{A,j}} - \frac{D_A - S_{ij}}{V_{A,i}} \tag{2.2}$$

$$\mu_{1,opening} = \frac{S_{ij}}{V_{A,j}} \tag{2.3}$$

The second regulation stated that the trailing aircraft is cleared to land when the leading aircraft has left the runway. This means that the trailing aircraft must be at least a certain distance from the runway where a missed approach procedure can be initiated the latest (D_{MAP}) when the leading aircraft has just cleared the runway. By doing this, the trailing aircraft can initiate a missed approach procedure without any risk. The time separation imposed by this regulation (μ_2) for both the opening and closing case is determined by Equation 2.4 and is added on top of the runway occupancy time of the leading arrival ($R_{A,j}$).

$$\mu_2 = \frac{D_A}{V_{A,j}} - \frac{D_A - D_{MAP}}{V_{A,i}} + R_{A,j} \tag{2.4}$$

The IAT between a leading aircraft passing the runway threshold and a trailing aircraft is calculated by adding the time separation resulting from Equation 2.1 to the difference in time needed for the two aircraft to fly the common approach path, see Equation 2.5.

$$IAT_{i,j} = \frac{D_A}{V_{A,i}} - \frac{D_A}{V_{A,j}} + \mu \tag{2.5}$$

Inter-Departure Time
The Inter-Departure Time (IDT) is described as the time between two consecutive starts of take-off rolls. Several regulations are of importance for determining the required IDT at airports using Standard Instrument Departures (SIDs). Firstly, the wake turbulence time-based separation is relevant. Secondly, only one aircraft is allowed to take off at a runway. Third, distance-based separation is needed between departing aircraft that have a longer common path due to heading the same Initial Departure Fix (IDF). Lastly, a communication buffer between departure clearance and the actual start of the take-off roll should be included. The communication buffer differs between operating airlines.

The IDT_{ij} between leading aircraft j and following aircraft i is equal to the maximum of (1) the departure runway occupancy time difference of of the leading aircraft j ($R_{D,j}$) and the trailing aircraft i ($R_{D,i}$) plus a time increment υ and (2) the required time based separation for aircraft combination i, j ($G_{i,j}$) plus a communication buffer $\bar{c}_{D2}$, see Equation 2.6.

$$IDT_{i,j} = max(R_{D,j} - R_{D,i} + \upsilon, G_{i,j}) + \bar{c} \tag{2.6}$$

The time increment υ depends on (1) the distance-based separation ($S_{i,j}$), (2) the length of the common departure path (D_D) and (3) the ground speed of both aircraft (V_D). When the length of the common path is smaller than the distance-based separation (i.e. $D_D \leq S_{i,j}$) the time increment is equal to the time the leading aircraft needs to leave the common departure path, see Equation 2.7.

$$\upsilon = \frac{S_{i,j}}{V_{D,j}} \tag{2.7}$$

When the length of the common path is larger than the distance based separation (i.e. $D_D \geq S_{i,j}$) the time increment depends on whether the aircraft run in ($V_{D,j} < V_{D,i}$) or separate from one another ($V_{D,j} \geq V_{D,i}$) over the course of time. When the aircraft separate from one another Equation 2.7 holds for the time increment υ, when the aircraft run in on another Equation 2.8 holds.

$$\upsilon = \frac{D_D}{V_{D,j}} - \frac{D_D - S_{i,j}}{V_{D,i}} \tag{2.8}$$

2.3.3. Dependent Arrival and Departure Runways

If operating one runway hinders the operation of another runway this is referred to as dependent runway use [2]. When operating dependent runways, at a certain point the number of departures will start to decrease when the number of arrivals increases any further. Four types of dependencies between runways can be distinguished: (1) parallel, (2) intersecting, (3) converging and diverging, and (4) mixed mode. Intersecting runway use occurs when runways physically intersect with each other. Converging and diverging runways do not physically intersect, but the lengths of the runways intersect one another. At this location, called the convergence point, a safety hazard exists. The layout of intersecting, converging and diverging runways causes sub-dependencies due to jet blast hindrance and missed approach operations.

The interaction between arrivals and departures for dependent runways composes of two interactions: (1) the arrival-departure interaction and (2) the departure-arrival interaction. The arrival-departure interaction for dependent runways requires a minimum time interval before an aircraft can take-off after an arrival, the Inter-Arrival-Departure Time (IADT). Likewise, the departure-arrival interaction for dependent runways requires a minimum time interval before an aircraft can arrive at the runway threshold after a departure took place, the Inter-Departure-Arrival Time (IDAT). Figure 2.3 gives an example of the interaction between arrivals and departures for dependent runways. van der Klugt [27] mathematically expressed the IADT and IDAT.

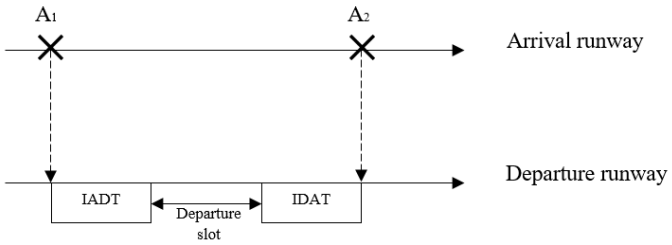

Figure 2.3: Example of an arrival-departure interaction

Converging Runways - Jet Blast Hindrance

Figure 4.5 presents two dependencies for an arrival at a runway and a departure at another runway [27]. A departure at runway one is only allowed when an arrival at runway two is at a certain distance from the runway threshold, see Figure 4.5(a). The minimum time between a departure at runway one followed by an arrival at runway two, the Inter-Departure-Arrival Time (IDAT), is equal to the minimum distance from the runway threshold (D_{min}) divided by the approach speed of the arrival (V_{A2}) minus a particular communication error ($\bar{c}_{D2}$), see Equation 2.9.

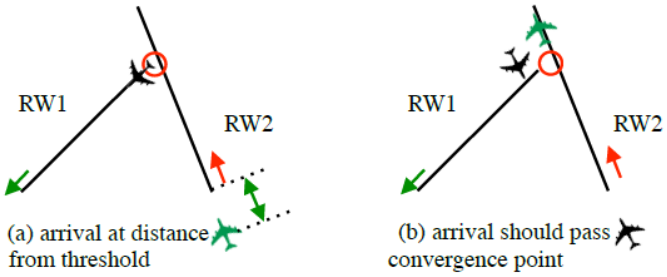

Figure 2.4: Jet blast hindrance between an arrival and departure for converging runways [27]

$$IDAT = \frac{D_{min}}{V_{A2}} - \bar{c}_{D2} \tag{2.9}$$

A line-up clearance for a departure at runway one is given when an arrival at runway two has passed the jet blast point, see Figure 4.2(b). Therefore, the time between an arrival followed by a departure, the Inter-Arrival-Departure Time (IADT) is equal to the ROT until the arrival has passed the jet blast point on runway two ($R_{A2,int}$) plus the line-up time of the departure ($t_{D1,lu}$) and a communication buffer ($\bar{c}_{D1}$), see Equation 5.21.

$$IADT = R_{A2,int} + t_{D1,lu} + \bar{c}_{D2} \tag{2.10}$$

Converging Runways - Missed Approach

Two potential safety hazards for missed approach operations were distinguished by [27]. Figure 2.8 shows the risk of a departing aircraft intersecting the missed approach path of an arrival van der Klugt [27]. A departure is only cleared for taking off when an arrival is at a minimum distance (D_{min}) from the runway threshold, see Figure 2.8(a). Consequently, the minimum time between a departure followed by an arrival (IDAT) is given by Equation 5.18.

$$IDAT = \frac{D_{min}}{V_{A2}} - \bar{c}_{D1} \tag{2.11}$$

When an arrival at runway two is already within the minimum distance from the runway threshold (D_{min}), a departure is cleared for taking off when the arrival has completed its landing. Therefore, the time between an arrival at runway two followed by a departure (IADT) at runway one is equal to the arrival completion time ($R_{A2,com}$) plus a communication buffer ($\bar{c}_{D1}$), see Equation 2.12.

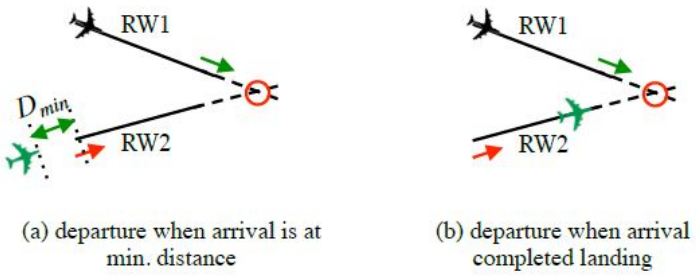

Figure 2.5: Missed approach dependency between an arrival and departure for converging runways [27]

$$IADT = R_{A2,com} + \bar{c}_{D1} \tag{2.12}$$

Intersecting Runways
Figure 2.9 shows the dependency for an arrival at a runway and a departure at two intersecting runways [27]. An arrival should be at a minimum distance (D_{min}) from the runway threshold or should have passed the intersection point before a departure is cleared. Furthermore, an arrival should be at the missed approach distance (D_{MAP}) from the runway threshold when a departure ends its take-off roll, to avoid the missed approach conflict. From this, the minimum time interval between a departure followed by an arrival (IDAT) is presented by Equation 2.13. Vice versa, the minimum time interval between an arrival followed by a departure (IADT) is presented by Equation 2.14.

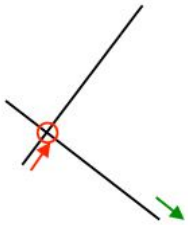

Figure 2.6: Dependency between an arrival and departure for intersecting runways [27]

$$IDAT = max(\frac{D_{min}}{V_{A2}} - \bar{c}_{D1}, \frac{D_{MAP}}{V_{A2}} + R_{D1,int}) \tag{2.13}$$

$$IADT = R_{A2,int} + \bar{c}_{D1} \tag{2.14}$$

2.4. Runway Capacity Allocation

The decision-making process of designating active runways, monitoring the performance of the active runways, predicting future runway configurations, and selecting the adequate airport acceptance en departure rates is complicated and depends on many factors, constraints, and competing interests of several stakeholders. This section presents the principles of runway configuration- and airport acceptance and departure rates selection.

2.4.1. Runway Configuration Selection

At airports that have access to multiple runways, often numerous combinations of active runways are possible given existing operational factors. The selected runways are used for arriving and departing aircraft or both and need to be managed such that system, airport, and user demands are met [18]. ATC supervisors are responsible for designating the optimal active runways by considering pre-determined runway configurations options for current and future operational circumstances. Multiple factors need to be taken into account by ATC supervisors when selecting a runway configuration for maintaining efficient air traffic operations [18]:

- Weather: e.g. weather minimums, convective weather
- Environment: e.g. noise and emissions
- Physical capacity-limiting factors: e.g. runway length, flight plan routing
- Airport layout: arrival and departure runways that are closest to the airport terminal and gates are preferred.
- Runway spacing: active runways need to be sufficiently spaced to allow maximum throughput
- Airspace restrictions: Special Use Airspace (SUA) near an airport can impose restrictions on arrival and departure flight plans
- Surface restrictions: e.g. taxi bottlenecks and space limitations
- Staffing factors: the required number of ATCOs for the operation of a runway configuration
- Terminal traffic flow of nearby airports: airports that have multiple proximate airports need to consider potential conflicting flight paths among airports.

2.4.2. Arrival and Departure Rate Selection

Airport acceptance rates represent the maximum number of arrivals and departures an airport can facilitate under specific operating conditions for a consecutive period of 60 minutes. They are called the Airport Acceptance Rate (AAR) and Airport Departure Rate (ADR) respectively for arrivals and departures. The rates are determined in collaboration between Tower Control and ACC supervisors and are used as input for Airport Traffic Management Systems, like Arrival and Departure Managers (which are explained in section 2.5). Common methods for determination are rules-of-thumbs and years of experience. The challenge within arrival and departure acceptance rates selection is to determine, implement, manage, and communicate these to all involved parties within a relatively short notice [18]. Once the rates are chosen, it is up to ATC to regulate traffic as such that the rates are not exceeded. Factors that influence the AAR and ADR are [18]:

- Availability of high-speed taxiways
- Runway conditions i.e. wet or dry
- Number of arrival and departure runways
- Traffic mix
- Procedural limitations i.e. noise and missed approach
- Mixed mode operations
- Distance between arrival and departure runways

2.5. Runway Capacity Utilization

At many U.S. and European airports the arrival and departure demand often exceeds the available airport capacity for specific periods. Therefore, the flow of arriving and departing aircraft needs to be adequately controlled to ensure safe and efficient operations. Many airports have been implementing Airport Traffic Management Systems that provide electronic assistance for ATCOs in planning and sequencing the flow of arriving and departing aircraft. Those systems are called the Arrival Manager (AMAN) and the Departure Manager (DMAN), respectively for the control of the arrival and departure flow. ATC uses AMANs and DMANs to schedule and meter inbound and outbound streams of aircraft [9]. Airports have been developing their AMAN and DMAN independently from one another, which resulted in different systems operating at different locations. The general working principles for both will systems will be outlined in this section.

2.5.1. Departure Management

The DMAN is a tactical planning tool supporting the departure scheduling of ground and tower control. The DMAN optimizes the flow of departing aircraft by taking into certain aspects of departure management, e.g. capacity and efficiency. From the scheduled departure times, the system derives the right times for (engine) start-up and push-back clearance. [6]

Objective

A DMAN is capable of continuously adapting to the progress of all departure procedures. An earlier departure clearance or a missed initial one may trigger the DMAN to reschedule the total outbound sequence. For this reason, a DMAN should not be seen as an advisory tool system, but as a control mechanism. The DMAN aims to increase departure throughput, the number of CFMU slot compliances, and the planning stability while minimizing the taxi-out delay by optimal departure sequencing. The complexity of the used algorithms, the system architecture, and the type of advisories differ from system to system. However, the underlying princi-

ples in each DMAN are often similar. [6]

Departure Management Process
When an aircraft is at the gate, the aircraft operator/handler estimates the time that the aircraft will be ready for engine start-up and push-back, the Target Off-Block Time (TOBT). This includes closed doors, the boarding bridge removed, the presence of a push-back vehicle. This time is continuously calculated and updated by the operator/handler to the airports DMAN. The Central Flow Management Unit (CFMU) issues the time the flight is expected to be airborne, the Calculated Take-Off Time (CTOT). This time is the result of tactical slot allocating, taking into account the constraints of airspace capacity.

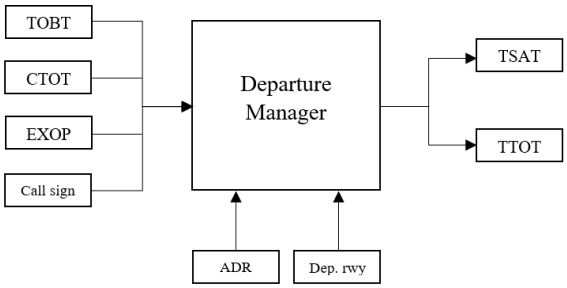

Figure 2.7: The input and output of the DMAN

The TOBT, CTOT, the call sign, the estimated outbound taxi time (EXOP), the Airport Departure Rate (ADR) and active departure runways are used as an input for the DMAN. With this information, the Departure Manager calculates the time that an aircraft can expect start-up/push-back approval from TWR Ground Control, called (TSAT). The TSAT is presented to the aircraft cockpit crew, and within a time frame of ± 5 minutes, the crew is allowed to ask for a start-up/push-back approval. The time difference between the TOBT and TSAT is the Expected Stand Waiting Period (ESWP). The DMAN also calculates the Target Take-Off Time (TTOT), which is the time that the aircraft becomes airborne.

After the aircraft has received its start-up/push-back clearance; the aircraft will start-up its engines and the aircraft will leave the parking area by the push-back vehicle until the aircraft is aligned with the taxiway. The TWR Ground Control provides the aircraft with its taxi route and departure runway. TWR Ground Control is responsible for providing the final sequence of departing aircraft in which aircraft WTCs and SIDs are taken into account. This is ensured by making last-minute tweaks in taxi routes or runway entries.

After taxiing, the aircraft reaches the runway holding point. Here it enters the queue of other departing aircraft. The Expected Runway Waiting Period (ERWP) is the time between entering the queue and the line-up at the runway. The ERWP plus the ESWP is the Expected Waiting period of the aircraft at the stand and runway holding point. A TWR ATCO verifies the runway is clear from any approaching or departing aircraft and ensures the sequence of arriving and departing aircraft meets the arrival/departure separation standards. When the clearance is received, the aircraft lines-up with the runway axis and roll to airborne from the runway holding point. This time interval is called the Estimated Line-up and Roll to Airborne Period (ELRP). After reaching V1, the take-off may no longer be aborted.

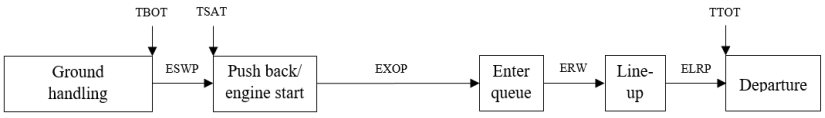

Figure 2.8: Departure management process

System Architecture
A description of the basic set of modules that are present in a DMAN can be found below. Figure 2.9 shows how modules are connected. [6]

- Supervisor module: the supervisor module is regarded as the central module of the DMAN and is responsible for data management and message handling. This ensures that all modules will be updated about flight plans, aircraft data, system parameters and, static data such as aircraft parking positions and SIDs. Furthermore, the supervisor module is responsible for the communication of dynamic data to the right ATCO resulting from the input of another ATCO. Moreover, the supervisor module calculates the ETOT, which is a hard constraint in departure planning. Based on the ETOT, the other time points are calculated using operational models.
- Planner module: the planner module is continuously optimizing the departure take-off schedule, taking into account the actual situation. The planner also manages data like aircraft separation tables and search-three information.
- HMI's for controllers: DMAN information is integrated into the electronic flight strips at the Controller Working Position (CWP) of at least: one clearance delivery position for issuing en-route clearances, one position of apron/ground control, one runway control position for line-up and take-off clearances.
- Gateway module: the gateway is responsible for translating communication between external systems and internal modules.

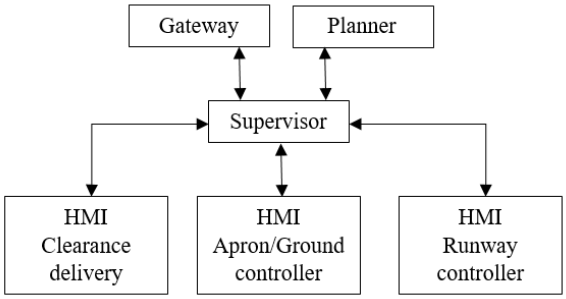

Figure 2.9: The basic system architecture of the DMAN

2.5.2. Arrival Management

An AMAN provides ATCOs electronic assistance in managing the flow of arriving aircraft to the runway threshold or metering points [13]. It optimizes the runway capacity by sequencing or metering the number of aircraft that enter particular airspace. To achieve this, the AMAN calculates expected and scheduled times for each aircraft at the runway threshold and IAFs [13].

Objective

The overall objectives of the AMAN are to increase safety, capacity, and efficiency and to reduce environmental impact. These objectives act in different directions, improving one often deteriorates the other. The AMAN needs to be implemented as such that it can find an optimal balance between the objectives to act as a useful support tool [13]. As the AMAN was developed and used at many airports independently from one another, considerable differences exist between them. The complexity of the used algorithms, the system architecture, and the type of advisories differ from system to system. However, the underlying principles in each AMAN are often similar.

Arrival Management Process

When an aircraft passes the Eligibility Horizon (EH), 150 to 200 NM from the runway threshold [28], the aircraft is taken into account for sequencing and scheduling, together with the other approaching aircraft. The AMAN uses flight plan data (FDPS), radar data (RDPS), weather data, and a trajectory prediction module to compute the Estimated Time Over (ETO) and the Estimated Time of Arrival (ETA). The ETA is the estimated time that the aircraft will reach the runway threshold (RWY) without considering any airport capacity constraint and is highly dependent on which runway is being operated [28]. The ETO is the estimated time the aircraft will arrive at the Initial Approach Fix (IAF).

Because the airport and airspace around it has limiting capacity; the possibility exists that an aircraft cannot arrive at its ETA because runway capacity is lacking. When this is the case, the aircraft needs to be delayed

before it can start its approach to ensure the required inter-arrival times between approaching aircraft. The AMAN determines this delay by calculating the Scheduled Time of Arrival (STA) for all approaching aircraft. The STA is the time the aircraft is allowed to reach the runway threshold. The time difference between the STA and ETA is the time delay or advance of the aircraft.

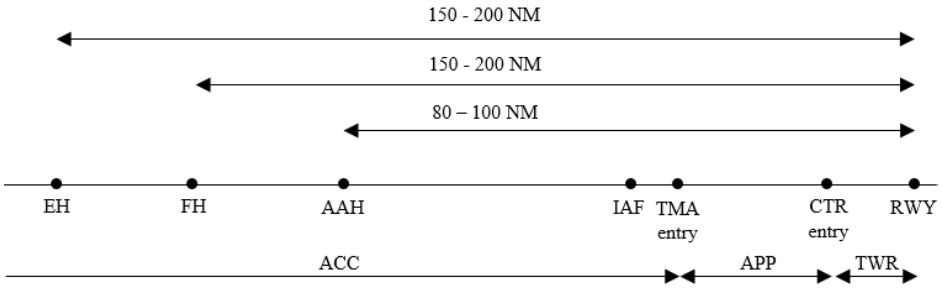

Figure 2.10: The locations of the different planning horizons used by an AMAN

Since the delay is not allowed to be absorbed within the TMA or CTR; the AMAN projects the delay in the Expected Arrival Time (EAT) at the IAF. The time difference between EAT and ETO equals the aircraft delay. The latter needs to be absorbed by ACC interference such that the aircraft reaches the IAF at its EAT. With the STA's of all approaching aircraft, the AMAN can start sequencing a stream of arriving air traffic. However, the STA is subject to change until the aircraft reaches the Freeze Horizon (FH), 150 to 200 NM from the runway threshold [28]. Once the aircraft passes the FH, its STA is fixed. Only when the aircraft reaches the Active Advisory Horizon (AAH), 80 to 100 NM from the runway threshold, ACC is allowed to send speed and direction commands actively. If the delay is too large to be solely resolved with speed vectoring, ACC can put the aircraft in the holding stacks near each IAF at the TMA boundary. When the aircraft enters the TMA, the control of the aircraft is handed over from ACC to APP. From this point onward, the AMAN is not used anymore. APP uses tactical control techniques like path stretching or shortening to create the arrival sequence and optimal inter-arrival spacing between an aircraft and its trailing and preceding one.

Figure 2.11: The planned times by the AMAN

System Architecture
A description of the basic set of modules that are present in an AMAN can be found below. Figure 4.4 shows how modules are connected. [13]

- Aircraft performance module: the aircraft performance module is a database that contains information about how different aircraft types perform. The databases can differ in accommodating a few aircraft models to an extensive amount.
- Trajectory prediction module: the trajectory prediction module predicts the flight progress of an aircraft based on aircraft performance, location, estimates of intent, expected environmental conditions, and procedures. The module computes the ETAs and ETOs for aircraft.
- Sequencer module: the sequencer module builds a sequence based on relative times using prescribed sequencing criteria.
- Weather data module: incorporating weather in the trajectory prediction module is vital for making predictions. The data can be loaded at specific time points or dynamically.
- Flight plan data source and radar data source: flight plan data and radar data are used as the basis of the trajectory prediction. Flight plan data is used to determine the intent of an aircraft and for predicting ETAs when no radar information is available. Radar information is used to determine the location,

altitude, and speed of an aircraft. The quality of the data depends on the accuracy of the radar system that is operated at the airport.

- SYSCO connection module: the SYSCO connection module is used to communicate computed information by the AMAN to the ATCOs and from ATCO to ATCO.
- Controller Working Position Human Machine Interface (CWP HMI) module: the CWP MHI is the graphic interface between the AMAN and the ATCO. Common interfaces are schedule lists and timelines [28].

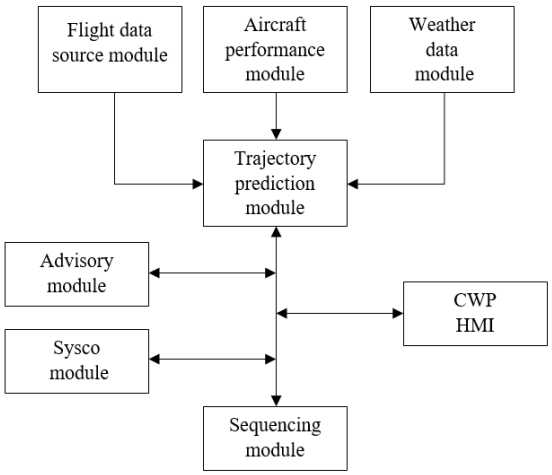

Figure 2.12: The system architecture of the AMAN

3

Previous Research

As explained previously, AMANs and DMANs are standalone systems [10], they are designed to optimize runway throughput by scheduling and metering the inbound and outbound stream of aircraft [9]. Past implementations of these systems share the same goal, but do not account for one another arrival or departure demand or delay ([6], [16]). The number of studies in implementations that did the latter is marginal. These studies differed from low-level of automation to high-level of automation and are elaborated upon below.

3.1. Coupled Arrival and Departure Management

Single European Sky ATM Research (SESAR) performed a study in flow-based integration of Arrival and Departure Management [8]. In this low-level of automation concept, the arrival and departure sequences of aircraft, including the predicted delay of each aircraft calculated by the AMAN and DMAN, were displayed alongside one another and presented identically to both supervisors. The supervisors were thus able to monitor the delay of both aircraft streams and could decide upon a runway spacing strategy to balance the required arrival and departure rates. This prototype was referred to as coupled AMAN-DMAN and was tested at Gatwick Airport (EGKK). Due to the poor data quality of the DMAN, the situational awareness between Arrival and Departure Management was not increased. Nonetheless, the concept is relatively easy to implement at airports without Time Based Separation (TBS) capabilities and advanced AMAN or DMAN systems.

3.2. Dynamic Aircraft Spacing

More advanced automation was obtained in concepts that provided dynamic inter-arrival spacing guidance to ATCOs using TBS slot markers that account for the departure demand. Diffenderfer et al. [10] showed that arrival and departure throughput can be improved and Air Traffic Controllers (ATCOs) were able to vector aircraft as advised when using TBS slot marker guidance based upon scheduled departure demand. However, no prioritization between arriving or departing aircraft flows was incorporated to create arrival free intervals that allowed for more than one departure. Yoo et al. [29] continued this study by extending the concept to allow for dynamical inter-arrival ATCO guidance at the entry of the TRACON. Furthermore, they designed and tested three arrival schedule adjustment strategies to create arrival free intervals large enough to enable the departure of more than one aircraft between two successive arrivals, while preserving arrival throughput.

In the first strategy called the Delay Control Strategy, for each arrival interval it is determined if delaying the trailing aircraft results in an AFI large enough to accommodate a take-off. It is only possible to delay the trailing aircraft when the delay does not cause a conflict with the minimum IAT with the subsequent aircraft. In the second strategy, called Delay and Advance Control Strategy, the leading aircraft is allowed to be advanced and the trailing aircraft is allowed to be delayed when there is sufficient slack to create an extra AFI. Again, advancing and delaying is only possible when minimum separation is not violated. The main concept of the last strategy is to discharge slack capacity from the arrival stream. For each pair of arriving aircraft it is determined if delaying the trailing aircraft results in an extra departure slot. If it does, the trailing aircraft will be delayed, else, the trailing aircraft is moved forward to remove slack capacity. [29]

The strategies were found to need sufficient natural slack between arrivals to generate additional departure capacity. Results showed that a 10 to 60% increase in the number of departures could be expected during peak hour operation, however, the impact of the uncertainty in arrival times was not verified. Also, it was not verified whether the extra departure slots matched the departure demand or not. Furthermore, the question arises whether the strategies will be useful at airports that are already operating at high arrival demand. A densely packed arrivals flow might not have sufficient slack to create extra departure slots.

3.3. Integrated Arrival and Departure Management

Near to fully automated concepts for coordinated Arrival and Departure Management integrates the AMAN and DMAN into one system which calculates and optimizes the arrival and departure sequence as a whole. Bohme et al. [7] used information from the AMAN and DMAN to tailor arrival free intervals in the arrival flow to account for the ground departure situation. This concept needs to be supported with an advanced AMAN capable of generating 4D-trajectories to stretch the paths of aircraft. The system applies an algorithm that uses fuzzy logic for the selection of a suitable time to introduce an arrival free interval.

The concept proved that integrating the AMAN and DMAN improves throughput at airports operating runways in mixed-mode operations. The throughput is expected to further increase when the fuzzy rule set will be optimised. However, a description of the defined rules was lacking, leaving the question of whether or not the implementation of such a system would increase the throughput at airports that operate dependent runways open. Considering that both arriving and departing aircraft trajectories carry a certain level of uncertainty and variability due to high order effects such as weather and human actions [15], it is questionable whether or not the optimized sequences calculated by an integrated AMAN and DMAN would be operationally deliverable by ATC once implemented in real-life.

3.4. Literature Gap

Research into the strategic coordination of Arrival and Departure Management was found to be marginal. Research that did focus on combined Arrival and Departure Management differed in the level of sophistication. The main advantage of the Coupled AMAN-DMAN is that it is accessible for airports to implement without major adjustments to their current AMAN and DMAN. However, the spacing setting is still chosen by human interpretation and entered manually. Also, ATCOs are still responsible for deciding when a departure will be fitted in the arrival sequence.

The Dynamic Aircraft Spacing strategy has the potential to create many extra departure slots as long as there is enough slack in the arrival sequence. At airports that are already operating at high demand or will be in the future, there might not be enough slack to generate the right number of departure slots. Since the algorithms cannot prioritize departures when needed, the Dynamic Aircraft Spacing strategies are less future proof.

The Integrated AMAN-DMAN exactly matches the arrival stream of aircraft to the departure demand. Therefore the systems need advanced Arrival and Departure Managers to overcome the stochastic nature of aircraft arrivals and departure to operationally execute the optimized sequence. This makes the Integrated AMAN-DMAN less attractive for airports to implement as many airports will have to make major adjustments to their operating AMAN and DMAN. Furthermore, when a departure misses its specially tailored slot and has to use another, the whole optimized sequence could be messed up. Table 3.1 summarizes how each study scored on different criteria.

Table 3.1: Summary of studies into coordinated Arrival and Departure Management

	Coupled AMAN-DMAN	Dynamic Aircraft Spacing	Integrated AMAN-DMAN
Implementable	++	+	- -
Departure demand	+	-	++
Robustness	+ +	+	-
ATCO influence	- -	-	-
Extra departure slots	-	++	+
Future proof	+	- -	++

4

Case Study: Amsterdam Airport Schiphol

With more than 71 million passengers in 2018, Amsterdam Airport Schiphol (AAS) is the largest airport in the Netherlands and the third-largest airport in Europe. It facilitates almost 500.000 flights per year and is known for its complex infrastructure [24]. The ATS to all incoming and outgoing aircraft is provided Air Traffic Control the Netherlands. This chapter aims to give the reader understanding of the operational complexity of Amsterdam Airport Schiphol by discussing its approach and departure routes, runway operations, and runway capacity utilization systems. Furthermore, a traffic analysis will be performed to quantify variables that might be of importance in future research.

4.1. Approach and Departure Routes

Inbound traffic to AAS uses predefined routes until reaching one of the three Initial Approach Fixes (IAFs): (1) ARTIP, (2) RIVER, and (3) SUGOL. Near each IAF a holding stack is available for aircraft to absorb delay when airport capacity is lacking, see Figure 4.1. In contrast with outbound traffic, no fixed route is defined from the IAFs towards Final Approach Fixes (FAFs). Instead, aircraft are vectored towards the FAF of the active runway by APP. The vectored approaches enable ATC to make maximum use of the available runway capacity as the common approach path between arriving aircraft is shorter. However, during off-peak hours fixed RNAV routes, such as Continuous Descent Approaches (CDAs), are used. Here, the common approach path is significantly longer, decreasing the runway capacity.

As no fixed approach routes are defined inside the TMA radar data was analyzed to find the most practised routes in the TMA from each IAF to each arrival runway. From the most practised routes, new waypoints are derived which can be used to simulate the trajectory of approaching aircraft inside the TMA at AAS. Table 4.1 shows the exact locations of the waypoints that describe the most practised trajectory from each IAF to arrival runway 18C.

Table 4.1: Coordinates of waypoints that descrbe the most practiced routes in the Schiphol TMA

IAF	Latitude	Longitude
ARTIP	52.566918	4.773036
RIVER	52.492041	4.510528
SUGOL	52.546030	4.684377

AAS uses Standard Instrument Departures (SIDs) to lead departing aircraft from the runway threshold to the upper airspace. All runways have one or more SID leading to each of the five different sectors in the Dutch airspace. Figure 4.3 shows part of a chart in which the SIDs for departures from runway 24 to sectors 1-3. In this chart, the geographic locations of the waypoints, VHF Omnidirectional Radio Ranges (VORs), and Distance Measuring Equipments (DMEs) that define a SID can be found. Furthermore, these charts show the common departure paths between different SIDs, which influences the separation that needs to be maintained between two departures. Departing aircraft from AAS are obliged to fly the horizontal path defined in a SID using their Area Navigation (RNAV) instruments unless ATC instructs them differently.

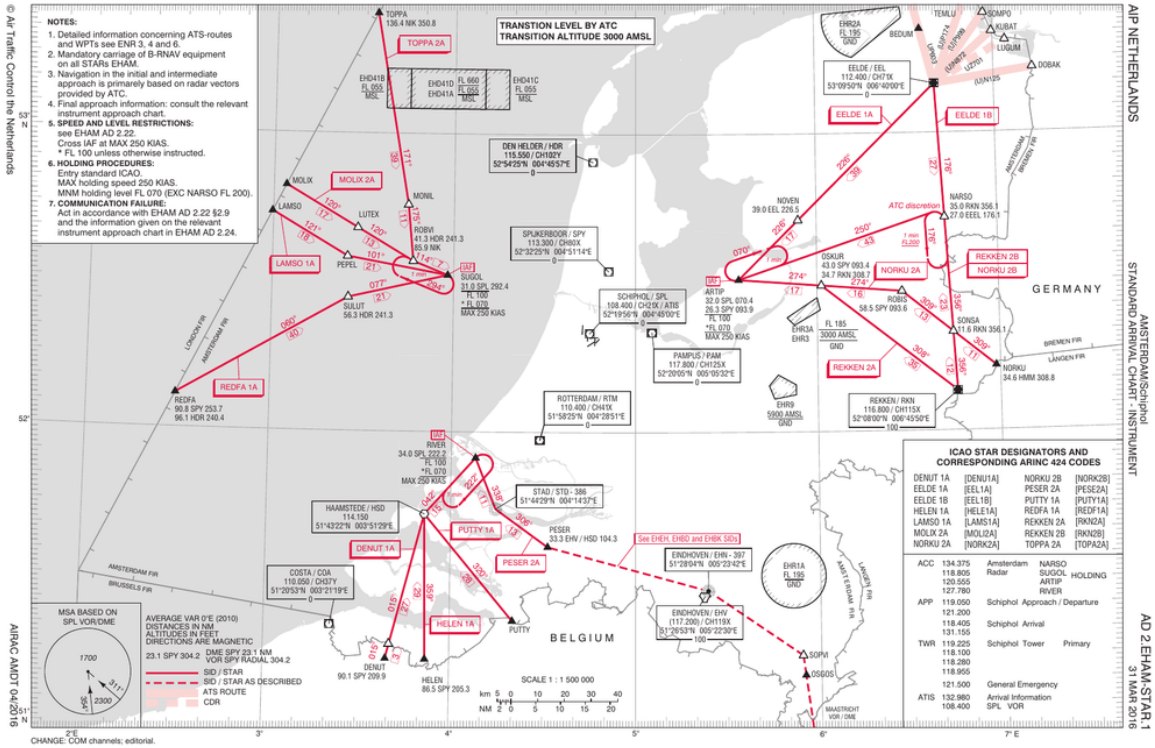

Figure 4.1: Standard Approach Route chart (source: Air Traffic Control the Netherlands)

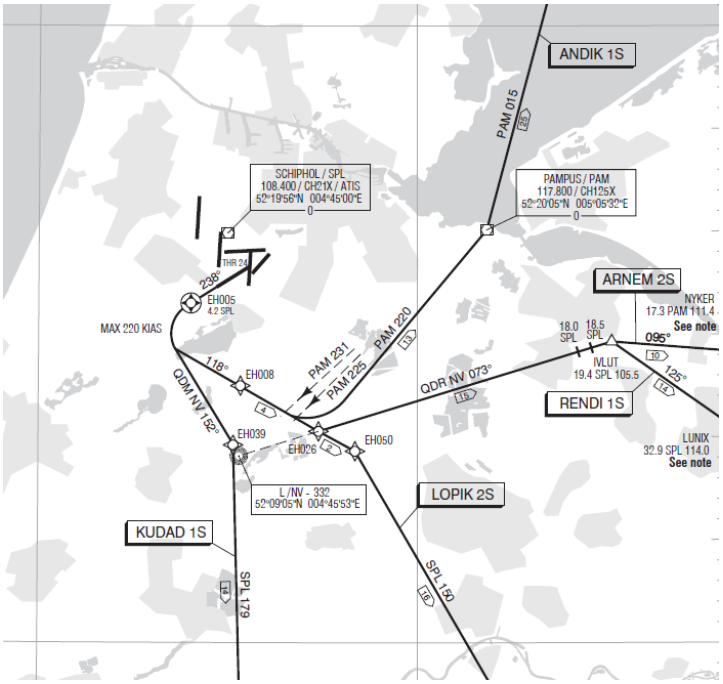

Figure 4.2: Part of a Standard Instrument Departure chart for departures from runway 24 (source: Air Traffic Control the Netherlands)

4.2. Runway Operations

Amsterdam Airport Schiphol operates using six runways, consisting of five long runways and one short runway. All runways are used both for take-offs and landings, and most of them can be used in both directions. The total of six runways resulted in the use of over a hundred different runway configurations in 2018. The locations of the runways relative to each other are depicted in Figure 4.1. [4]

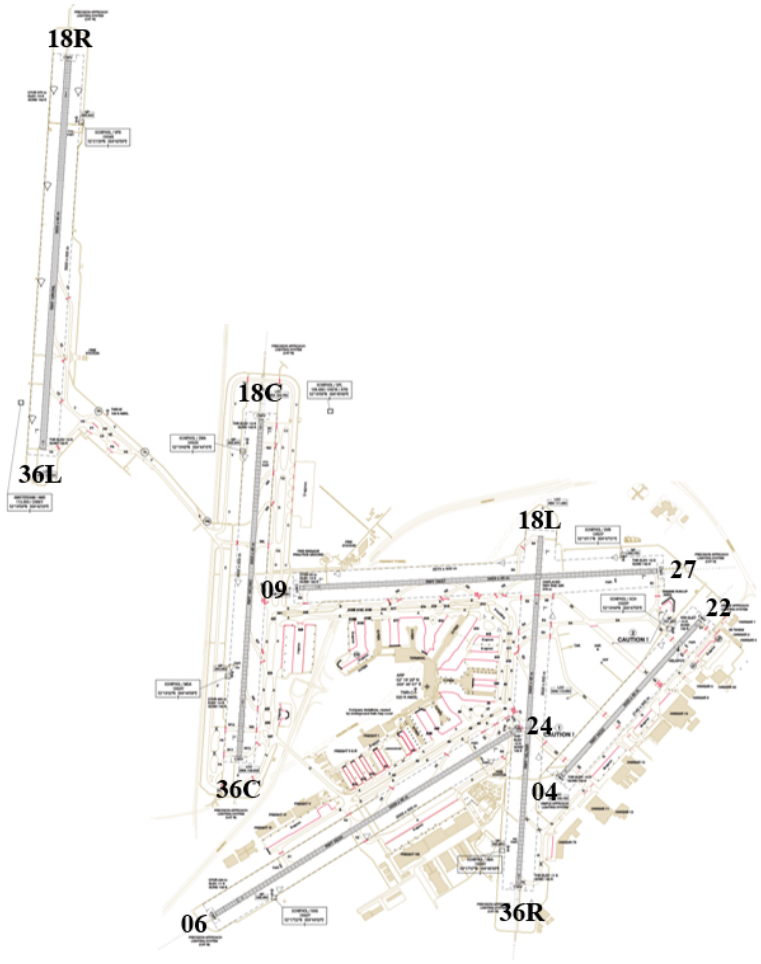

Figure 4.3: Runway layout of Amsterdam Airport Schiphol (Source: Air Traffic Control the Netherlands)

Table 4.2: Runway characteristics at Amsterdam Airport Schiphol

Runway name	Designator	Length [m]	Remarks
Aalsmeerbaan	18L/36R	3400	Take-offs 36R and arrivals 18L not allowed
Buitenveldertbaan	09/27	3453	-
Kaagbaan	06/24	3500	-
Oostbaan	04/22	2014	-
Polderbaan	18R/36L	3800	Take-offs 18R and arrivals 36L not allowed
Zwanenburgbaan	18C/36C	3300	-

4.2.1. Runway Selection

The use of the runways is restricted due to noise abatement agreements with the Dutch government. Therefore the use of the runways should follow the "Nieuw Normen- en Handhavingstelsel" (NNHS). The NNHS includes a framework of rules concerning runway use, which aim to create as little as possible nuisance to the communities surrounding Schiphol. The number of active arrival and departure runways is dependent on the time of the day. During the daytime, Schiphol uses three runways simultaneously. This means that ei-

ther two runways are used for departure and one runway for arrival, or vice versa. To accommodate a smooth transition from inbound peak to outbound peak, a fourth runway may be used with some restrictions. Operating a fourth runway is allowed for a maximum of 80 movements and a duration of 20 minutes per day and an annual average of 40 per day. During the night and off-peak periods, one arrival and one departure runway are used.

Table 4.3: Preference runway configurations during daytime (06:00h - 23:00h)

Preference	Arrival 1	Arrival 2	Departure 1	Departure 2
1(*)	06	(36R)	36L	(36C)
2(*)	18R	(18C)	24	(18L)
3(*)	06	(36R)	09	(36L)
4(*)	27	(18R)	24	(18L)
5a(**)	36R	(36C)	36L	(36C)
5b(**)	18R	(18C)	18L	(18C)
6a(***)	36R	(36C)	36L	(09)
6b(***)	18R	(18C)	18L	(24)

(*) When visibility > 5000 m, cloud base > 1000 ft (2000 ft for converging runways) during UDP
(**) When visibility > 5000 m, cloud base > 1000 ft
(***) When visibility > 1500 m, cloud base > 300 ft

The selection of active runways is based on the sequence of preferred runway configurations. During good weather conditions, the APP supervisor and TWR supervisor choose the runway configuration with the highest preference, see Table 4.3. During an inbound- or outbound peak, a change of runway configuration is not necessary when another configuration has a higher preference due to changed weather conditions. However, the APP supervisor and TWR supervisor need to reconsider the active runways, thus the configuration, when (1) rainstorms or wind shear is present in the approach or departure areas, (2) the wind at low altitude (until 2000 ft) deviates from the wind speed at the ground, or (3) when the cross- or tailwind component of the wind speed exceeds the limits. The capacity of the Main Landing Runway (MLR) and secondary landing runway (SLR) is determined based on the crosswind component, see Table 4.4.

Table 4.4: Capacity limits due to cross wind

Cross wind	Capacity
25 kt	No air traffic flow and capacity management
30 kt	50 aircraft per hour (34 at MLR and 16 at SLR)
35 kt	40 aircraft per hour (34 at MLR and 6 at SLR)
> 35 kt kt	34 aircraft per hour (34 at MLR and no SLR)

4.3. Dependent Arrival and Departure Runways

As at many other airports, dependencies exist between the runways available at Schiphol as well. A dependency between runways does not indicate that runways cannot be operated simultaneously. Air Traffic Control the Netherlands has additional procedures for the use of dependent runways at Amsterdam Airport Schiphol. For example, additional limitations for the visibility and cloud base are imposed, and different procedures need to be followed during the night. Table 4.5 summarizes the dependencies that exist between arrival and departure runways due to missed approach conflicts, jet blast hindrance, and intersecting runways at AAS. Table 4.5 also shows the occurrence of the dependency within a runway configuration in percentage. Over 2018 and 2019 in 23.1% of the time a runway configuration was used with dependent arrival and departure runways. [2]

4.3.1. Missed Approach Dependency

During missed approach conflicts, several procedures exist for the Tower Control ATCOs. The ATCO is allowed to give a take-off clearance when he/she has established the arrival at the other (dependent) arrival. Furthermore, the ATCO must give the take-off clearance such that the departing aircraft begins its take-off roll before

the approaching aircraft to the dependent runway is less than 2 NM away from the runway threshold. If the take-off roll has not started early enough, the take-off or landing from one of the aircraft has to be aborted by the ATCO. Also, the ATCO must always monitor the arrivals to recognize a missed approach on time and take proper action. A separation of less than 2 NM between the runway threshold and the arriving aircraft is allowed during UDP when the visibility is higher than 5 km, and the cloud base is higher than 2000 ft under the condition that the ATCO informs the arriving aircraft about the departing aircraft.

4.3.2. Intersecting Runways

When operating intersecting runways, the take-off clearance must be given as such that the departing aircraft has passed the intersection point before the arriving aircraft is less than 1 NM from the runway threshold. The ATCO must time the departures and arrivals at runways that experience jet blast hindrance as such that the departure started before the arriving aircraft is within 1 NM distance away from the runway threshold. The ATCO is only allowed to give a take-off clearance after the arriving aircraft has passed the jet blast intersection point.

Table 4.5: Dependent departure and arrival runway combinations at Amsterdam Airport Schiphol

Departure	Arrival	Dependency	Percentage [%]
04	06	Missed approach	0.0
09	06	Missed approach	5.6
	36R	Missed approach	1.4
18L	06	Missed approach	0.0
	22	Missed approach	0.4
	09	Jet Blast(*) / Intersecting runways (**)	0.0
	27	Jet Blast(*) / Intersecting runways (**)	1.7
18C	22	Missed approach	0.1
	27	Missed approach	0.2
36C	27	Missed approach	0.5
27	36R	Missed approach	0.0
24	18C	Missed approach	13.0
	36R	Jet blast (***)(****)	0.2

(*) When departure enters runway 18L from E5
(**) When departure enters runway 18L from E6
(***) When departure enters runway 36R from S7E
(****) When departure enters runway 36R from S8, S5 or S6 and WTC is equal to M or H

4.4. Runway Capacity Utilization

As at many U.S. and European airports, the arrival and departure demand often exceeds the available capacity at Amsterdam Airport Schiphol during periods of the day. Therefore, the flow of arriving and departing aircraft is controlled to ensure safe operations by an Arrival and Departure Manager. Air Traffic Control the Netherlands uses an AMAN and DMAN to meter the number of aircraft movements in the Schiphol TMA. This section will explain the fundamental principles of the AMAN and DMAN that are currently used at AAS.

4.4.1. Departure Management

Amsterdam Airport Schiphol uses a DMAN called Pre-Departure Sequencer (PDS) to calculate at what time and from which runway each aircraft is allowed to depart. Currently, a custom made sequencing component called CPDSP is used. In the future, this component is updated by a new sequencer called CPDS. In this section, the working principles of the new CPDS will be given.

System Initialization and Triggers

The PDS needs to be initialized with the available departure runways and its properties. The runway configuration is filed by an APP- or ACC supervisor in consultation with other parties. The period for which a specific runway configuration is selected is subdivided into multiple periods. For each period, the declared

capacity and TMA Exit Points that are assigned to each runway need to be specified. The PDS only includes an aircraft in its sequence if the aircraft is an IFR-flight, the flight plan is available in its system, the aircraft is planned to depart from the main runway, TOBT plus EXOT is not more than 10 hours away, and the aircraft is not suspended. Aircraft that are suspended are obliged to change their flight plan before it is allowed to depart. The PDS is triggered to update the planning when a TOBT update of an aircraft with the TOBT earlier than the previous TOBT or later than the current TSAT, a CTOT update is given by NMOC, a change in runway configuration of capacity is issued, or the de-icing information is updated.

Runway Allocation
PDS assigns runways to departing aircraft using the runway configuration that is planned for the TTOT time of the aircraft. When only one departure runway is planned, the aircraft is assigned to that runway. If there are two departure runways, the PDS uses the TMA Exit Point of the aircraft and selects the runway to which this TMA Exit Point is allocated to. Aircraft that do not have a TMA Exit Point, as a domestic flight, the default runway is chosen as the departure runway. When the TTOT changes as such that there is a different departure runway at that time, PDS automatically changes the departure runway as long as no airway clearance is given. When an airway clearance is already given, the PDS will give the Outbound Planner (OPL) a conflict notification. Thereafter, the OPL either chooses to cancel the clearance or adjust the runway configuration such that the aircraft can depart from its initially planned runway.

Variable Taxi Times
The PDS uses variable taxi times to estimate the time that is needed for an aircraft to taxi from the gate to the runway (EXOT). The DMAN uses Variable Taxi Time tables (VTT tables) to determine the taxi-out time. The tables include parameters like the gate, runway, aircraft type, time of the day, time of the year, weather conditions, and the availability of taxiways to estimate the taxi time. The taxi times include the average times for waiting clearances (push-back, taxi, runway) and for the aircraft waiting time in the queues near the runway. During situations for which the VTT tables do not account for, the Outbound Planner (OPL) is allowed to adjust all EXOTs by entering a multiplication factor, for example, 10%, when the taxiways are incredibly crowded. The OPL can also modify the EXOT of an individual flight when needed.

TTOT and TSAT Determination
PDS used time blocks of 10 minutes with a predefined number of aircraft that may depart in each time block. For regulated aircraft, TTOT is equal to CTOT. For non-regulated aircraft, TTOT is equal to TTOT-target by default as long as the capacity of the time block is not exceeded. This implies that PDS accepts aircraft having the same TTOT. In practice, two aircraft cannot depart from the same runway at the same time. However, Air Traffic Control the Netherlands thought it was not desirable to let PDS calculate the exact departure sequence of aircraft within a time block since aircraft often request a departure clearance minutes earlier or later. The exact departure time of an aircraft is determined by the OPL themselves.

When an aircraft has its CTOT, or TTOT-target planned within a time block which has not enough capacity left, this aircraft or anther aircraft within the time block will be moved to the next time block where enough capacity is left. Priority rules determine which flight will be moved to the next time block. The aircraft that is moved to another time block will get a new TTOT equal to the start time of the time block. This means that when there is a high demand, and many aircraft need to be moved to other time blocks, those aircraft will receive the same TTOT. Since the taxi-out times are different, the aircraft will still get different TSATs. Therefore, the aircraft will not call for a push-back clearance at the same time. Once TTOT is determined by PDS, TSAT is equal to TTOT minus the estimated taxi-out time when no de-icing is required, see Equation 4.1.

$$TSAT = TTOT - EXOT \tag{4.1}$$

De-icing Operations
At Amsterdam Airport Schiphol aircraft de-icing is possible at either the gate or at a remote platform and is performed by a de-icing company. When a pilot requests de-icing, the de-icing company chooses whether the de-icing will be done at the gate or remote and determines the estimated duration of the operation (EDIT). This data is communicated to Air Traffic Control the Netherlands. Thereafter, PDS calculates the deadline for de-icing to start in order to depart at TTOT (SCZT) and sends it to the de-icing company. The calculation of SCZT for both gate and remote de-icing is respectively presented in Equation 4.2 and 4.3 and Figure 4.4.

$$SCZT_{Gate} = TTOT - EXOT - EDIT \tag{4.2}$$

$$SCZT_{Remote} = TTOT - EXOT2 - EDIT \tag{4.3}$$

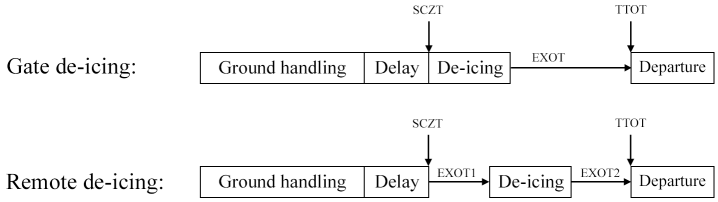

Figure 4.4: SCZT calculation

When the de-icing company receives (SCZT) it schedules the aircraft for de-icing (ECZT). If ECZT is later than SCZT the ECZT is communicated with Air Traffic Control the Netherlands. Otherwise, ECZT is not communicated, and the planning is completed. In the case of de-icing at the gate, de-icing cannot start until ground handling has finished. Furthermore, depending on the weather, the time between the end of de-icing and start-up (TSAT) cannot be too long, to prevent new ice being formed. If Air Traffic Control the Netherlands receives an ECZT, PDS needs to recalculate TTOT (based on ECZT), the sequence and re-determines the SCZT (see Figure 4.5 and Equation 4.5 and 4.5). The updated SCZT is sent back to the de-icing company. This time it is likely that the SCZT is accepted by the de-icing company and the planning is completed.

$$TTOT_{Gate} = ECST + EDIT + EXOT \tag{4.4}$$

$$TTOT_{Remote} = ECST + EDIT + EXOT2 \tag{4.5}$$

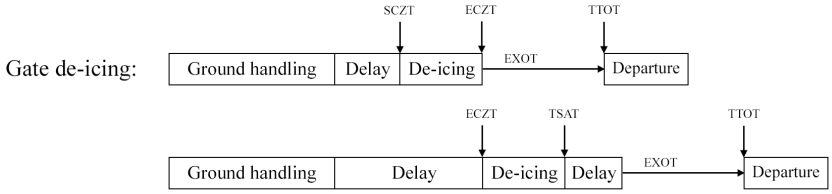

Figure 4.5: When Air Traffic Control the Netherlands receives ECZT later than SCZT, it adjusts TTOT and TSAT

4.4.2. Arrival Management

From 1998 onwards Amsterdam Airport Schiphol uses an AMAN system called the Inbound Planner (IBP) to manage the incoming aircraft. IBP was one of the elements of the Amsterdam Advanced ATC system (AAA). Compared to other AMAN systems in Europe, its TP module was less advanced. IBP was outdated and in need of an upgrade [28]. However, improving IBP would affect the whole AAA system. Therefore, the decision was made in 2011 to develop an independent AMAN, called the Advanced Schiphol Arrival Manager (ASAP). ASAP has similar functionalities as IBP, and for most ATCOs, no shift in responsibilities was made.

Working principles

ASAP uses horizons that are defined as categories of aircraft depending on their location. The three categories are pre-planned flights, planned flights, and under control of APP flights. Pre-planned flights are the aircraft that are available at radar but are not yet under the control of the Amsterdam FIR. Its STA and EAT are calculated by the TP module but are not yet fixed due to too large uncertainty in the calculation of them. About 14 minutes before ETO, the STA and EAT of the aircraft are fixed, and ACC is allowed to begin delaying and advancing aircraft to meet their EAT. ACC must deliver the aircraft within a margin of ± 2 minutes relative to their EAT at the IAF. When the aircraft enters the TMA control is taken over by APP, and ASAP is not actively used anymore. However, the flights are still visible at the CWP HMI of ACC and APP. APP is responsible for the adequate spacing of the aircraft in its final approach. Generally, ASAP automatically allocates an aircraft to an active runway based on the IAF. Nonetheless, ATCOs can adjust the allocated runway in ASAP when a

situation calls for it. ASAP can show how the aircraft would fit in the arrival stream on the other runway.

Once an aircraft is within the pre-planned horizon, the TP module of ASAP calculates ETA. Knowing the ETA, the STA can be determined using Equation 4.6 4.7 and 4.10. When the amount of traffic is low, the STA is equal to the ETA. If not, the STA is equal to the Last Assigned Slot (LAS) plus the Dynamic Landing Interval (DLIV). DLIV is based on the declared arrival capacity of the runways or the WTC distance-based separation minima on approach. The declared arrival capacity is inserted per runway and is defined in spatial distance. The separation minima that is the most constraining is used for calculating DLIV between two aircraft. The approach planner, usually the APP supervisor, is responsible for interacting with ASAP. The sequencer and scheduling algorithm uses the First Come First Serve (FCFS) principle.

The sequence of aircraft created by ASAP is communicated to ACC. ACC receives the information from ASAP as a stack list on their radar screen, showing an overview of which aircraft needs to be delayed how much (the difference between EAT and ETO). At the moment, ACC is not aiming to minimize the difference between EAT and ETO. This is due to the inaccuracy of the current TP module. As the Active Advisory Horizon (AAH) is located 14 minutes from the IAF, space and time to absorb delays are limited. ACC has three options to absorb delay (1) speed reduction, (2) vectoring, or (3) stacking. When delays build up and become too large, speed reduction and vectoring will not be an option anymore. ACC will need to stack aircraft in holding patterns, which is highly unfavourable.

$$STA_1 = ETA \tag{4.6}$$

$$STA_2 = LAS + DLIV \tag{4.7}$$

$$STA = max(STA_1, STA_2) \tag{4.8}$$

$$DLIV = S/CAS_{final} \tag{4.9}$$

$$S = max(S_{wtc}, S_{declared}) \tag{4.10}$$

Trajectory Prediction Module
ASAP uses a TP module called Speed And Route Advisor (SARA) to calculate the ETA and ETO. SARA uses the horizontal path, the vertical path, and speed profile to determine the 4D trajectory from its current location to the runway threshold. Using flight plan data, which includes all active waypoints, the horizontal path of the aircraft to reach the IAF is relatively easy to determine. Determining the time the aircraft takes to reach the runway threshold from entering the TMA is more challenging because no fixed trajectories are specified within the TMA. Therefore, SARA uses trajectory data deduced from numerous landings to determine the most likely trajectory for a particular IAF and runway combination. To determine the vertical path and speed profile, the trajectory of the aircraft is segmented in phases from cruise until touchdown. Within each segment, certain parameters like indicated airspeed, Mach number, flight path angle, rate of descent are assumed to be constant and determined using historical data. With the calculated ETAs and ETOs by SARA other ASAP modules can derive the EATs and STAs.

4.5. Traffic Analysis

Each arriving and departing aircraft reaches the airport through respectively one of the IAFs or sectors. The arriving and departing traffic at AAS is not equally distributed over the IAFs and sectors. This means that one sector may be overloaded while at the same time, another is not. Table 4.6 and 4.7 show the percentage of arriving traffic over each initial approach fix and the percentage of departure traffic through each sector in 2018. The unequal distribution of departure traffic over the different sectors has the consequence that the distribution of departure traffic over each SID is not equal as well. Table 4.8 shows the distribution of departing traffic from runway 24 to each of the SIDs.

The distribution of aircraft WTCs influences the capacity of runways since larger separation is required for specific pairs of aircraft WTCs. Also, the approach and departure speed of aircraft influences the IAT and IDT times when there is a speed difference between two aircraft at a common approach or departure path. The total WTC distribution for arriving and departing aircraft throughout the day at AAS in 2018 is depicted in Table 4.9.

Table 4.6: Arriving traffic distribution at AAS

Initial Approach Fix	Percentage [%]
SUGOL	31
ARTIP	42
RIVER	27

Table 4.7: Departing traffic distribution at AAS

Sector	Percentage [%]
1	16
2	30
3	24
4	15
5	15

Table 4.8: Departing traffic distribution at AAS

SID	Percentage [%]
ANDIK	9.6
ARNEM	10.6
RENDI	16.0
LOPIK	6.0
KUDAD	18.4
VALKO	14.1
BERGI	25.3

Table 4.9: Fleet mix and characteristics at Amsterdam Airport Schiphol in 2018

WTC	Occurrence[%]	ROT arr RWY 18C	ROT dep RWY 24
Light	2.1	59.7	50.4
Medium	80.5	55.7	50.1
Heavy	17.1	71.9	49.4
Super	0.3	78.2	54.6

The fleet mix fluctuates during the day and differs for arriving and departing traffic. Table 4.10, 4.11, 4.12 and 4.13 show that the number of heavies AAS is higher in the morning than in the evening. The combinations of arriving traffic mix and departing traffic mix during the same time interval influences the magnitude of arrival and departure capacity interference. For example, when the percentage of heavies in the arriving traffic high, larger arrival gaps will be created. After that, it is easier to interweave departing aircraft through the arriving aircraft.

Table 4.10: Arriving fleet mix in the morning (7.40h - 9.20h) at AAS

WTC	Occurrence[%]
Light	0.7
Medium	72.1
Heavy	27.2
Super	0.0

Table 4.11: Arriving fleet mix in the evening (17.40h - 20.20h) at AAS

WTC	Occurrence[%]
Light	0.7
Medium	95.9
Heavy	2.7
Super	0.7

Table 4.12: Departing fleet mix in the morning (7.40h - 9.20h) at AAS

WTC	Occurrence[%]
Light	0.1
Medium	64.9
Heavy	35.0
Super	0.0

Table 4.13: Departing fleet mix in the evening (17.40h - 20.20h) at AAS

WTC	Occurrence[%]
Light	0.1
Medium	89.9
Heavy	9.7
Super	0.3

Furthermore, for each aircraft type that landed at AAS in 2018 the average approach ground speed on the descent path from 2000 to 70 ft was calculated using radar data obtained from Air Traffic Control the Netherlands. This should reflect aircraft speed for different types at the common approach path, assuming that it starts at approximately 2000 ft and ends at 70 ft above the runway threshold. Also, the average departure ground speed for each aircraft type between 0 and 3000 ft is calculated using the radar data from 2018. Table 4.14 shows the speeds mentioned above for the five most frequently occurring aircraft types at AAS in 2018.

Table 4.14: Top 5 most frequently occurring aircraft types and their characteristics for AAS in 2018

Aircraft type	Occurrence [%]	Approach speed [knots]	Departure speed [knots]
B738	21.6	156.4	167.5
E190	13.6	152.7	148.8
A320	10.6	149.5	161.1
B737	8.5	152.6	158.8
A319	6.3	146.4	153.8

In Chapter 2 it was described that the IDT, IAT, IDAT, and IADT are also influenced by the time a departing aircraft takes between getting a departure clearance and start its take-off roll and by the time an arriving aircraft passes the runway threshold and the actual arrival is established. The estimates of these times for AAS were made by operational experts of Air Traffic Control the Netherlands and are presented in Table 4.15.

Table 4.15: Estimates of departure communication and arrival completion times by operational experts

WTC category	Communication buffer time [s]	Arrival completion time [s]
Light	5	7
Medium	10-15	14
Heavy	20-30	10
Super	20-30	18

4.6. Arrival and Departure Capacity Interference Assessment

A capacity assessment of arrival and departure runway combinations is performed to give insight into what extend the capacity of Amsterdam Airport Schiphol is currently affected by the use of dependent arrival and departure runways. The data that was needed to perform the assessment was obtained from Air Traffic Control the Netherlands and concerned the total number of air traffic movements at AAS in 2018 and 2019. The results are obtained for the two most occurring arrival and departure runway dependencies that were found in Table 4.5, departure runway 24, and 09.

The departure capacity of runway 09 and 24 is calculated for different combinations of arrival runways for marginal weather conditions and good weather conditions. Since arrival and departure capacity interference will only appear when the runways are operating at maximum capacity, and the data also included off-peak hours, the calculated departure capacities at the moments that there was not enough departure demand to pressurize the runway capacity had to be filtered out.

4.6.1. Results

Departures from runway 09 have a missed approach dependency with arrivals at runway 06 and 36R. Figure 4.6a and 4.6b shows that departures at runway 09 were not operated in combination with arrivals at 36R frequently enough to generate enough data samples. Furthermore, Figure 4.6a shows that the departure capacity at runway 09 is almost the same in combination with dependent and non-dependent arrival runways. During marginal visibility, the dependency between departures at runway 09 and arrivals at runway 06 is slightly visible as the departure capacity of runway 09 in combination with arrivals at 06 is lower than non-dependent combinations.

Departures from runway 24 have a missed approach dependency with arrival runway 18C and jet blast hindrance with arrivals on runway 36R. Figure 4.7a shows that the departure capacity of runway 24 is lower for dependent arrival runways than for non-dependent arrival runways during good visibility. However, this observation is drawn from a relatively small sample size. For marginal visibility, the sample size of the departure

capacity of runway 24 in combination with arrivals on runway 36R is too small, see Figure 4.7b. The departure capacity of runway 24 in combination with arrivals on runway 18C is respectively 4.3 and 2.5 atm/hour lower than in combination with non-dependent arrival runways 27 and 18R.

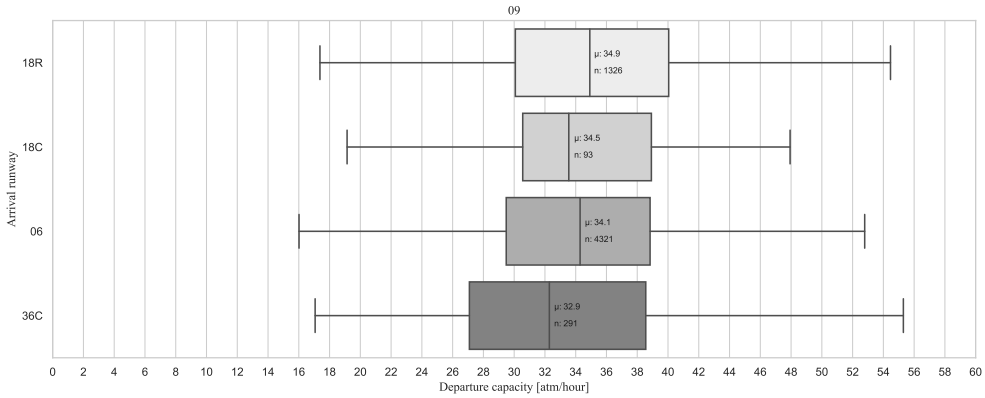

(a)

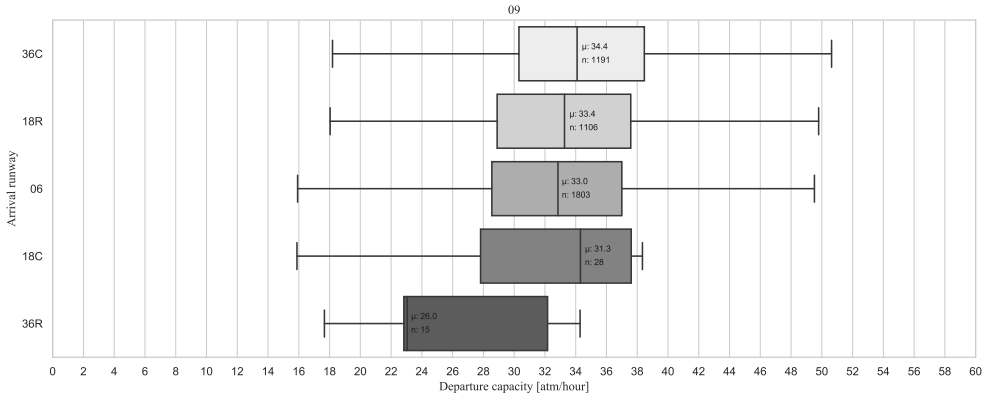

(b)

Figure 4.6: Departure capacity of 09 in combination with different arrival runways for (a) good, and (b) marginal weather conditions

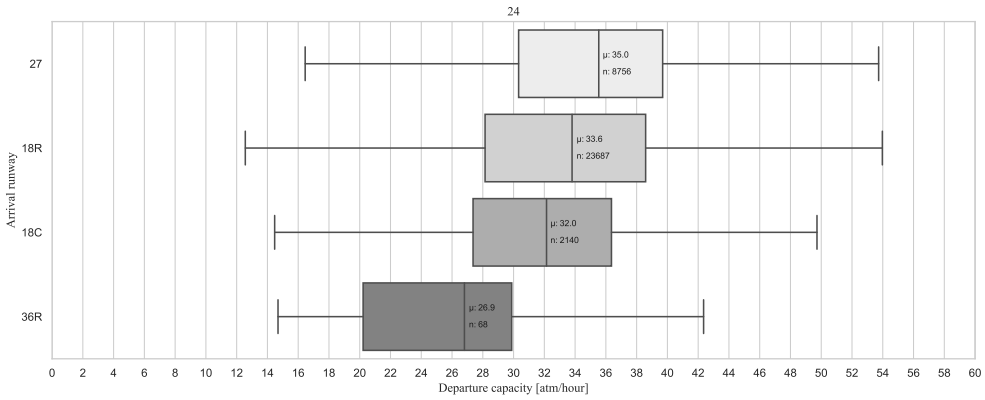

(a)

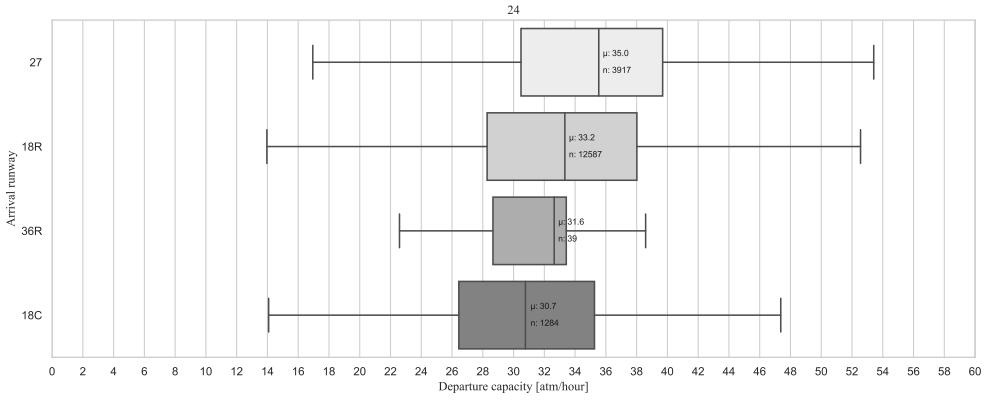

(b)

Figure 4.7: Departure capacity of 24 in combination with different arrival runways for (a) good, and (b) marginal weather conditions

- End preliminary study -

The preliminary study was already graded for AE4020

II

Arrival and Departure Management Simulator

5

Uncoordinated Arrival and Departure Management Simulator

The uncoordinated Arrival and Departure Management (ADMAN) simulator will serve as a baseline model to evaluate. The performance of any future coordinated ADMAN(s). This model should represent the current management of arrivals and departures. This chapter will elaborate on the conceptual design, the working principles and algorithms active in the uncoordinated ADMAN. First, it explains the overview of the model, including its elements, after which it explains each element separately.

5.1. Model Overview

Figure 5.1 shows the different modules that are present in the uncoordinated ADMAN. The flight data of arriving and departing aircraft will serve as the input of the arrival manager (AMAN) and departure manager (DMAN) modules. The AMAN sequences and schedules all arriving aircraft at the runway threshold and the DMAN sequences and schedules all departing aircraft at the runways. In the uncoordinated ADMAN the AMAN and DMAN schedule inbound and outbound independently from one another. The ATC module uses the scheduled arrival and departure times as input. The ATC module ensures that arriving and departing aircraft land and take-off at their assigned times. For this, the ATC module changes the states of aircraft by adjusting the flight plan.

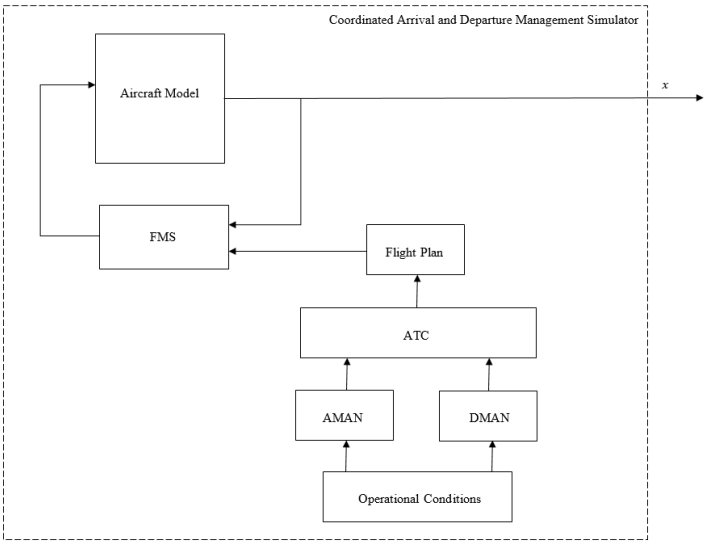

Figure 5.1: Framework for the uncoordinated model

5.2. Arrival Manager

The Arrival Manager is based on the knowledge from Chapter 2, and 4 on general Arrival Management and the Arrival Management implemented at Amsterdam Airport Schiphol. The main goal of the Arrival Manager (AMAN) implemented in this study is to mimic the effect of an Arrival Manager on the number of arriving aircraft in the TMA and their respective spacing rather than the exact functioning of an Arrival Manager.

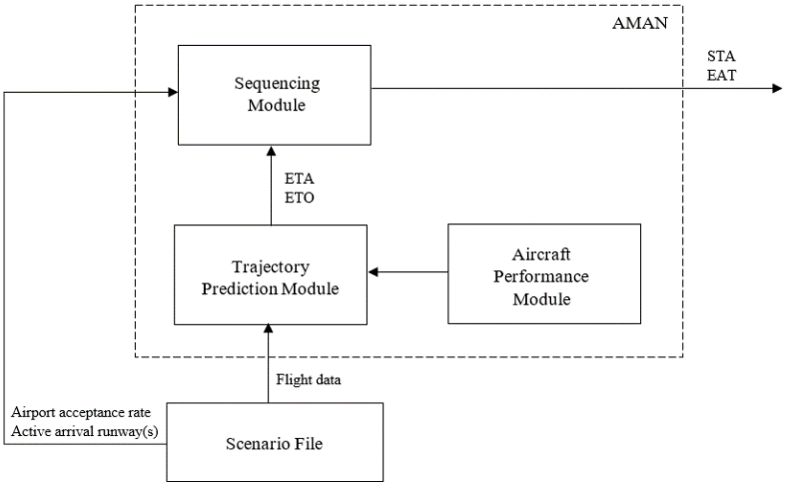

Figure 5.2: Framework of the AMAN module

Chapter 2 introduced the different modules which an Arrival Manager uses: (1) the Trajectory Predictor (TP) module, and (2) the Sequencing module. Figure 5.2 shows the location of these modules relative to one another. The TP calculates the Estimated Time Over (ETO) at the Initial Approach Fix and the Estimated Time of Arrival at the runway threshold (ETA) for each arriving aircraft that crosses its horizon. With the expected arrival times of all approaching aircraft, the sequencing module establishes a sequence and calculates for each aircraft their Scheduled Time of Arrival (STA) and delay. The sequencing module uses the same principles as the arrival manager at LVNL, the First Come First Served (FCFS) principle, and it uses Dynamic Landing Intervals (DLIVs).

5.2.1. Trajectory Predictor

The Trajectory Predictor (TP) predicts the Estimated Time of Arrival (ETA) of aircraft at the runway threshold and the Estimated Time Over (ETO) of aircraft at the Initial Approach Fix (IAF). These predictions are used by the sequencer to set up sequences of arriving aircraft and determine delays. Therefore, the accuracy of the predictions is of crucial importance in the functionality of an AMAN. This section presents the theory behind calculating the ETA and ETO.

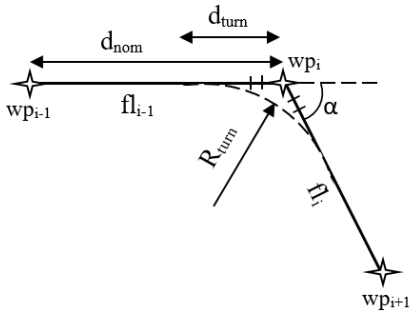

Figure 5.3: Track distance of an aircraft when turning

Track Distance
The nominal track distance (d_{nom}) of a flight leg between two waypoints (wp_i and wp_{i+1}) in the horizontal trajectory of an aircraft is calculated using the flat earth approximation. In the flat earth approximation the distance between two location is calculated using geographical coordinates defined in terms of latitude (lat) and longitude (lon), see Equations 5.1 - 5.3. Figure 5.3 supports the variables presented in these equations. The calculation does not provide the exact distance due to some abstractions. However, as waypoints are usually not spaced too far away from one another, this error is negligible.

$$\Delta y = 60 \cdot (lat_{wp_{i+1}} - lat_{wp_i}) \tag{5.1}$$

$$\Delta x = 60 \cdot (lon_{wp_{i+1}} - lon_{wp_i}) \cdot cos((lat_{wp_{i+1}} + lat_{wp_i}) \cdot 0.5) \tag{5.2}$$

$$d_{nom} = \sqrt{\Delta y^2 + \Delta x^2} \tag{5.3}$$

Aircraft do not manoeuvre directly from waypoint to waypoint but manoeuvre in flyby modus. Flyby modus anticipates for tangential interception of the next flight leg of a route by making a turn. The actual track distance (d_{act}) is, therefore, shorter than the nominal track distance. To find the actual track distance Equations 5.4 - 5.7 are used. First the turn radius (R_{turn_i}) of an aircraft is calculated using its current TAS and bank angle (ϕ), see Equation 5.4. After that, the distance (d_{turn_i}) from which the turn is initiated and ends relative to wp_i can be determined knowing the heading difference (α) between the two flight legs, see Equation 5.6. The length of the turn arc (d_{arc_i}) equals the heading difference multiplied by the turn radius. Finally, the actual track distance can be determined using Equation 5.7.

$$R_{turn_i} = \frac{TAS_i^2}{g_0 \cdot tan(\phi)} \tag{5.4}$$

$$d_{turn_i} = R_{turn_i} \cdot tan(0.5 \cdot \alpha) \tag{5.5}$$

$$d_{arc_i} = \alpha \cdot R_{turn_i} \tag{5.6}$$

$$d_{act} = d_{nom} - d_{turn_i} + 0.5 \cdot d_{arc_i} \tag{5.7}$$

Estimated Flying Time
The calculation of the Estimated Flying Time (EFT) over each flight leg can start once the actual track distances between the waypoints are known. In this calculation, two situations are distinguished. In the first situation the assigned speed of the aircraft at wp_i is equal to the assigned speed at wp_{i+1}, meaning no acceleration or deceleration will occur at fl_i. In the second situation the aircraft accelerates or decelerates due to a difference in the assigned speeds at wp_i and wp_{i+1}. Considering that TAS is equal to the Ground Speed (GS) and an aircraft is not accelerating or decelerating, Equation 5.8 shows the calculation of the EFT (EFT_i) over fl_i.

$$EFT_i = \frac{d_{act}}{TAS_{i+1}} \tag{5.8}$$

If an aircraft is accelerating because the assigned speed at wp_{i+1} is higher than the speed at wp_i, Equation 5.8 no longer applies. Since the aircraft does not fly the whole flight leg at TAS_{i+1}, the EFT is lower than Equation 5.8 would give. The same holds for flight legs where aircraft decelerate, instead here the EFT would be higher than Equation 5.8 would give. Equations 5.9 - 5.12 describe how to calculate the EFT for flight legs where aircraft accelerate or decelerate. First the time an aircraft needs to accelerate or decelerate from TAS_i to TAS_{i+1} ($EFT_{acc,dec}$) is calculated, see Equation 5.9. In BlueSky the default acceleration (a_{acc}) and decelerating (a_{dec}) equals respectively 1 kts/s and -1 kts/s for for all flight phases. The travelled distance during accelerating or decelerating ($d_{acc,dec}$) equals to the average speed multiplied by the time that is needed to accelerate or decelerate. Then, the time that is needed for an aircraft to cover the remaining distance equals the actual track distance minus the acceleration or deceleration distance divided by TAS_{i+1} (EFT_{left}), see Equation 5.11. The total EFT is the sum of the acceleration or deceleration time and the time that is needed to cover the remaining distance.

$$EFT_{acc,dec} = \frac{TAS_{i+1} - TAS_i}{a_{acc,dec}} \tag{5.9}$$

$$d_{acc,dec} = \frac{TAS_{i+1} + TAS_i}{2} \cdot EFT_{acc,dec} \tag{5.10}$$

$$EFT_{left} = \frac{d_{act} - s_{acc,dec}}{TAS_{i+1}} \tag{5.11}$$

$$EFT_i = EFT_{acc,dec} + EFT_{left} \tag{5.12}$$

Estimated Time Over and Estimated Time of Arrival
By summing all EFT per flight leg i, the ETA of aircraft j can be calculated and by summing all EFT up to the waypoint that equals the IAF will result in the ETO of aircraft j. The ETA and ETO are relative to the creation time of an aircraft; therefore, the simulation time needs to be added to the ETA and ETO, see Equation 5.19 and 5.20.

$$ETA_j = t_{sim} + \sum_{i=0}^{N} EFT_i \tag{5.13}$$

$$ETO_j = t_{sim} + \sum_{i=0}^{N=iaf} EFT_i \tag{5.14}$$

5.2.2. Sequencer

The sequencer module establishes a sequence of arriving aircraft based on relative times using prescribed sequencing criteria. In this implementation, the sequencing strategy uses the principles of ASAP. ASAP uses the First Come First Served (FCFS) principle and Dynamic Landing Intervals.

$$DLIV_i = \frac{max(s_{wtc},\ s_{dec})}{TAS_{i,final} + wind_{final}} \tag{5.15}$$

$$STA_i = max(ETA_i, LAS + DLIV_i) \tag{5.16}$$

$$Delay_i = STA_i - ETA_i \tag{5.17}$$

$$EAT_i = ETO_i + Delay_i \tag{5.18}$$

An aircraft i is allowed to be scheduled when its ETO relative to the current time is smaller or equal to the Eligibility Horizon. Knowing the ETA of an aircraft, the STA can be determined using Equations 5.21 - 5.18. When the amount of traffic is low, the STA is equal to the ETA. If not, the STA is equal to the Last Assigned Slot (LAS) plus the Dynamic Landing Interval (DLIV). The DLIV depend on either the declared arrival capacity (s_{dec}) of the runway or the WTC distance-based separation minima on final approach (s_{wtc}). The declared arrival capacity is inserted per runway and is defined by the spatial distance. The sequencer in ASAP corrects the TAS for the wind component at final. However, this implementation neglects the weather conditions, and therefore, the wind speed at final is non-existing. The DLIV between two aircraft uses the separation minima that is the most constraining. When the STA is determined, the delay that needs to be absorbed by an aircraft equals the difference between STA and ETA. A positive delay means an aircraft needs to absorb time while a negative delay means an aircraft needs to be advanced to meet its assigned STA.

5.3. Departure Manager

Chapter 2 and 4 presented the complexity of general Departure Management and the Departure Management implemented at Amsterdam Airport Schiphol. The goal of the Departure Manager in this implementation is to mimic the effect of a Departure Manager on the number of departing aircraft at the runway threshold aiming to take-off. Therefore, the implemented DMAN includes several simplifications. In this implementation, the Departure Manager (DMAN) assigns each departing aircraft a Target Take-Off Time (TTOT) by only taking the minimum required IDT between two consecutive aircraft and the Declared Airport Departure Capacity (DADC) into account.

$$ADR = \frac{3600}{DADC} \tag{5.19}$$

$$TTOT_j = max(LAS + ADR,\ LAS + IDT_{j-1,j}) \tag{5.20}$$

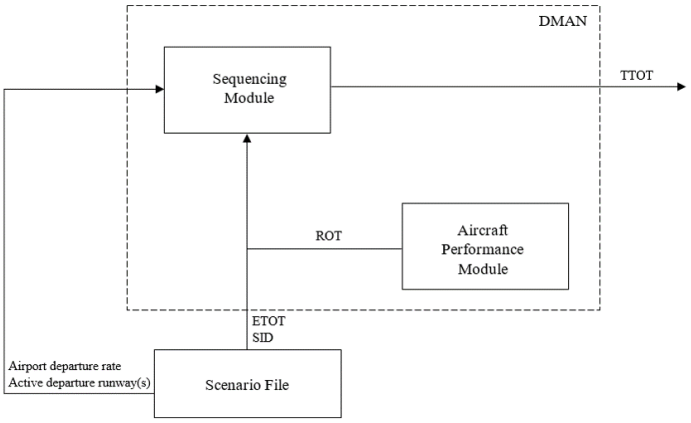

Figure 5.4: Framework of the DMAN module

Figure 5.4 shows the different elements present in the DMAN. The Declared Airport Departure Capacity (DADC) equals the total number of departing aircraft allowed to take off in one hour. Subsequently, the Airport Departure Rate (ADR) can be calculated, see Equation 5.19. The ADR represents the minimum IDT between two aircraft due to the metering constraint of the DMAN. The TTOT of departing aircraft j equals the Last Assigned Slot (LAS) plus the most constraining time between ADT and the minimum required IDT between departing aircraft j and $j-1$, see Equation 5.20.

5.4. Air Traffic Control

The Air Traffic Control (ATC) module mimics the role of ATC by making sure that arriving aircraft are at the IAF and runway threshold around their assigned STA and EAT and departing aircraft take-off around their TTOT. Figure 5.5 shows which elements are included in the Air Traffic Control module to perform this task. For arriving aircraft, the Speed Advisory module performs this role.

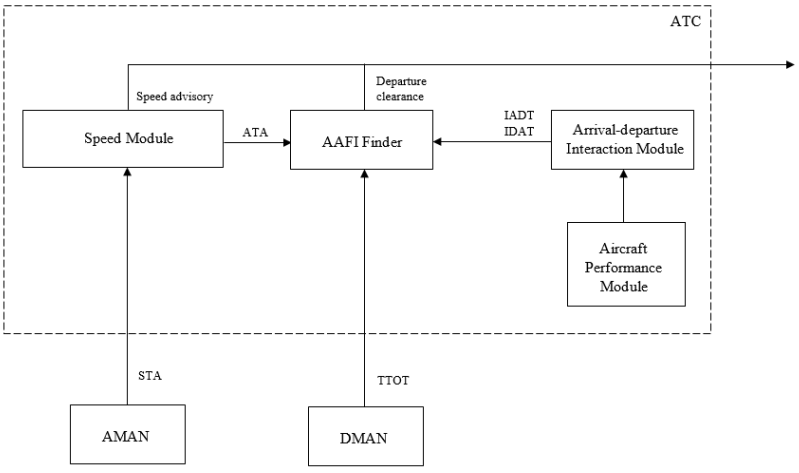

Figure 5.5: Framework of the ATC module

Since the arrival runway which the AMAN uses and departure runway which the DMAN uses may be dependent; the departing aircraft cannot just start its take-off roll at its TTOT. In real-life, TWR has to confirm that there is sufficient time between the departure and a possible arrival before giving a departure clearance. It might be the case that right at the TTOT of the departing aircraft an arriving aircraft is already in its final approach as scheduled by the AMAN, hindering the departure clearance. As arriving aircraft in their final descent cannot be delayed anymore, aircraft arrivals are assumed to take priority over aircraft departures in the uncoordinated model, meaning that the departing aircraft has to wait until TWR finds an arrival interval

that is wide enough to serve the required IADT and IDAT. In the uncoordinated ADMAN, this role of TWR is replaced by an algorithm that searches for arrival intervals large enough to fit the planned departure by DMAN, which is named the Actual Arrival Free Interval Finder (AAFI Finder).

5.4.1. Speed Advisor

Once the TP and sequencer have determined the delay that needs to be absorbed by an aircraft, a speed advisory module performs the role of ATC to provide commands to let the aircraft absorb its delay. In real life, ACC is responsible for providing the appropriate commands such that an aircraft arrives at the IAF around its EAT. ACC can choose to follow the advice of the speed, and route advisory module or they can discard the advice and follow their plan. Generally, three types of delay adsorption can be distinguished: (1) speed reduction, (2) vectoring, and (3) holding. The goal of the uncoordinated ADMAN is to simulate the effect of an AMAN on the number of aircraft in the TMA rather than simulating the exact functioning of an AMAN. Therefore, the ATC module solely gives speed commands to arriving aircraft by assigning each aircraft a Required Time of Arrival (RTA).

$$ATA_j = STA_j + rand(-SD, SD) \tag{5.21}$$

In reality, the work of an AMAN stops when the arriving aircraft enters the TMA. ATC tactically performs the actual sequence of arriving aircraft and their respective IAT. Therefore it is likely that arriving aircraft do not arrive at their assigned STA. Since modelling the decision-making process of ATC is complicated and time-consuming; in this implementation, the actual arrival sequence is the same as the arrival sequence planned by the AMAN. However, because the TP will have a small error when calculating the ETAs, the Actual Time of Arrival (ATA) is not equal to the Scheduled Time of Arrival (STA). The RTA will be set at the calculated ATA once an aircraft has passed the Freeze Horizon.

5.4.2. Arrival- Departure Interaction Module

The Arrival- Departure Interaction module the required Inter-Arrival-Departure Time (IADT) between an arriving aircraft $i-1$ and departing aircraft j and the required Inter-Departure-Arrival Time (IDAT) between departing aircraft j and arriving aircraft i. These times are used by the Actual Arrival Free Interval Finder to determine whether a departure fits between two arrivals. The Inter-Arrival-Departure Time (IADT) and the Inter-Departure-Arrival Time (IDAT) were already mathematically expressed in Chapter 2.

5.4.3. Actual Arrival Free Interval Finder

The layout of intersecting, converging and diverging runways hinders departing aircraft from being cleared for take-off independently from arriving aircraft. In the uncoordinated ADMAN, the AMAN schedules incoming aircraft without taking into account the departure ground situation. Aircraft arrive at the runway threshold as such that two successive arrivals create Actual Arrival Intervals (AAIs). In the uncoordinated ADMAN, departing aircraft are interweaved in the arrival sequence when an AAI offers enough time to account for the required separation between the arriving and departing aircraft and between departing aircraft themselves.

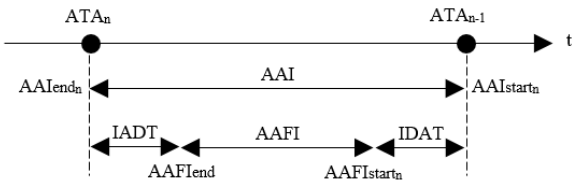

Figure 5.6: Definitions that are used in the Actual Arrival Free Interval Finder

The AMAN schedules arriving aircraf $i-1$ and i at the arrival runway at times STA_{i-1} and STA_i which results in ATA_{i-1} and ATA_i. Each pair of arriving aircraft creates an Actual Arrival Interval (AAI), see Equation 5.22 and 5.23. During the simulation, the size of an AAI shrinks once the time of the simulation (t_{sim}) has passed AAI_{start_i}.

$$AAI_{start_i} = ATA_{i-1} \tag{5.22}$$

$$AAI_{end_i} = ATA_i \tag{5.23}$$

For each departure that is ready to take-off, when t_{sim} is larger or equal to TTOT, all available AAIs will be evaluated until an AAI is large enough for the departing aircraft to take-off. The evaluation starts with the AAI of which AAI_{start_i} is the earliest. To determine whether an AAI is large enough to accommodate a departure, the module calculates the minimum required $IADT_{i-1,j}$ and $IDAT_{i,j}$ between arriving aircraft $i-1$, departing aircraft j, and arriving aircraft i. The IADT and IDAT determine the size of the Actual Arrival Free Interval (AAFI), see Equation 5.24 and 5.25.

$$AAFI_{start_i} = AAI_{start_i} + IADT_{i-1,j} \tag{5.24}$$

$$AAFI_{end_i} = AAI_{end_i} - IDAT_{i,j} \tag{5.25}$$

$$AAFI_{length_i} = AAFI_{end_i} - AAFI_{start_i} \tag{5.26}$$

When the length of the AAFI is smaller than zero, the AAI is not large enough to accommodate the departure, and the AAFI Finder needs to evaluate the next AAI. When the length of the AAFI is larger than zero, the AAI is large enough to accommodate the departure. Figure 5.6 visualizes the latter. The time interval between arrival 1 and 2 is too small to accommodate departing aircraft 2, therefore departing aircraft 2 takes-off in the subsequent AI.

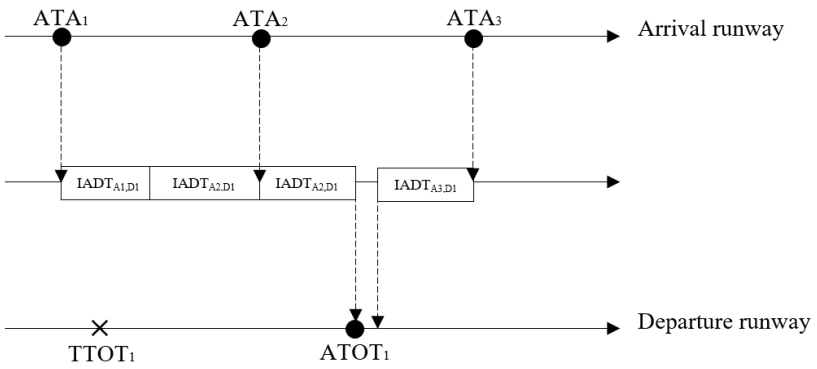

Figure 5.7: Visualization of an example

However, the minimum required IDT with the previously planned take-off still has to be checked. It may be that a departure in AFI $i-1$ blocks a departure in AFI i due to the required IDT. When the previous assigned ATOT ($ATOT_{j-1}$) plus IDT for departure j with the previous cleared departure is not larger than $AAFI_{start_i}$, the Actual Take-Off Time ($ATOT_j$) of departing aircraft j equals $AAFI_{start_i}$, see Figure 5.8.

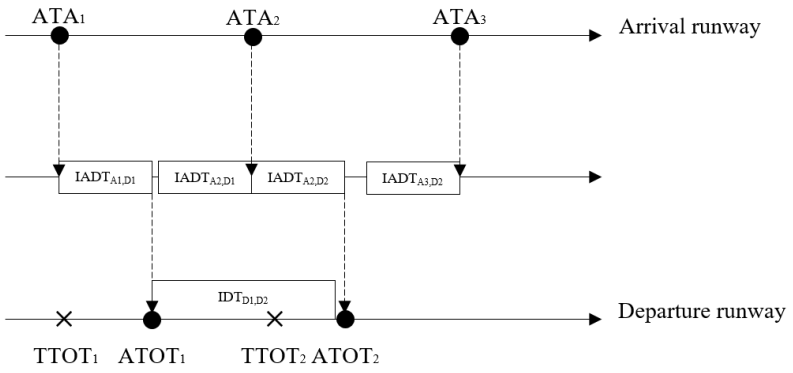

Figure 5.8: Visualization of an example

When the previous assigned ATOT ($ATOT_{j-1}$) plus IDT for departure j with the previous cleared departure is larger than $AAFI_{start_i}$ but smaller than AFI_{end_i}, the Actual Take-Off Time ($ATOT_j$) of departing aircraft j equals $ATOT_{j-1} + IDT_{j,j-1}$, see Figure 5.10.

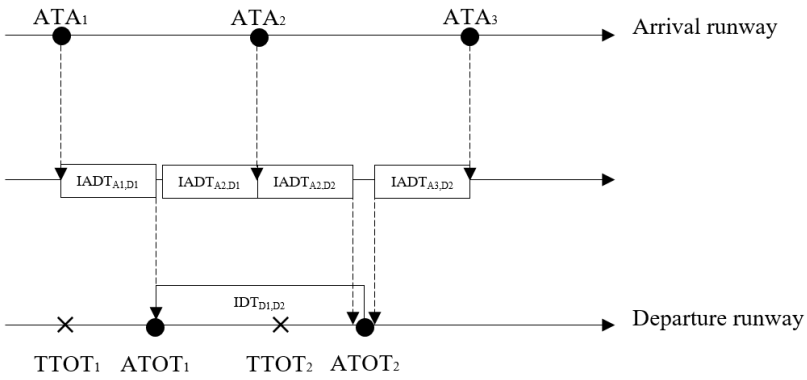

Figure 5.9: Definitions that are used in the Actual Arrival Free Interval Finder

$$ATOT_j = max(AAFI_{start_i}, ATOT_{j-1} + IDT_{j,j-1}) \tag{5.27}$$

If the previous assigned ATOT ($ATOT_{j-1}$) plus IDT for departure j with the previous planned departure is larger than $AAFI_{start_i}$ and $AAFI_{end_i}$, AFI_i is not available for departure j and the next AAI will need to be evaluated.

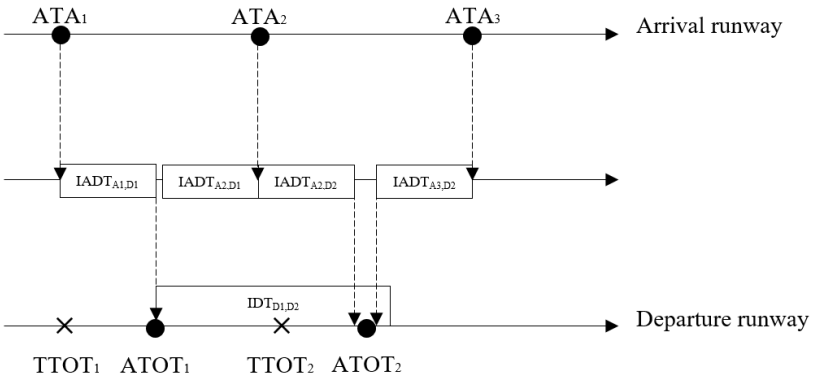

Figure 5.10: Visualization of an example

When a departure is cleared for take-off within AAI i, the starting time of the AAI is adjusted to the ATOT of that specific departing aircraft. Doing this, the AAI may be re-evaluated for the take-off of another departure, and if it is sufficiently another departing aircraft can be planned in the same AAI. When determining if a second to n^{th} is allowed to be cleared departure in the same AAI, the IADT does not play a role anymore. An AAI allows for a second to n^{th} departure when the length of the AAFI is larger than the IDT.

$$AAFI_{start_i} = AAI_{start_i} \tag{5.28}$$

$$AAFI_{end_i} = AAI_{end_i} - IDAT_{i,j} \tag{5.29}$$

$$AAFI_{length_i} = AAFI_{end_i} - AAFI_{start_i} \tag{5.30}$$

Furthermore, it may be the case that the first departure in line for take-off does not fit in the nearest available AFI due to a too large IDT with the previous departure. This causes the AAFI finder to schedule the departure

in another available AFI. The first AFI will remain open for scheduling departing aircraft further down the line. Therefore a departure which was released later for take-off than another departure may receive an earlier ATOT.

6

Coordinated Arrival and Departure Management Simulator

Past research in coordinated arrival and departure management showed that no optimal strategy was found that takes the actual departure demand into account while at the same time creating robust arrival and departure sequences and being easily implementable at the same time. Moreover, no study has yet focused on developing a coordination mechanism between the AMAN and DMAN for airports that use converging or intersecting runways. Instead, they were all aimed at mixed-mode operations. This chapter presents a coordinated Arrival and Departure Management simulator (coordinated ADMAN). The coordinated ADMAN includes three different coordination mechanisms between the AMAN and DMAN that aims to increase the operational efficiency of dependent arrival and departure runway combinations.

6.1. Design Requirements

Since AMANs and DMANs are developed and used at many airports independently from one another, considerable differences exist between them. The complexity of the used algorithms, the system architecture, and the type of advisories differ from system to system. Therefore, the coordination mechanism should be universally applicable and should not require advanced arrival and departure managers to function sufficiently. This also means that the coordination between the AMAN and DMAN should provoke at least as possible adjustments to the core working principles of the AMAN and DMAN. Additionally, the coordination cannot change the existing division of responsibilities between ATCOs.

6.2. Model Overview

Figure 6.2 shows an overview of the coordinated Arrival and Departure Management model (coordinated ADMAN). The difference with the uncoordinated ADMAN is the presence of a coordination module between the arrival manager and departure manager. As in the uncoordinated ADMAN, a scenario file contains arriving and departing aircraft to and from a particular airport. The flight data of these aircraft are used by the arrival and departure manager to schedule them for arrival and departure. The coordination module uses information from the AMAN and DMAN to check whether the number of planned departures matches the arrival stream of aircraft. If this is not the case, the coordination module should take action. In the coordinated model, the AMAN and DMAN do not work independently anymore, the AMAN schedules using the departure ground situation as input.

The AMAN module in the coordinated model uses the same working principles and algorithms as presented for the uncoordinated model. The same holds for the departure manager and the ATC module, in the coordinated ADMAN, the DMAN and ATC module use the same working principles and algorithms as in the uncoordinated ADMAN.

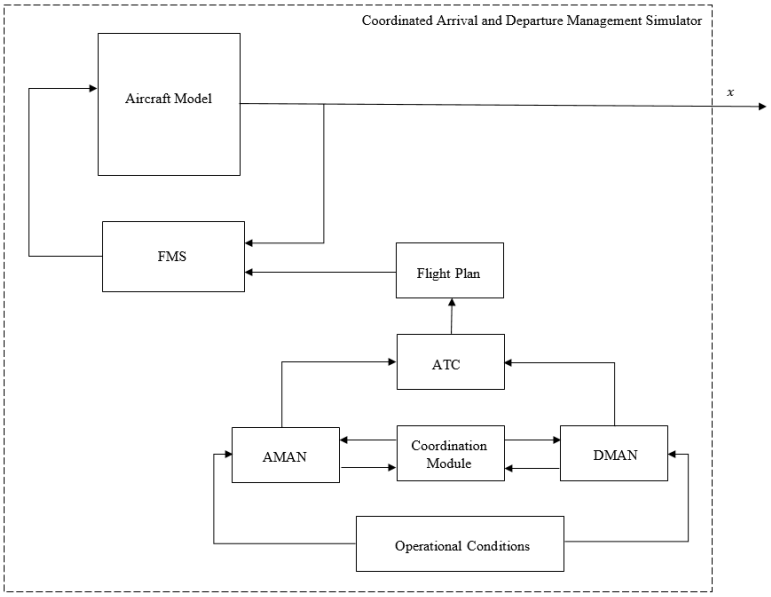

Figure 6.1: Framework for the coordinated ADMAN model

6.3. Coordination Module I: M only

Figure 6.2 shows an overview of the different elements present in the coordination module. The module obtains the arrival planning and departure planning every time the AMAN pushes a schedule update. With the STAs of the AMAN, the conflict detector sets up the Scheduled Arrival Intervals (SAIs). The conflict detector calculates the expected number of departure slots that fit in the arrival stream as was sent by the AMAN considering the specific arrival and departure runway dependency. The module compares the expected number of departure slots to the preferred number of departure slots. The difference between the two represents the number of departure slots that need to be created by the coordination module. The conflict solver creates these departure slots in the arrival schedule by changing the STAs of the arriving aircraft. Subsequently, the AMAN receives the adjusted STAs. The following section explains each element of the coordination module in more detail.

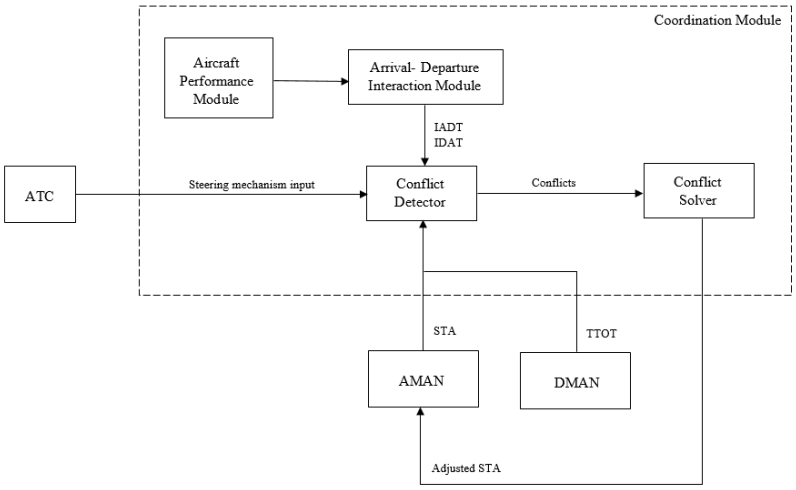

Figure 6.2: Framework of the coordination module

6.3.1. Horizon of Action

Once arriving aircraft have passed the Eligibility Horizon (EH), AMAN takes the aircraft into account for scheduling. However, the assigned STA is still subject to change until the aircraft reaches the Freeze Horizon (FH). As the STAs of arriving aircraft are only allowed to change in this time interval between EH and FH, the coordination module should also work in this time interval. This way, the STAs of arriving aircraft can be assigned as a function of the departure ground situation.

As the horizon of action of the coordination module lies between EH and FH, the planning horizon of the DMAN must be equal or greater than the planning horizon of the AMAN. When taking the AMAN of Amsterdam Airport Schiphol as an example, the EH is 14 minutes away from the IAF, and considering that the time from IAF to runway threshold is approximately 10 minutes, the planning horizon of the DMAN should be at least 24 minutes.

6.3.2. Steering Mechanism

Several options exist to steer the level of coordination between arrival and departure management. The coordinated ADMAN uses preferred departure-to-arrival ratio (α_{pref}) as a steering mechanism between the arrival and departure rate. The preferred departure-to-arrival ratio represents the minimum required departure slots (n_{dep}) that fit should in the arrival stream relative to the number of planned arrivals (n_{ar}) by the AMAN. As α_{pref} and the number of planned arrivals is known, the minimum required departure slots in the planned arrival stream can be calculated, see Equation 6.1.

$$n_{dep} = \alpha_{pref} \cdot n_{ar} \tag{6.1}$$

6.3.3. Conflict Detector

The conflict detector element of the coordination module calculates the estimated number of departure slots that fit in the stream of arriving aircraft as is planned by the arrival manager each time the AMAN updates its schedule. By obtaining the unfixed STAs of the AMAN, the conflict detector can set up the Scheduled Arrival Intervals (SAIs). An SAI is the scheduled time between arrival i and the previously scheduled arrival $i-1$. The starting time of an SAI i is the STA of arrival $i-1$ and the end time of the SAI is equal to the STA of the arrival i, see Equation 6.2 and 6.3.

$$SAI_{start_i} = STA_{i-1} \tag{6.2}$$

$$SAI_{end_i} = STA_i \tag{6.3}$$

After this, the conflict detector will calculate the number of departure slots that fit in each SAI. Aa Schedule Arrival Free Interval (SAFI) defines a departure slot, and its length depends on the minimum required time between an arriving aircraft $i-1$ and a departing aircraft j, the IADT, the minimum required time between a departing aircraft j and an arriving aircraft i, the IDAT. The arrival-departure interaction module calculates the IADT and IDAT. In chapter 2 it was mentioned that the length of the IADT and IDAT depends on aircraft type and WTC. Since the AMAN knows the aircraft type of each arriving aircraft, for the calculation of IADT and IDAT the actual aircraft WTCs of the arriving aircraft can be used.

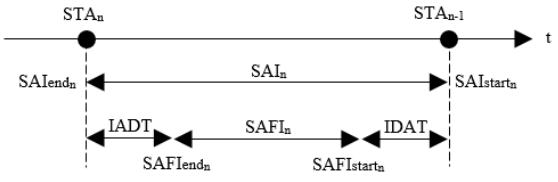

Figure 6.3: Definitions used in the conflict detector

However, for the departing aircraft, this is different. As the DMAN is assumed to be rather a metering system instead of a sequencer, the exact departure sequencing is tactically performed last-minute by ground and tower control. Hence, the DMAN cannot give exact information on which departing aircraft will depart

between which combination of arriving aircraft. Therefore, for the calculation of the IADT and IDAT, the departing aircraft WTC remains unknown. As at AAS over 80% of the arriving and departing aircraft is of aircraft WTC M, coordination module I assumes all departing aircraft in coordination module I of category M. Therefore, the module neglects the presence of heavy aircraft in the departing aircraft traffic mix.

If the length of an SAI is larger than the sum of IADT and IDAT, this does not directly mean that a departure slot is available in the SAI due to the minimum required IDT. The minimum IDT between two departing aircraft must be taken into consideration as well. A departure slot in a prior SAI may block the presence of another departure slot in the subsequent SAI. Since coordination module I considers all departing aircraft as WTC M, the conflict detector calculates with an IDT of 80 seconds between two departing aircraft. Taking the latter into consideration, the starting time of a SAFI ($SAFI_{start_i}$) is the most constraining time of the end time of the previous SAFI $i-1$ plus the IDT of 80 seconds and the starting time of SAI i plus the minimum required IADT, see Equation 6.4. The end time of SAFI i is equal to the end time of SAI i minus the minimum required IDAT, see Equation 6.5.

$$SAFI_{start_i} = max(SAFI_{end_{i-1}} + IDT,\ SAI_{start_i} + IADT) \tag{6.4}$$

$$SAFI_{end_i} = SAI_{end_i} - IDAT \tag{6.5}$$

The length of the SAFI can be calculated with Equation 6.6. If the length of a SAFI i is larger than zero, at least one departure fits in the SAI. Subsequently, the number of departure slots that fit in SAI i is equal to the length of the SAFI divided by IDT rounded down to the closest integer. The total number of departure slots that fit in the scheduled arrival stream is the sum of the departure slots per SAI, see Equation 6.7.

$$SAFI_{length_i} = SAFI_{end_i} - SAFI_{start_i} \tag{6.6}$$

$$Slots_{dep} = \sum_{i=0}^{n_{ar}} \frac{SAFI_{length_i}}{IDT} \tag{6.7}$$

Using the previously explained steering mechanism, the preferred departure-to-arrival ratio (α_{pref}), the minimum required departure slots ($Slots_{dep_{min}}$) to meet α_{pref} is known. The DMAN gives the number of planned departures within the same time interval. ($Slots_{dep_{scheduled}}$). Since it is unfavourable to create more departure slots than is scheduled by the DMAN, the minimum required number of departure slots is compared by the actual number of scheduled departures. If the minimum required departure slots are larger than the actual number of scheduled departures, the minimum required departure slots is equal to the actual number of scheduled departures.

$$Conflicts = Slots_{dep_{min}} - Slots_{dep} \tag{6.8}$$

Subsequently, the number of extra departure slots, defined as conflicts, that needs to be created by the coordination module is equal to the minimum number of departure slots minus the number of departure slots currently available in the scheduled arrival stream, see Equation 6.8. If the number of conflicts is larger than zero, the coordination module needs to reschedule the STAs of the arriving aircraft such that the arrival stream accommodates the minimum number of departure slots.

6.3.4. Conflict Solving

The previous section explained the calculation of the number of extra departure slots, called conflicts, that needs to be created by the coordination module. The so-called conflict solver element of the coordination module solves the conflicts. The conflict solver rearranges the STAs of the arriving aircraft such that the minimum required IAT is maintained and at the same time the minimum needed departure slots are available. The conflict solver consists of three parts: (1) the SAI selector, (2) the slack shifter, and (3) the aircraft delayer, see Figure 6.4. The following section explains the working principles of the conflict solver.

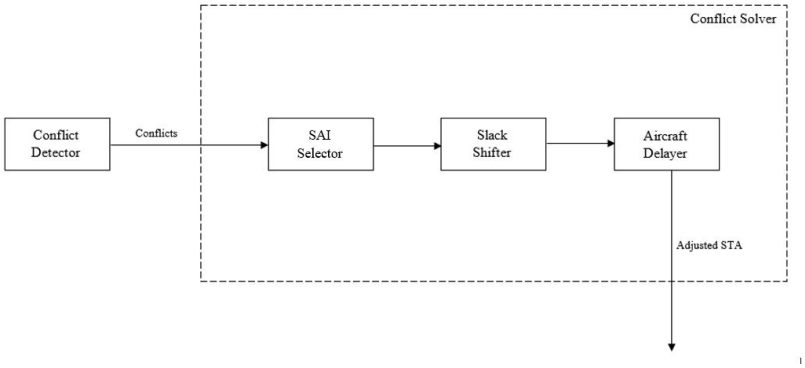

Figure 6.4: Framework of the conflict solver element of the coordination module

SAI Selection

The previous chapter explained that the DMAN is a metering system rather than a sequencing system. Hence, no information on which departure takes-off in which SAI is available. The coordination module does not precisely know which SAIs are too small to accommodate a departure; it has solely information about the number of conflicts that need to be solved. Therefore, a so-called SAI selector selects the SAIs that will be enlarged to create the extra needed departure slots and resolve the conflicts.

The selection of SAIs is performed by a Mixed Integer Programming (MIP) optimization algorithm. The algorithm selects SAIs such that it minimizes the extra time added to the sequence of arriving aircraft. To do this, for each SAI two variables need to be known: (1) the time needed to create one extra departure slot (t_{extra}), and (2) the slack SAI time (t_{slack}). When the number of departure slots in SAI i is equal to zero, the length of the SAI is too short of overcoming the minimum required IADT and IDAT. The time needed to create one departure slot is then the difference between the length of the SAI, and the sum of IADT and IDAT, see Equation 6.9. When the number of departure slots in SAI i is nonzero, the SAI needs extra time to overcome the IDT between two departures to create an extra departure slot. The extra needed time is equal to the number of departure slots that are currently available in the SAI times the IDT, minus the length of the SAFI, see Equation 6.10.

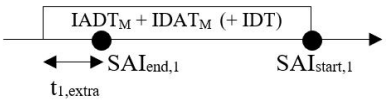

Figure 6.5: SAI extra needed time

$$t_{i_{extra}} = (IADT + IDAT) - (SAI_{end_i} - SAI_{start_i}) \tag{6.9}$$

$$t_{i_{extra}} = Slots_{dep} \cdot IDT - SAFI_{length_i} \tag{6.10}$$

The slack SAI time can be defined as the time that comes available when the SAI does not get selected. When the number of departure slots in SAI i is equal to zero, the slack SAI time is equal to the arrival slack time, see equation 6.11. The arrival slack time is the difference between the minimum required IAT and the scheduled IAT, see Figure 6.6.

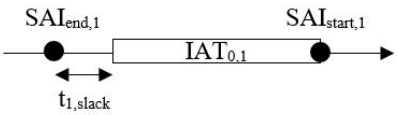

Figure 6.6: SAI slack time when no departure slot is available in the SAI

$$t_{i_{slack}} = (SAI_{end_i} - SAI_{start_i}) - IAT \tag{6.11}$$

When the number of departure slots in SAI i is nonzero, the slack SAI time is equal the most constraining slack time between the arrival slack and departure slot slack, see Equation 6.12. Figure 6.7 depicts the situation when the IAT between two arrivals is the most constraining, and Figure 6.8 shows when the required minimum departure slot length is constraining the SAI slack time.

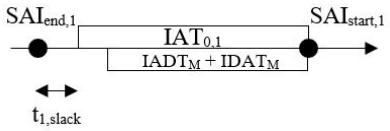

Figure 6.7: SAI slack time when one departure slot is available in the SAI

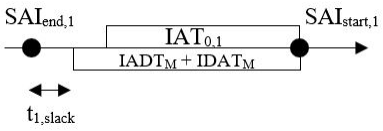

Figure 6.8: SAI slack time when one departure slot is available in the SAI

$$t_{i_{slack}} = min((SAI_{end_i} - SAI_{start_i}) - IAT,\ (SAI_{end_i} - SAI_{start_i}) - (IADT + IDAT) - (Slots_{dep} - 1) \cdot IDT) \quad (6.12)$$

As said before; the algorithm selects SAIs such that it minimizes the extra time added to the sequence of arriving aircraft. If a SAI is selected, $d_i = 1$, the SAI will be enlarged by $t_{i_{extra}}$ and its SAI slack time will not become available. When an SAI is not selected, $d_i = 0$, the SAI will not be enlarged and its SAI slack time will become available. Equation 6.13 presents the objective of the optimization algorithm. The total number of selected SAIs needs to be equal to the number of conflicts, see Equation 6.14.

$$z = minimize \sum_{i=0}^{n_{ar}} d_i \cdot t_{i_{extra}} + (d_i - 1) \cdot t_{i_{slack}} \quad (6.13)$$

$$\sum_{i=0}^{n_{ar}} d_i = conflicts \quad (6.14)$$

Slack Shifting

When the SAIs are selected, the module checks if somewhere in the scheduled arrival stream SAIs with available slack is present. If there is, the module uses the slack of those SAIs to enlarge the selected SAIs and create the extra departure slots. The scheduled arrival times (STAs) of the arriving aircraft are rearranged in the same time interval without violating the minimum IAT. This way, extra departure capacity may be created without losing arrival capacity.

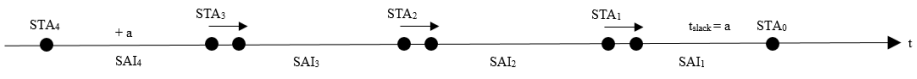

Figure 6.9: Slack advancing

Figure 6.9 shows that SAI 1 has a seconds of slack time, and the SAI selector selected SAI 4 for creating an extra departure slot by adding b extra time to SAI 4. As no more slack can be shifted from SAI i to SAI j than is available and it is unfavourable to shift more seconds of slack than is needed, the allowable slack that the module can shift is equal to the minimum of the two, see Equation 6.16. Assuming that $t_{1_{slack}}$ is smaller than $t_{4_{extra}}$, the slack capacity of SAI 1 can be shifted from SAI 1 to SAI 4 by advancing the intermediate STAs by a.

$$t_{shifted_{i,j}} = min(t_{i_{slack}}, t_{j_{extra}}) \quad (6.15)$$

Figure 6.10 the opposite situation is presented; here slack will be shifted from SAI 1 to SAI 4. Now the intermediate arriving aircraft are not advanced by a but are delayed by a. So, when the slack shifter moves slack from SAI, i to SAI j and i is larger than j the intermediate arriving aircraft will be delayed. When slack is shifted from SAI i to SAI j, and i is smaller than j, the intermediate arriving aircraft will be advanced.

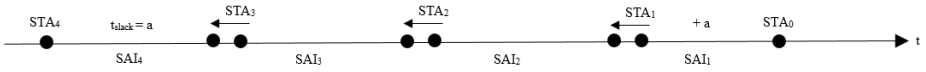

Figure 6.10: Slack delaying

Aircraft Delaying
When there is no slack or not enough slack in the scheduled arrival stream of aircraft to solve all the conflicts, the module adds time to SAIs by delaying the trailing aircraft. Figure 6.11 shows that after slack shifting SAI 2 still needs a seconds to create an extra departure slot. As no more slack is available, the module adds a seconds to SAI 2 by delaying the trailing aircraft by a.

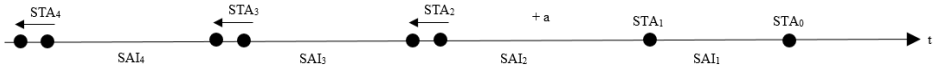

Figure 6.11: Aircraft delaying

6.4. Coordination Module II: Heavy Time Margin

The previous section explained that coordination module I assumes all departing aircraft as WTC M since over 80% of the departing aircraft is of this category. In coordination module II it is chosen to account for the number of heavy departing aircraft by applying an extra time margin over the minimum time between arriving and departing aircraft, IADT and IDAT. This difference between coordination mechanism I and coordination mechanism II results in a slightly modified conflict detector; however, the horizon of action, steering mechanism and conflict solver remain the same. The following sections explain the calculation of the heavy time margin and its implementation in the conflict detector.

6.4.1. Heavy Time Margin

When the AMAN updates its schedule, the coordination module retrieves the number of heavy departing aircraft from the DMAN (n_{dep_H}). The number of scheduled heavy departures is multiplied by the difference in IADT and IDAT between a medium and heavy departure ($\Delta IADT_{M,H}$ and $\Delta IDAT_{M,H}$) to obtain the total time difference. The total time difference is divided by the number of arrival slots (n_{ar}) to obtain the heavy time margin each SAI has to account for on top of $IADT_M$ and $IDAT_M$ (t_{hm}).

$$t_{hm} = \frac{n_{dep_H} \cdot (\Delta IADT_{M,H} + \Delta IDAT_{M,H})}{n_{ar}} \tag{6.16}$$

6.4.2. Conflict Detector

As each SAI has to account for the number of heavies in the departing aircraft traffic mix, the length of each SAFI is decreased by t_{hm}, see Equation 6.17. This means that, when calculating the number of departure slots, the length of an SAI has to be larger compared to coordination module I before at least one departure slot is assigned to the SAI. If the length of a SAFI is larger than zero, at least one departure slot fits in the SAI. For assigning second or more departure slots to the SAI the same equation holds as in coordination module I, see Equation 6.18.

$$SAFI_{length_i} = SAFI_{end_i} - SAFI_{start_i} - t_{hm} \tag{6.17}$$

$$Slots_{dep} = \sum_{i=0}^{n_{ar}} \frac{SAFI_{length_i}}{IDT} \tag{6.18}$$

6.4.3. Conflict Solver

In coordination module II the selection of SAIs is the same as in coordination module I. However, the input variables, $t_{i_{extra}}$ and $t_{i_{slack}}$, are slightly different. When the number of departure slots in SAI i is equal to zero, the length of the SAI is too short of overcoming the minimum required IADT and IDAT. The time needed to create one departure slot is then the difference between the length of the SAI, and the sum of IADT, IDAT and the heavy time margin, see Equation 6.19. When the number of departure slots in SAI i is nonzero, the SAI needs extra time to overcome the IDT between to departures to create an extra departure slot. The extra needed time is equal to the number of departure slots that are currently available in the SAI times the IDT, minus the length of the SAFI, which already included the heavy time margin, see Equation 6.17 and 6.20.

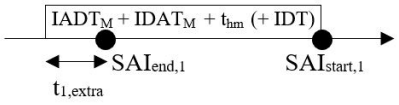

Figure 6.12: SAI extra needed time

$$t_{i_{extra}} = (IADT_M + IDAT_M + t_{hm}) - (SAI_{end_i} - SAI_{start_i}) \tag{6.19}$$

$$t_{i_{extra}} = Slots_{dep} \cdot IDT - SAFI_{length_i} \tag{6.20}$$

When the number of departure slots in SAI i is equal to zero, the slack SAI time is equal to the arrival slack time, see equation 6.22. The arrival slack time is the difference between the minimum required IAT and the scheduled IAT, see Figure 6.13.

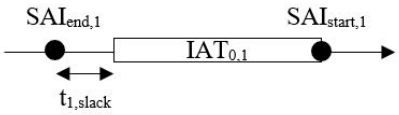

Figure 6.13: SAI slack time when no departure slot is available in the SAI

$$t_{i_{slack}} = (SAI_{end_i} - SAI_{start_i}) - IAT \tag{6.21}$$

When the number of departure slots in SAI i is nonzero, the slack SAI time is equal the most constraining slack time between the arrival slack and departure slot slack, see Equation 6.22. Subsequently, the conflict solver will adjust the STAs of the arriving using the same principles as in coordination module I.

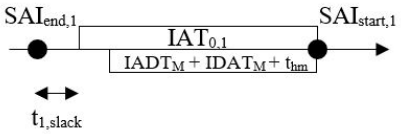

Figure 6.14: SAI slack time when one departure slot is available in the SAI

$$t_{i_{slack}} = min((SAI_{end_i} - SAI_{start_i}) - IAT,\ (SAI_{end_i} - SAI_{start_i}) - (IADT_M + IDAT_M + t_{hm}) - (Slots_{dep} - 1) \cdot IDT) \tag{6.22}$$

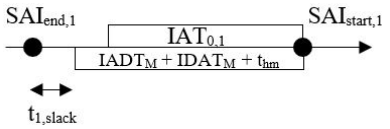

Figure 6.15: SAI slack time when one departure slot is available in the SAI

6.5. Coordination Module III: M and H

Coordination module II accounts for the number of heavy departures by counting a heavy time margin over the IADT and IDAT. Coordination module III accounts for the scheduled heavy departures differently; it distinguishes between departure slots that fit aircraft WTC M and departure slots that fit aircraft WTC H. The coordination module evaluates for each SAI specifically whether it can accommodate a heavy departure slot, a medium departure slot, or possibly a combination both. Subsequently, it determines the number of extra medium departure slots and the number of extra heavy departure slots that need to be created by the coordination module. This results in a different conflict detector and conflict solver compared to coordination module I. However, the horizon of action, steering mechanism are the same. The following sections will explain the working principles of the conflict detector and conflict solver of coordination module III.

6.5.1. Conflict Detector

The conflict detector element of coordination module III calculates the estimated number of departure slots that fit in the stream of arriving aircraft as is planned by the arrival manager each time the AMAN updates its schedule. It calculates two variables: (1) the number of departure slots that fit a departing aircraft of WTC M ($Slots_{dep_M}$) and (2) the number of departure slots that fit a departing aircraft of WTC H ($Slots_{dep_H}$). As in coordination module I, by obtaining the unfixed STAs of the AMAN, the conflict detector can set up the Scheduled Arrival Intervals (SAIs).

$$SAI_{start_i} = STA_{i-1} \tag{6.23}$$

$$SAI_{end_i} = STA_i \tag{6.24}$$

$$SAI_{length_i} = SAI_{end_i} - SAI_{start_i} \tag{6.25}$$

After this, the conflict detector will calculate the number of departure slots that fit in each SAI. For each pair of arriving aircraft i and $i-1$ the conflict detector calculates two time intervals: (1) the minimum time between that is needed between the two arriving aircraft to accommodate a departing aircraft of WTC M, and (2) the minimum time between that is needed between the two arriving aircraft to accommodate a departing aircraft of WTC H. These time intervals are respectively called AFI_M and AFI_H. AFI_M is equal to the minimum IADT between arriving aircraft $i-1$ and departing aircraft j plus the minimum IADT between arriving aircraft i assuming departing aircraft j to be of WTC M, see Equation 6.26. AFI_H is equal to the minimum IADT between arriving aircraft $i-1$ and departing aircraft j plus the minimum IADT between arriving aircraft i assuming departing aircraft j to be of WTC H, see Equation 6.27.

$$AFI_{i_M} = IADT_{i-1,j_M} + IDAT_{i,j_M} \tag{6.26}$$

$$AFI_{i_H} = IADT_{i-1,j_H} + IDAT_{i,j_H} \tag{6.27}$$

Depending on the length of each SAI, different actions are required. Here, three circumstances are distinguished: (1) when SAI_{length_i} is smaller than AFI_{i_M}, (2) when SAI_{length_i} is greater than AFI_{i_M} and smaller than AFI_{i_H}, and (3) when SAI_{length_i} is greater than AFI_{i_M} and AFI_{i_H}. Each of them will be explained below.

(1) When SAI_{length_i} is smaller than AFI_{i_M}

If the length of SAI i is smaller than AFI_{i_M} the SAI cannot accommodate a departure slot for an aircraft of WTC M. In addition to that, the length of SAI i is not sufficient to accommodate a departure slot for an aircraft of WTC H as well. The number of departure slots for WTC M, and the number of departure slots for WTC H that fit in the SAI is equal to zero.

(2) When SAI_{length_i} is greater than AFI_{i_M} and smaller than AFI_{i_H}
If the length of SAI i is larger than AFI_{i_M}, it is checked if the length is also larger than AFI_{i_H}. If the length is not larger than AFI_{i_H}, SAI i has the potential to accommodate a departure slot for WTC M, but certainly cannot accommodate a departure slot for WTC H. An expected departure slot in a prior SAI $i-1$ may block the presence of another departure slot in SAI i. Therefore, whether or not a departure slot is present in SAI $i-1$ and whether the departure slot is intended for a departing aircraft of WTC M or H has to be checked. If no departure slot is present in SAI $i-1$ the number of departure slots for WTC M that fit in the SAI is equal to 1, and the number of departure slots for WTC H that fit in the SAI is equal to zero.

$$SAFI_{start_i} = max(SAFI_{end_{i-1}} + IDT_{j-1,j_M},\ SAI_{start_i} + IADT_{i-1,j_M}) \tag{6.28}$$

$$SAFI_{end_i} = SAI_{end_i} - IDAT_{i,j_M} \tag{6.29}$$

$$SAFI_{length_i} = SAFI_{end_i} - SAFI_{start_i} \tag{6.30}$$

If a departure slot is present in SAI $i-1$, the module calculates the start and end time of SAFI i. The starting time of the SAFI is then most constraining starting time of the end time of the previous SAFI $i1$ plus the minimum required IDT between the WTC of departure slot $j-1$and the current departure slot of WTC M, and the starting time of SAI i plus the minimum required IADT, see Equation 6.28. Figure 6.16 shows the situation when the IADT is the most constraining when determining the starting time of the SAFI. Figure 6.17 depicts the opposite situation. Here the IDT with the previous departure slot constrains the starting time of the SAFI. The end time of SAFI i is equal to the end time of SAI i minus the minimum required IDAT, see Equation 6.29. If the length of SAI i is larger than zero the number of departure slots for WTC M that fit in the SAI is equal to 1, and the number of departure slots for WTC H that fit in the SAI is equal to zero. Else, the number of departure slots for WTC M and H are both equal to zero.

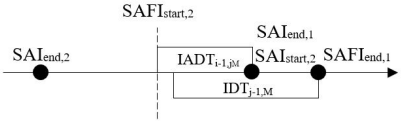

Figure 6.16: SAI slack time when one departure slot is available in the SAI

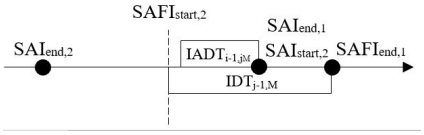

Figure 6.17: SAI slack time when one departure slot is available in the SAI

(3) When SAI_{length_i} is greater than AFI_{i_M} and AFI_{i_H}
If the length of SAI i is larger than AFI_{i_M}, and also larger than AFI_{i_H}. SAI i has the potential to accommodate a departure slot for both WTC M and H. Assuming the departure slot accommodating a departure for WTC H; the module checks the presence of a departure slot in SAI $i-1$. If no departure slot is present in SAI $i1$ at least one departure slot for WTC H is available in the SAI. The start, end time and length of the SAFI are calculated respectively with Equation 6.31, 6.32 and 6.33. Subsequently, the number of departure slots of WTC H that fit in SAI i equal to the length of the SAFI divided by IDT rounded down to the closest integer, see Equation 6.34.

$$SAFI_{start_i} = SAI_{start_i} + IADT_{i-1,j_H} \tag{6.31}$$

$$SAFI_{end_i} = SAI_{end_i} - IDAT_{i,j_H} \tag{6.32}$$

$$SAFI_{length_i} = SAFI_{end_i} - SAFI_{start_i} \tag{6.33}$$

$$Slots_{dep_H} = 1 + \frac{SAFI_{length_i}}{IDT_{H,H}} \tag{6.34}$$

If a departure slot is present in SAI $i-1$, the start and end time of SAFI i is calculated. The starting time of the SAFI is then most constraining starting time of the end time of the previous SAFI $i1$ plus the minimum required IDT between the WTC of departure slot $j-1$and the current departure slot of WTC H, and the starting time of SAI i plus the minimum required IADT, see Equation 6.35. This process was already depicted in Figure 6.16 and Figure 6.17. The end time of SAFI i is equal to the end time of SAI i minus the minimum required IDAT, see Equation 6.36. If the length of SAI i is smaller than zero, it is checked if the SAI could still accommodate a departure slot by performing option 2. If the length of SAI i is larger than zero, the number of departure slots of WTC H that fit in SAI i equal to the length of the SAFI divided by IDT rounded down to the closest integer, see Equation 6.34.

$$SAFI_{start_i} = max(SAFI_{end_{i-1}} + IDT_{j-1,j_H},\ SAI_{start_i} + IADT_{i-1,j_H}) \tag{6.35}$$

$$SAFI_{end_i} = SAI_{end_i} - IDAT_{i,j_H} \tag{6.36}$$

$$SAFI_{length_i} = SAFI_{end_i} - SAFI_{start_i} \tag{6.37}$$

Conflicts

When for every SAI the number of departure slots that fit a departing aircraft of WTC M and H are calculated, the total number of available departure slots ($slots_{dep_{total}}$) can be calculated according to Equation 6.38. Using the previously explained steering mechanism, the preferred departure-to-arrival ratio (α_{pref}), the minimum required departure slots ($Slots_{dep_{min}}$) to meet α_{pref} is known. If the minimum required departure slots is larger than the available departure slots, the coordination mechanism will have to create extra departure slots.

$$Slots_{dep_{total}} = \sum_{i=0}^{n_{ar}} Slots_{dep_{M_i}} + Slots_{dep_{H_i}} \tag{6.38}$$

$$Conflicts_M = Slots_{dep_{min}} - Slots_{dep} \tag{6.39}$$

$$Conflicts_H = Slots_{dep_{min}} - Slots_{dep} \tag{6.40}$$

6.5.2. Conflict Solving

As in the previous coordination modules, the conflict solver has to rearrange the STAs of the arriving aircraft to accommodate the extra needed departure slots. Since coordination module III distinguishes between departure slots that fit a departing aircraft of WTC M and departure slots that fit departing aircraft of WTC H, the SAI selector has to choose which SAIs will be enlarged to fit a medium departure and which SAI will be enlarged to fit a heavy departure. This results in a different compared to coordination module I and II. This section explains the SAI selector of coordination mechanism III.

SAI Selector

The selection of SAIs is performed by a Mixed Integer Programming (MIP) optimization algorithm. The algorithm selects SAIs such that it minimizes the extra time added to the sequence of arriving aircraft. To do this, for each SAI specific three variables need to be known: (1) the time needed to create one extra slot for a medium departure (t_{extra_M}), (2) the time needed to create one extra slot for a heavy departure (t_{extra_H}) and (3) the slack SAI time (t_{slack}).

When the number of departure slots in SAI i is equal to zero, the length of the SAI is too short of overcoming the minimum required IADT and IDAT for a medium or heavy departure. The time needed to create one departure slot for a medium or heavy is then the difference between the length of the SAI, and the sum of IADT and IDAT, see Equation 6.42 and 6.43. The slack SAI time is equal to the arrival slack time, see Equation 6.43.

$$t_{i_{extra_M}} = (IADT_{i-1,j_M} + IDAT_{i,j_M}) - (SAI_{end_i} - SAI_{start_i}) \tag{6.41}$$

$$t_{i_{extra_H}} = (IADT_{i-1,j_H} + IDAT_{i,j_H}) - (SAI_{end_i} - SAI_{start_i}) \tag{6.42}$$

$$t_{i_{slack}} = (SAI_{end_i} - SAI_{start_i}) - IAT_{i,i-1} \tag{6.43}$$

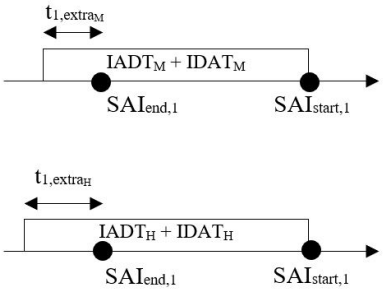

Figure 6.18: The extra time needed to create a departure slot for a medium and heavy departure slot

When a medium departure slot is available in an SAI, the SAI needs extra time to overcome the IDT between to medium departures to create an extra departure slot for a medium departure, see Equation 6.44. The time that is needed to create an extra departure slot for a heavy aircraft is more complicated. When a heavy departure slot is added behind a medium departure slot in the same SAI, the size of minimum required IDAT becomes larger. However, the size of the IADT remains the same. So the SAI has to be enlarged to overcome the minimum IDT between a leading medium and trailing heavy and the difference in IADT between a medium departure and heavy departure, see Equation 6.45.

$$t_{i_{extra_M}} = IDT_{M,M} - SAFI_{length_i} \tag{6.44}$$

$$t_{i_{extra_H}} = (IDT_{M,H} + IDAT_{i-1,j_H}) - (SAI_{end_i} - SAFI_{start_i}) \tag{6.45}$$

$$t_{i_{slack}} = min((SAI_{end_i} - SAI_{start_i}) - IAT_{i,i-1},\ (SAI_{end_i} - SAFI_{start_i}) - IDAT_{i,j_M}) \tag{6.46}$$

When one or more heavy departure slots are available in an SAI, the SAI needs extra time to overcome the IDT between to heavy departures to create an extra departure slot for a heavy departure, see Equation 6.47. When a medium departure slot is added behind a heavy departure slot in the same SAI, the size of minimum required IDAT becomes smaller. However, the size of the IADT remains the same.

$$t_{i_{extra_H}} = Slots_{dep_{H_i}H,H} - SAFI_{length_i} \tag{6.47}$$

$$t_{i_{extra_M}} = (IDT_{H,M} + IDAT_{i-1,j_M}) - (SAI_{end_i} - SAFI_{start_i}) \tag{6.48}$$

$$t_{i_{slack}} = min((SAI_{end_i} - SAI_{start_i}) - IAT_{i,i-1},\ (SAI_{end_i} - SAFI_{start_i}) - IDAT_{i,j_H}) - (Slots_{dep_{H_i}-1)_{H,H}} \tag{6.49}$$

The optimization algorithm decides which SAIs will be enlarged such that it minimizes the extra time added to the arrival sequence. If an SAI is selected to be enlarged to create a medium departure slot, $d_{M_i} = 1$, the SAI will be enlarged by $t_{i_{extra_M}}$ and its SAI slack time will not become available. If an SAI is selected to be enlarged to create a heavy departure slot, $d_{H_i} = 1$, the SAI will be enlarged by $t_{i_{extra_H}}$ and its SAI slack time will not become available. When a SAI is not selected, $d_{M_i} = 0$ and $d_{H_i} = 0$, the SAI will not be enlarged and its SAI slack time will become available. Equation 6.50 presents the objective of the optimization algorithm. The total number of selected SAIs needs to be equal to the number of conflicts, see Equation 6.52 and 6.53.

$$z = minimize \sum_{i=0}^{n_{ar}} d_{M_i} \cdot (d_{M_i} \cdot t_{i_{extra_M}} + (d_{M_i} - 1) \cdot t_{i_{slack}}) + d_{H_i} \cdot (d_{H_i} \cdot t_{i_{extra_H}} + (d_{H_i} - 1) \cdot t_{i_{slack}}) \tag{6.50}$$

$$d_{M_i} + d_{H_i} \leq 1 \tag{6.51}$$

$$\sum_{i=0}^{n_{ar}} d_{M_i} = conflicts_M \tag{6.52}$$

$$\sum_{i=0}^{n_{ar}} d_{H_i} = conflicts_H \tag{6.53}$$

7

Software Implementation

The previous chapters the conceptual working principles and applied algorithms of the uncoordinated and coordinated models were explained. In this chapter it will be explained which software is chosen and how the models are implemented.

7.1. Software

BlueSky Open Air Traffic Simulator (BlueSky) was chosen as software for implmentation. BlueSky is meant as a tool to perform research on Air Traffic Management and Air Traffic Flows. Its goal is to provide everybody who wants to visualize, analyze or simulate air traffic with a tool to do so without any restrictions, licenses or limitations. For the uncoordinated model, in which a small optimization problem is included, Gurobi Optimizer was chosen as solver. Since BlueSky uses the programming language Python, the python version of Gurobi Optimizer will be used and the implementation of both models is done in python as well.

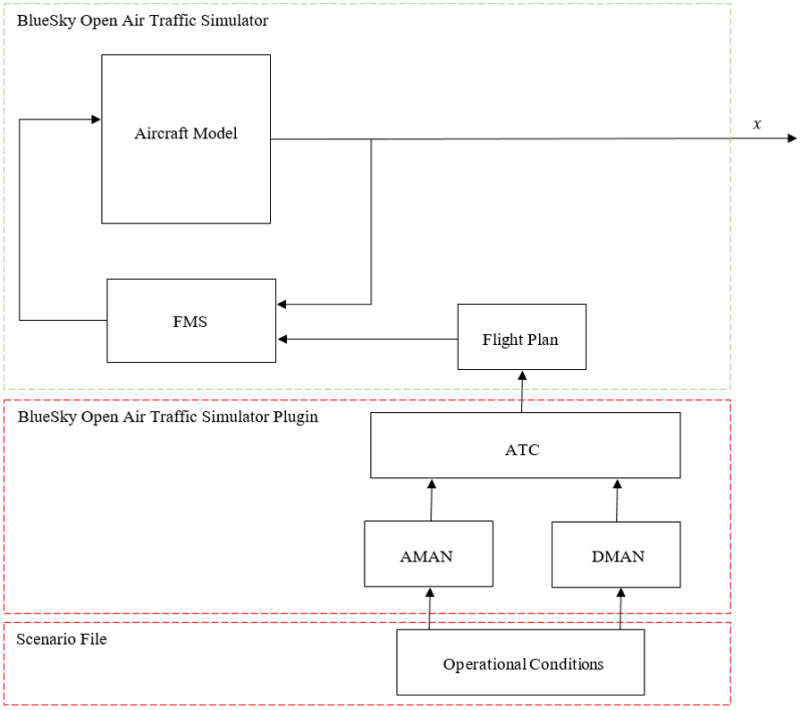

Figure 7.1: Framework for the uncoordinated ADMAN implemented in software

Figure 8.1 and 7.2 show the implementation of the uncoordinated and coordinated ADMAN in BlueSky. The uncoordinated ADMAN and coordinated ADMAN will be implemented in BlueSky by creating a plugin object because this is the easiest way to implement it in de existing modules of Bluesky. A plugin object has direct access to the traffic object, which requires for calculating and adjusting per-aircraft states. Furthermore, by creating a plugin object, new per-aircraft states can be defined, and BlueSky tools can be used. A BlueSky scenario file feeds the operational conditions into the model.

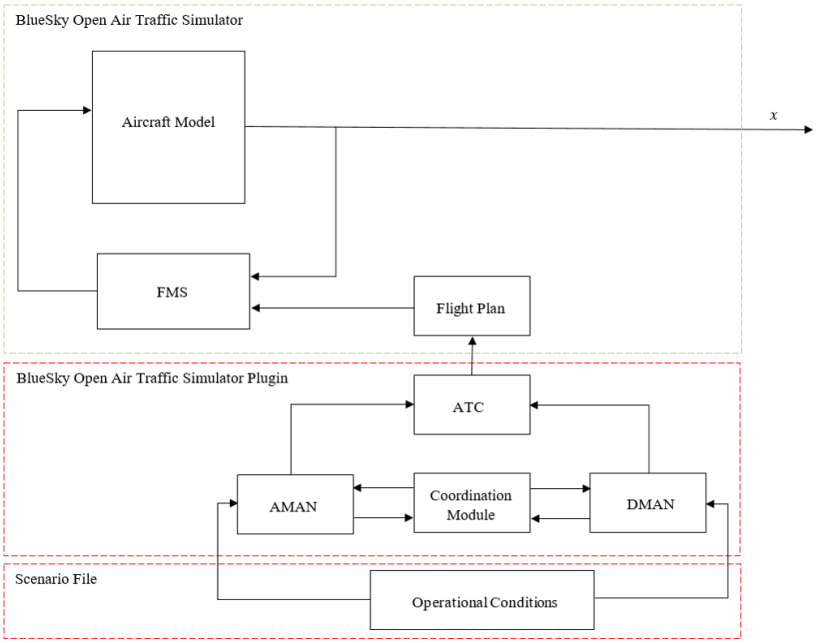

Figure 7.2: Framework for the coordinated ADMAN implemented in software

7.2. Plugin Architecture

For the implementation of the uncoordinated model, four scripts are written: (1) the uncoordinated ADMAN plugin, which is the main file that communicates with the traffic object of BlueSky. It includes the AMAN module, the DMAN module and the ATC module. During the simulation, the per aircraft variables are continuously monitored and if needed to be updated by the plugin. (2) The Trajectory Predictor function that is called by the uncoordinated ADMAN plugin every time it needs to revision ETA and ETO of an arriving aircraft. The function uses the index of the arriving aircraft as input to retrieve the flight plan of the aircraft from the BlueSky's route object and returns its ETA and ETO using the equations presented in the previous chapter. (3) The arrival-departure interaction function that is called every time the AFI finder wants to evaluate whether an arrival interval is large enough to suit the departure of a specific departure. The function uses the arrival completion time of the leading arriving aircraft, the average approach speed of the trailing arriving aircraft and the communication buffer time of the departing aircraft as input. It returns the minimum IADT and IDAT between arriving and departing aircraft pairs. (4) The aircraft performance function that is called when variables are needed that is not defined in any of BlueSky's object. The function uses the arriving or departing aircraft type as input and returns several variables like aircraft WTC, average approach speed, average departure speed, arrival completion time, runway occupancy time, runway occupancy time, and distance- and time-based separation minima.

The implementation of the coordinated ADMAN uses one script more compared to the uncoordinated model. The Trajectory Prediction function, the arrival-departure interaction function and the aircraft performance function are the same files as for the uncoordinated ADMAN. The coordinated ADMAN plugin is different than for the uncoordinated model. It includes the AMAN module, the DMAN module, the ATC module and the coordination module. Furthermore, the coordinated ADMAN uses two optimizer functions, one for coordination module I and II and one for coordination module III. Within the coordinated ADMAN plugin, the

specific coordination module I, II or III can be activated.

7.3. Model Parameters

The functioning of modules and elements of both the uncoordinated and coordinated ADMAN depends on many different variables. Table 7.1 and 7.2 give an overview of the arriving and departing variables used by the uncoordinated and coordinated ADMAN. Most of the variables presented here do not need any explanation. However, the arrival status and departure status do.

To keep track of where each arriving aircraft is in the arrival process, each arriving aircraft is given an arrival status which is continuously updated in the simulation. The arrival process uses seven different states are used: (1) aircraft arrival status 0 represents the arriving aircraft that exist in the scenario, but is still too far away to take into account for scheduling by the AMAN. (2) Aircraft arrival status -1 represents the arriving aircraft that have passed eligibility horizon of the AMAN, and are therefore allowed to be taken into account for scheduling. (3) Aircraft arrival status 1 represents the arriving aircraft that have been scheduled by the AMAN, and so, these aircraft have been given an arrival slot. However, since the aircraft has not passed the active advisory horizon, the assigned slot time is still subject to change. (4) Aircraft arrival status -2 represents the aircraft that have passed the active advisory horizon of the AMAN and is therefore allowed to receive a speed advisory by the ATC module to absorb its delay. (5) Aircraft arrival status represents the aircraft that have received a speed advisory from the ATC module. (6) Aircraft arrival status -3 represents the aircraft that have completed their arrival process and are allowed to be deleted from the scenario. (7) Aircraft arrival status 3 represent the aircraft that are deleted from the scenario.

Table 7.1: Arriving aircraft variables

Variable
Aircraft ID
Latitude
Longitude
Altitude
Ground Speed
Calibrated Air Speed
Average Approach speed
Destination
Flight plan
Aircraft type
Aircraft WTC
Minimum distance-based separation
Arrival completion time
Expected Time of Arrival (ETA)
Expected Time Over (ETO)
Scheduled Time of Arrival (STA)
Actual Time of Arrival (ATA)
Arrival status

Table 7.2: Departing aircraft variables

Variable
Aircraft ID
SID
Destination
Aircraft type
Aircraft WTC
Minimum distance-based separation
Minimum time-based separation
Communication buffer time
Average departure speed
Average runway occupancy time
Target Take-Off Time (TTOT)
Actual Take-Off Time (ATOT)
Departure status

Departing aircraft use less states compared to the arriving aircraft. For the same reason, to keep track of where each departing aircraft is in the departing process, each departing aircraft is given a departure status which is continuously updated in the simulation. Departing aircraft use four different states: (1) Aircraft departure state 0 represents a departing aircraft that is allowed to be scheduled in by the DMAN (TTOT). (2) Aircraft departure state 1 represents a departing aircraft that has moved to the runway threshold and is allowed to be given a take-off clearance by the ATC module (ATOT). (3) Aircraft departure state 2 represents a departing aircraft that has received an actual departing slot (ATOT) but has not departed yet because the simulation time has not passed its ATOT yet. (4) Aircraft departure state 3 represents a departing aircraft that has taken off.

Table 7.3: AMAN input variables

Variable
Active arrival runway
Declared capacity
Eligibility horizon
Active Advisory horizon

Table 7.4: DMAN input variables

Variable
Active departure runway
Declared capacity

The AMAN, DMAN and coordination module use specific input variables before it is operational, see Table 7.3, 7.4, and 7.5. For both the AMAN and DMAN the active runway and its declared capacity are needed. Furthermore, the AMAN needs to know the locations of the eligibility and active advisory horizons. The coordination modules require the preferred departure-to-arrival ratio and need to know which of the three coordination modules is active. As said before, the aircraft performance module is a function that is called when variables are needed that are not available in any of BlueSky's objects. Therefore, the performance function demands data concerning the variables presented in Table 7.6

Table 7.5: Coordination module input variables

Variable
Preferred departure-to-arrival ratio
Active coordination module

Table 7.6: Performance module input data

Variable
Average approach speed
Average departure speed
Arrival completion time
Departure communication buffer time
Runway occupancy time
SID common departure path
Distance-based separation minima
Time-based separation minima

7.4. Model Update

The plugins of the uncoordinated ADMAN and coordinated ADMAN together with the other supporting files updates its variables and, if needed, changes the per-aircraft variables every second in the simulation. This section demonstrates the update of the plugin for both the uncoordinated ADMAN and the coordinated ADMAN.

7.4.1. Uncoordinated Model

At the start of the update, possible new arriving aircraft are identified. If there are new arriving aircraft, which were not there in the previous time step, the empty variables of the new arriving aircraft are added to the variables of the already existing arriving aircraft. Hereafter, the variables of all the arriving aircraft are updated with the help of the TP and the traffic object. The updated aircraft arrival states determine the subsequent action for each aircraft. Figure 9.1 presents an overview of this process.

The arriving aircraft assigned with aircraft arrival status -1, have just passed the eligibility horizon of the AMAN and are allowed to be scheduled. The arrival manager sorts the ETA of all arriving aircraft with aircraft arrival status -1 in ascending order and assigns each aircraft an arrival slot (STA) using the sequencing method previously described. The last fixed arrival slot is the starting point from which the AMAN is allowed to schedule. Arriving aircraft with status -2 have just passed the active advisory horizon. Their assigned STA and their arriving aircraft status will be fixed and set to 2 respectively. Arriving aircraft with status 2 are assigned an ATA. Once the ATA is known, the RTA of the aircraft will be activated. Every time a new ATA is added, a new Actual Arrival Interval (AAI) is known. The start time of the new AAI is the ATA of the previous arrival and the end time of the AAI is the new added ATA. Since no departure has been planned yet in the AAI, the AAI planning status equals 0.

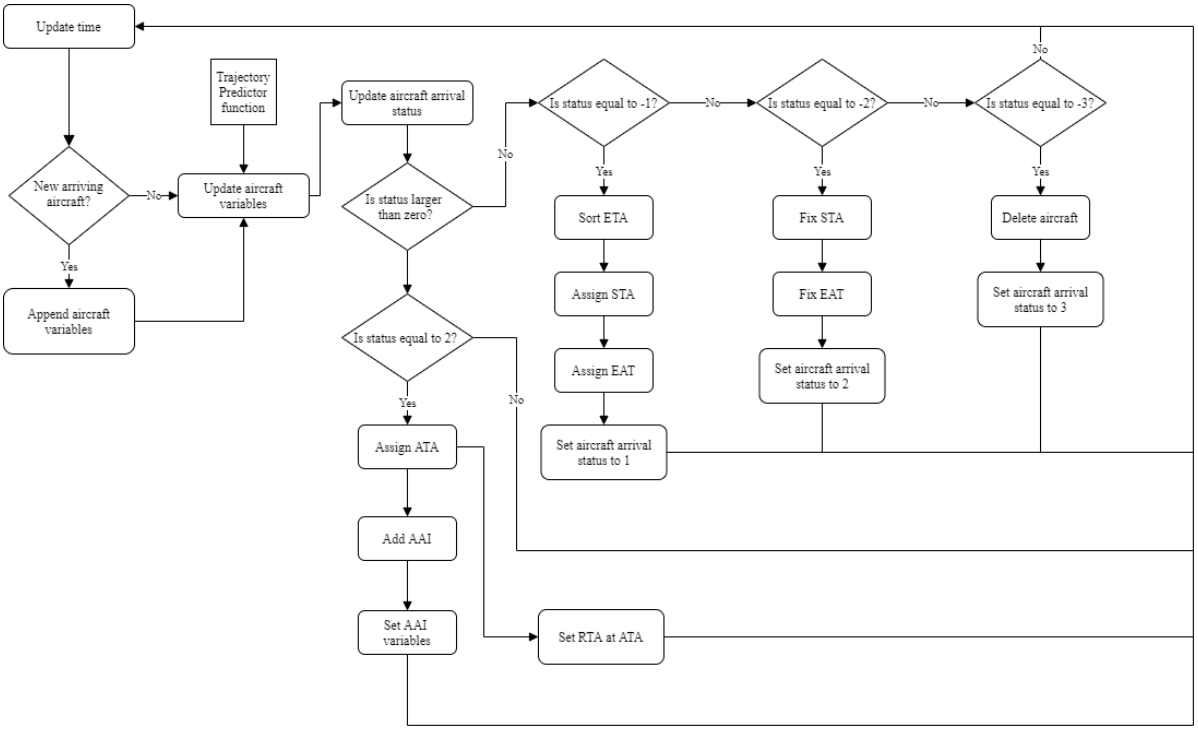

Figure 7.3: Model update of the arrival process in the uncoordinated ADMAN

Parallel to the planning of the arrivals, departing aircraft are processed as well. At the start of the update, possible new departing aircraft will be identified. If there are new departing aircraft, empty variables of the new departing aircraft will be added to the variables of the already existing departing aircraft. Also, the TTOT of the departing aircraft is assigned right away as it has no constraining factor. Hereafter, the variables of all the departing aircraft are updated. The updated aircraft departure states indicate the subsequent action of each aircraft. Figure 9.2 presents an overview of this process.

The aircraft with departure status 1 will be moved to the runway threshold, and the AAFI finder will try to find a suitable AAI. If the AAFI finder does, the ATOT was determined, and its status will be changed to 2. Also, the concerned AAI variables are updated; the starting time of the AAI equals the ATOT of the departure. The aircraft ID of the departing aircraft is logged as an AAI variable as well. From now, at least one departure takes-off in the AAI. Therefore, the AAI status will be updated to 1. Departing aircraft with status 2 will take-off when the simulation time is equal to the ATOT of the departing aircraft.

To ensure that departing aircraft will not be planned in an AAI that has already passed in time, in every update, it checks for each AAI whether the simulation time is larger than the starting time of the AAI. If it is, the simulation time is catching up with the position of the AAI in time. In this case, the start time of the AAI will continuously be equal to the simulation time. Furthermore, when the starting time of the AAI is equal to the end time of the AAI, the AAI is closed for planning by setting its status to 3. Figure 7.5 depicts this process.

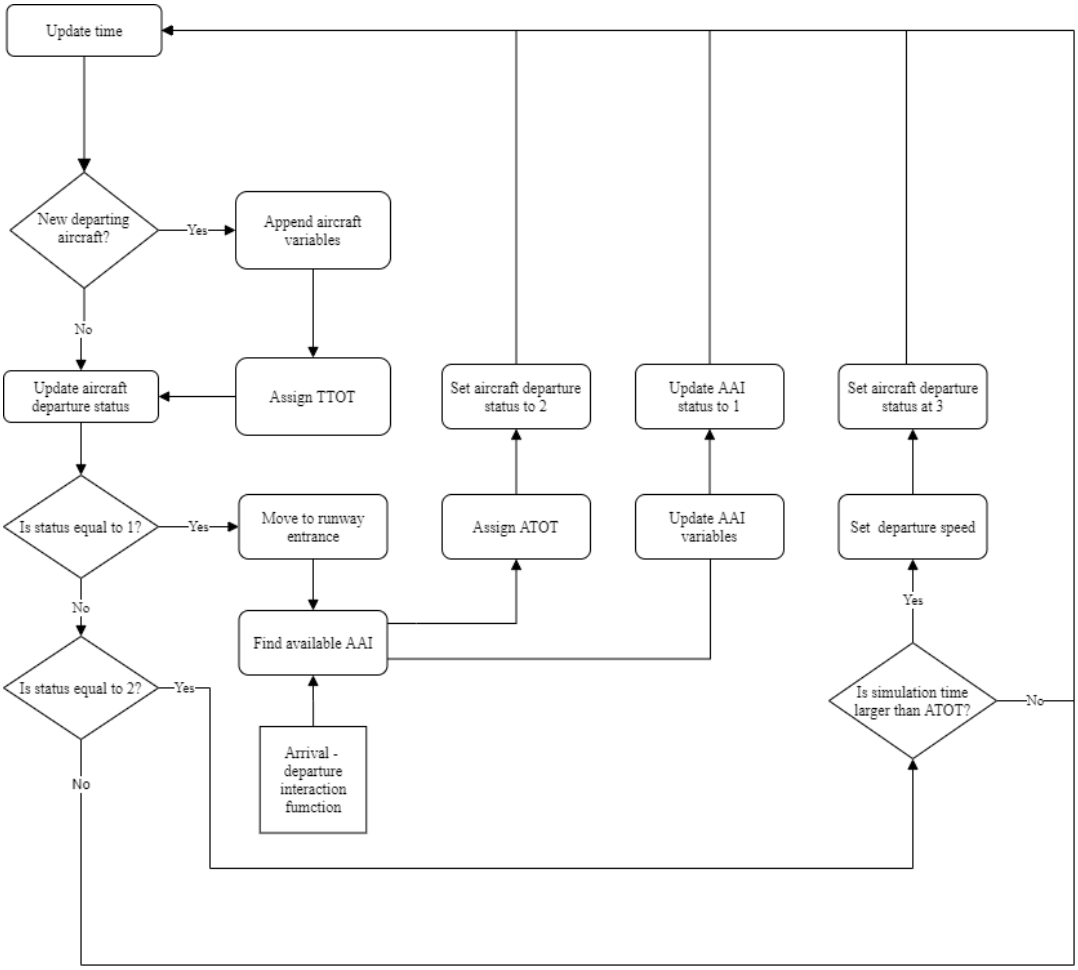

Figure 7.4: Model update of the departure process in the uncoordinated ADMAN

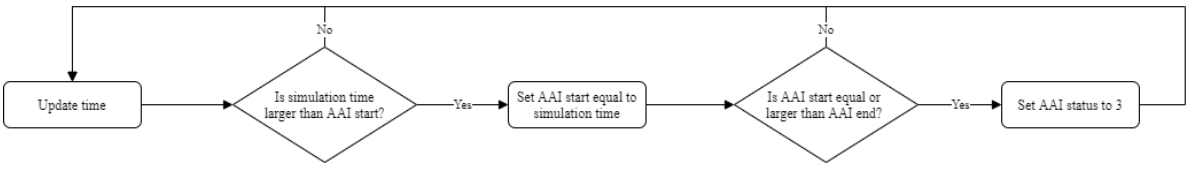

Figure 7.5: Model update of the AAIs in the uncoordinated ADMAN

7.4.2. Coordinated Model

At the start of a model update of the coordinated ADMAN, the arriving aircraft and departing aircraft are processed according to Figure 7.3 and 7.4. Hereafter, the coordination module will start acting. The previous chapter explained the development of three different coordination modules. Even though the used algorithms and working principles are different between the three, how each coordination module is updated is the same. Figure 7.5 shows how the coordination module is updated each time step.

In every time step, the coordination module retrieves the unfixed STAs from the AMAN. With the unfixed STAs of the arriving aircraft, the coordination module can establish the SAIs and calculate the number of departure slots that are available in the scheduled arrival stream. If the number of departure slots is larger than the minimum required departure slots, the coordination module does not need to proceed. However, when the number of departure slots is smaller, the coordination module will have to calculate the number of conflicts that will have to be solved by the conflict solver.

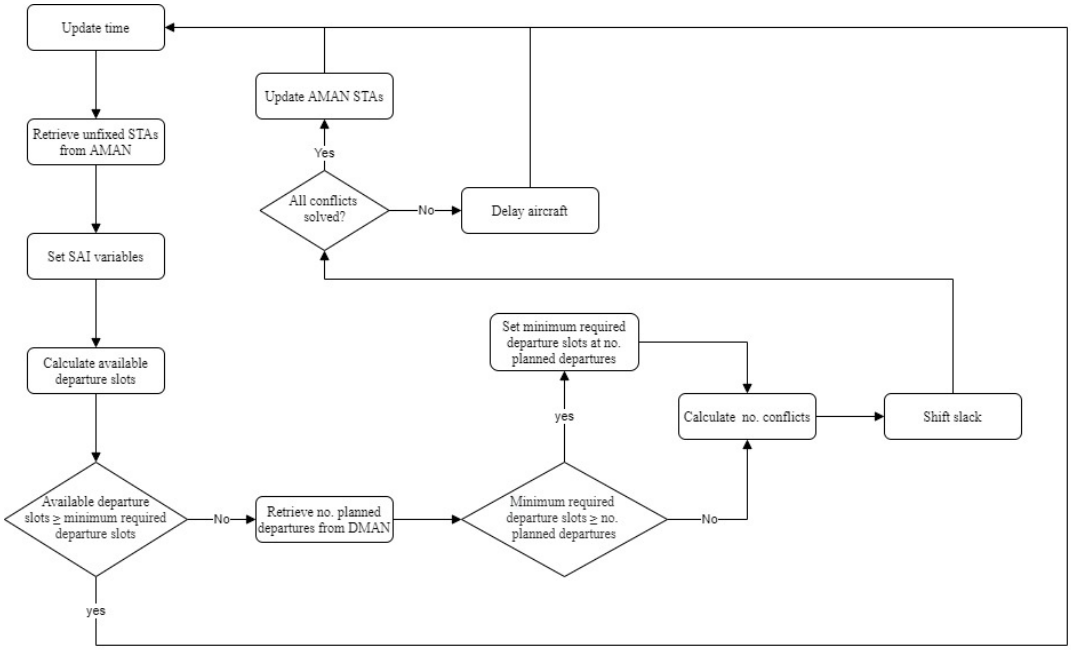

Figure 7.6: Model update of the coordination module of the coordinated ADMAN

8

Scenario Generator

The previous chapters outlined the working principles of the uncoordinated and coordinated ADMAN. Here it was explained that the models require a scenario file containing arriving and departing aircraft to and from a specific airport. The flight data of these flights is input for the AMAN and DMAN. This chapter explains the generation of scenario files that can be run in BlueSky Open Air Traffic Simulator (BlueSky) and obtain results.

8.1. Overview

The goal of the scenario generator is to construct scenario files for different operational conditions such that experiments can be performed with the uncoordinated and coordinated models. BlueSky uses *.scn* files as an input. In these files, plugins are loaded into BlueSky and aircraft, and their flight plans are defined. Figure 8.1 shows an overview of the scenario generator. The scenario generator uses two types of input to generate scenarios: (1) user input, and (2) airport-specific input. Table 8.1 and 8.2 show the user and airport input variables.

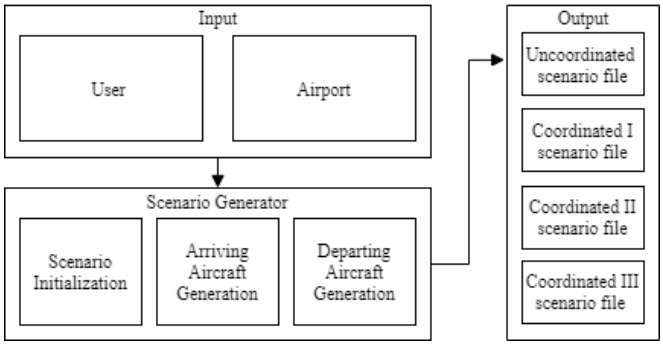

Figure 8.1: Overview of the scenario generator

With the specified input, the different elements of the scenario generator will write a scenario. Since the scenario generator uses distributions as input, it uses a fixed seed to generate semi-random scenarios. This means that it generates identical scenarios at another time with the same input. Furthermore, the number of repeats is used as input to generate n different scenarios using the same input.

The scenario generator consists of roughly three elements. The first element will initialize the settings of the model, the second part will generate the arriving aircraft at specific times in the scenario, and the last element will generate the departing aircraft at specific times as well. Each scenario will be written four times, one time in which the uncoordinated plugin will be loaded and three times in which the different coordinated modules will be loaded. Scenario i for the uncoordinated model is identical to scenario i for the coordinated models. Because of this, a fair comparison can be made between different coordination strategies.

Table 8.1: User input

Variable
Number of arrivals per hour
Number of departures per hour
Scenario duration
Declared arrival capacity
Declared departure capacity
Eligibility horizon
Active advisory horizon
Number of repeats
Output directory

Table 8.2: Airport input

Variable
Active arrival runway
Active departure runway
Arrival routes
Departure routes
IAF-runway combination
SID-runway combination
Arrival fleet mix distribution
Departure fleet mix distribution
IAF traffic load distribution
SID traffic load distribution

8.2. Scenario Initialization

The model initialization element will specify at the start of a simulation specific parameters. First of all, the right plugin file will have to be loaded in the scenario. After this, the AMAN, DMAN and coordination module input variables according to Table X, Y and Z are initialized. The output directory is used such that the plugin file knows where to dump its data at the end of a simulation.

8.3. Arriving Aircraft Generation

The number of arrivals per hour, and the scenario duration determines the total number of arriving aircraft that the scenario has to contain. Each arriving aircraft gets a distinct aircraft ID. First of all, each arriving aircraft will be assigned to a specific aircraft type using the airports arriving traffic mix distribution. Using a traceable seed, semi-random p values (p_{ACtype}) between 0 and 1 are generated for each arriving aircraft i ($AC_{arriving}$). The airports' traffic mix distribution includes all occurring aircraft types and their respective p-value interval. If the p-value of arriving aircraft i falls within the p-value interval of aircraft type j, arriving aircraft i will be of aircraft type j, see Equation 8.1.

$$d_{ACtypes_{j-1}} < p_{ACtype_i} \leq d_{ACtypes_j} \tag{8.1}$$

Hereafter, it is determined over which IAF each aircraft will approach the airport. Using a traceable seed, semi-random p values (p_{IAF}) between 0 and 1 are generated for each arriving aircraft i ($AC_{arriving}$). The IAF traffic load distribution input includes which IAFs are present and their respective p-value interval. If the p-value of arriving aircraft i falls within the p-value interval of IAF j, arriving aircraft i will approach the airport over IAF j, see Equation 8.2.

$$d_{IAF_{j-1}} < p_{IAF_i} \leq d_{IAF_j} \tag{8.2}$$

Subsequently, the scenario generator needs to determine the creation time of each arriving aircraft in the scenario. The arrivals must be reasonably equally distributed over time such that the arriving aircraft do not arrive all around the same time. The total number arriving aircraft over each IAF is calculated. With the total number of arriving aircraft per IAF, the average inter-generation time per IAF can be calculated by dividing the scenario duration by the number of arriving aircraft per IAF. Subsequently, the creation time of arriving aircraft i is equal to i times the average inter-generation time plus a semi-random integer to include some variability. As in this research, it is less important how the arriving aircraft reach the horizon of AMAN; each IAF connects to one origin flight plan. The creation time is the time the aircraft appears at the origin.

8.4. Departing Aircraft Generation

Likewise generating the arriving aircraft, the number of arrivals per hour, and the scenario duration determines the total number of departing aircraft that the scenario has to contain. Each departing aircraft gets a distinct aircraft ID. For generating the aircraft types for each departure, the same method holds as for the arrivals. However, here the airports departing traffic mix distribution is used.

Furthermore, each departing aircraft is allocated to a SID. Using a traceable seed, semi-random p values (p_{SID}) between 0 and 1 are generated for each departing aircraft i ($AC_{departing}$). The airports' traffic load SID distribution includes all SIDs and their respective p-value interval. If the p-value of departing aircraft i falls within the p-value interval of SID j, departing aircraft i will take-off via SID j, see Equation 8.3.

$$d_{SID_{j-1}} < p_{SID_i} \leq d_{SID_j} \tag{8.3}$$

The airports' gate coordinates input is used to assign each departing aircraft to a gate location. To avoid each departure being generated at the same location; for each departing aircraft, the scenario generator uses semi-random integers to match a departing aircraft to a gate at the specific airport.

Last, the creation time of each departure must be determined. The departures must be relatively equally spread throughout the scenario. Moreover, it is crucial to make sure that the AMAN and DMAN schedule their aircraft in the same time interval, otherwise arriving and departing aircraft do not conflict with one another. Assuming that DMAN know at time t-50 minutes, the first departing aircraft need to appear 50 minutes in advance to the first arrival reaches the AMANs EH. The SID number of the departing aircraft determines the trajectory of the departing aircraft within the TMA. Each SID connects to one destination. Once a departing aircraft is below 50 ft. at its destination, the scenario file deletes the aircraft.

III

Experiments

9

Experiment I: Arrival and Departure Capacity Interference

Chapter 4 showed that the departure capacity of dependent arrival and departure runways combinations is lower than the departure capacity of independent arrival and departure runways. These results contributed to answering the first part of research question X: what is the current magnitude of arrival and departure capacity interference? However, the second part of the research question, which investigates the future magnitude of arrival and departure capacity interference, cannot be answered with empirical data. Therefore experiment I is designed to give insight into the future magnitude of arrival and departure capacity interference. This experiment may also demonstrate the importance of a coordination mechanism between the management of arrivals and departures.

9.1. Experimental Set-Up

Table 4.5 showed that arrival runway 18C and departure runway 24 is the most frequently used arrival and departure runway combination at AAS which is affected by the missed approach dependency, see Figure 9.1. Therefore, experiment I uses arrival and departure runway combination to assess future arrival and departure capacity interference. The 1+1 configuration causes arriving aircraft from each IAF will all land on the same runway. Likewise, departing aircraft for all sectors will depart from the same runway.

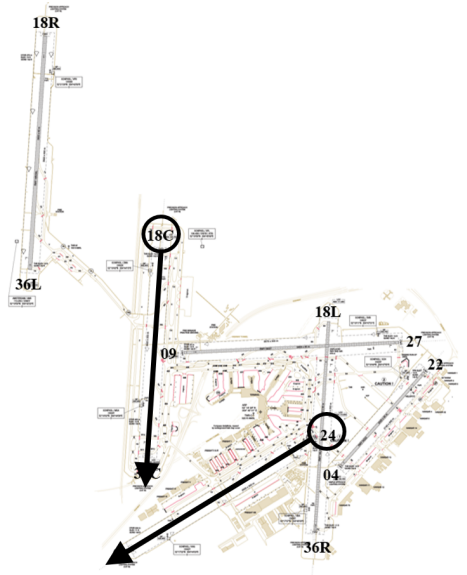

Figure 9.1: Arrival runway 18C in combination with departure runway 24 at AAS

The missed approach dependency at AAS states that a departing aircraft receives a take-off clearance when the nearest arriving aircraft is at least 2 NM away from the runway threshold. When the next arriving aircraft is already within 2 NM distance from the runway threshold, the departing aircraft will only be released when the arriving aircraft has completed its landing. Chapter 2 mathematically expressed this dependency.

9.1.1. Apparatus

As the uncoordinated model aims to mimic current day arrival and departure management, this model can be used to investigate the severeness of arrival and departure capacity interference now and in the future. In the uncoordinated model, arrivals are scheduled independently from departures and departures are interweaved in the arrival sequence when an arrival interval is large enough to accommodate a departure.

9.1.2. Independent Variables

The results of this experiment depend on many inputs of the different modules and elements of the uncoordinated model. Since this research is in collaboration with the Knowledge and Development Center, Air Traffic Control the Netherlands provides the empirical data and expert knowledge used as input by the modules. Table 9.1 shows an overview of the required input of the uncoordinated model and which input is used for it.

Table 9.1: AMAN input variables

Variable	Input
Active arrival runway	18C
Eligibility horizon	30 min
Active Advisory horizon	15 min
Declared capacity	3 NM
TP SD	3 NM

Table 9.2: DMAN input variables

Variable	Input
Active departure runway	24
Declared capacity	variable

Table 9.3: Performance module input data

Variable	Input	Defined per
Average approach speed	EHAM runway 18C	aircraft type
Average departure speed	EHAM runway 24	aircraft type
Arrival completion time	SYSTEM X	aircraft WTC
Departure completion time	LVNL operational expert	aircraft WTC
Runway occupancy time	EHAM runway 24	aircraft WTC
SID common departure path	AIP the Netherlands	SID combination
Distance-based separation minima	ICAO	aircraft WTC
Time-based separation minima	ICAO	aircraft WTC

9.1.3. Traffic Scenarios

In the conditional set-up of experiment I, three levels of arrival loads are chosen, (1) a low level of arrival load, 30 arrivals per hour, (1) an medium level of arrival load, 35 arrivals per hour, and (3) a high level of arrival load, 40 arrivals per hour. For the departing aircraft load, the experiment only uses levels to decrease the total number of experimental set-ups, (1) a low level of departure load, 30 departures per hour, and (2) a high level of departure load, 40 departures per hour. The declared capacity of the DMAN is equal to one of the two loads.

The arriving and departing aircraft traffic mix at AAS differs during the day. The number of heavies is higher in the morning than in the evening due to the transatlantic traffic. Therefore, a distinction between the traffic mix in the morning and the evening in the conditional set-up. The morning uses the arriving and corresponding departing traffic mix distribution of an arrival peak period. Likewise, the evening uses the arriving and corresponding departing traffic mix distribution of an arrival peak period.

The scenario generator described in Chapter 10.1.3 is used to generate scenarios according to the experimental set-ups presented in Table 9.4 and the independent variables. Each scenario performs 25 repeats. In total, 12 scenarios will be examined in this experiment and thus, 300 simulations.

Table 9.4: Traffic scenarios

Scenario	Arrivals	Departures	Traffic mix distribution	Duration	Repeats
1	30/hour	30/hour	Morning arrival peak	1.5 hour	25
2			Evening arrival peak	1.5 hour	25
3		40/hour	Evening arrival peak	1.5 hour	25
4			Morning arrival peak	1.5 hour	25
5	35/hour	30/hour	Morning arrival peak	1.5 hour	25
6			Evening arrival peak	1.5 hour	25
7		40/hour	Evening arrival peak	1.5 hour	25
8			Morning arrival peak	1.5 hour	25
9	40/hour	30/hour	Morning arrival peak	1.5 hour	25
10			Evening arrival peak	1.5 hour	25
11		40/hour	Evening arrival peak	1.5 hour	25
12			Morning arrival peak	1.5 hour	25

9.1.4. Measurements

To express the severeness of arrival and departure capacity interference, experiment I uses capacity as Key Performance Area (KPA). Therefore, each repeat will be evaluated using the following metrics:

1. Arrival capacity: the number of arrivals that landed per hour, which is equal to the total number of arrivals (n_{ar}) divided by the arrival time interval times the number of seconds in one hour, see Equation 10.1. The arrival time interval equals the Actual Time of Arrival of the last arriving aircraft ($ATA_{i=n}$) relative to the Actual Time of Arrival of the first arriving aircraft ($ATA_{i=0}$). The arrival capacity is calculated per repeat.

$$C_{ar} = \frac{n_{ar}}{ATA_{i=n_{ar}} - ATA_{i=0}} \cdot 3600 \tag{9.1}$$

2. Departure capacity: the number of departures that landed per hour, which is equal to the total number of departures (n_{ar}) that took off divided by the departure time interval times the number of seconds in one hour, see Equation 10.2. Since the time interval in which aircraft arrive and the time interval in which aircraft depart may not fully align, the departure time interval starts when the first departure takes off, the Actual Take-Off Time ($ATOT_{i=0}$). Considering that the AFI finder cannot give departure clearances anymore after the last arrival has landed, the end of the departure time interval is equal to the Actual Time of Arrival of the last arriving aircraft ($ATA_{i=n}$). As the latter may cause that not all departing aircraft take-off within the arrival time interval, the departure time interval is divided by the number of departures that took-off. The departure capacity is calculated per repeat.

$$C_{dep} = \frac{n_{dep}}{ATA_{i=n_{ar}} - ATOT_{i=0}} \cdot 3600 \tag{9.2}$$

3. Arrival delay: the time difference between the Actual Time of Arrival (ATA_i) and the Earliest Time of Arrival (ETA_i) summed over all arriving aircraft and divided by the total number of arriving aircraft (n_{ar}), see Equation 10.3. The latter is the average delay imposed by the AMAN to ensure the minimum required time between two arriving aircraft. The arrival delay is calculated per repeat.

$$D_{ar} = \frac{\sum_{i=0}^{n_{ar}} ATA_i - ETA_i}{n_{ar}} \tag{9.3}$$

4. Departure delay: the time difference between the Actual Take-Off Time ($ATOT_i$) and the Target Take-Off Time ($TTOT_i$) summed over all departing aircraft that took-off and divided by the total number of departing aircraft that took-off (n_{dep}), see Equation 10.4. This delay represents the delay that is due to the dependency between the arrival and departure runway. The departure delay is calculated per repeat.

$$D_{dep} = \frac{\sum_{i=0}^{n_{dep}} ATOT_i - TTOT_i}{n_{dep}} \tag{9.4}$$

9.1.5. Hypotheses

Assuming that the arrival load will increase due to RECAT and TBS in the future, the AMAN will schedule tighter arrival streams. Subsequently, it becomes harder to interweave departing aircraft in the arrival stream when the arrival intervals are smaller. This will probably result in a lower departure capacity and higher departure delay compared to lower arrival load scenarios. So, the expectation is that the arrival and departure capacity interference will worsen in the future.

When distinguishing between the arrival and departure capacity interference during morning arrival peaks and evening arrival peaks at AAS, the outcomes are hard to predict. Table 4.10 and 4.11 show that the number of heavies is higher in the morning than in the evening. More heavies in the arriving fleet mix will result in larger arrival intervals. Theoretically, this would make it easier to interweave departures in the arrival stream. However, the number of heavies in the departing fleet mix is even higher than the number of heavies in the arriving fleet mix. Due to the increased spacing between departing aircraft, the benefit of the increased arrival spacing may fade away. The exact interaction between the arriving fleet mix and the departing fleet mix is unknown, and therefore this part of the experiment is exploratory.

9.2. Results

The results of experiment 1 are presented for: (1) when no distinction is made in the time of the day, and (2) when a distinction is made between morning and evening. Arrival and departure capacity interference becomes most apparent when the pressure at the departure runway is high, this section presents the results for a departure load of 40 atm/hour. Appendix B presents the same results for a departure load of 30 atm/hour.

9.2.1. Total

Figure 9.2 and 9.3 shows the departure capacity as a function of the arriving capacity when no distinction is made between morning and evening. The figures depict the interaction between arrival capacity and departure capacity. The departure capacity decreases as a result of an increase in the arrival capacity. When the arrival load increases with 10 atm/hour, the departure capacity drops with almost 5 atm/hour.

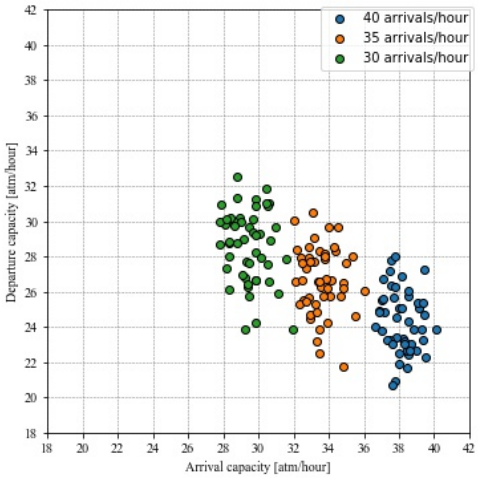

Figure 9.2: Departure capacity as a function of the arrival capacity

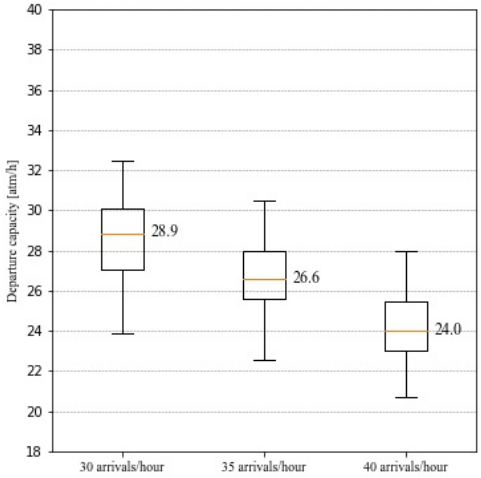

Figure 9.3: Departure capacity as a function of the arrival load

Figure 9.2 also shows that the arrival capacity at an arrival load of 30 arrivals per hour approximately ranges between 28 and 31.5 atm/hour. For an arrival load of 35 atm/hour, the arrival capacity ranges between 31.5 and 36 atm/hour. For the highest arrival load, the arrival capacity ranges between 36.5 and 41 atm/hour. Figure 9.2 and 9.3 show the spread of the departure capacity. The spread of the departure capacity is significantly larger compared to the spread arrival capacity. For each of the arrival load, the departure spread is approximate ± 3.5 atm/hour relative to the median.

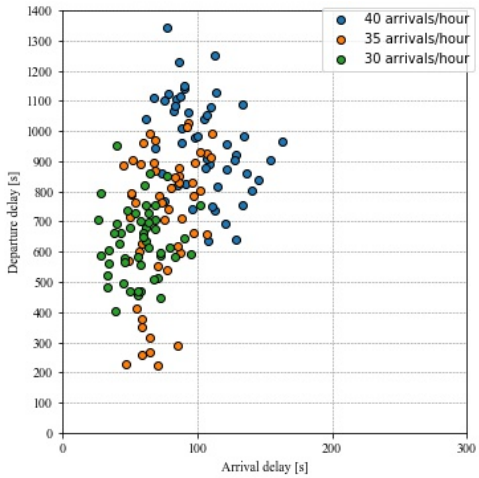

Figure 9.4: Departure delay as a function of the arrival delay

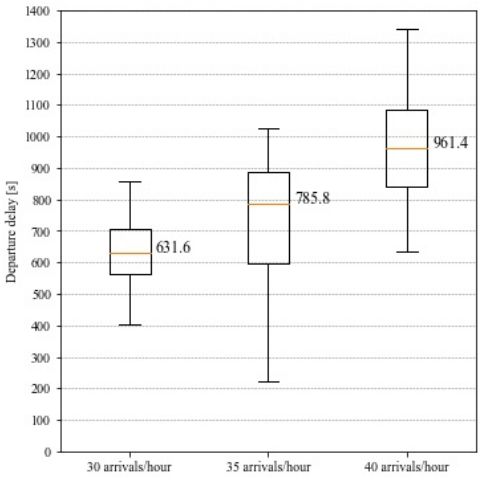

Figure 9.5: Departure delay as a function of the arrival load

Figure 9.4 and 9.5 respectively show the average departure delay as a function of the arrival delay and arrival load. Figure 9.4 shows that the arrival delay increases for higher arrival loads. Also, the departure delay increases for higher arrival loads. For each increase of 5 atm/hour in arrival load, the departure delay increases with over 20%.

9.2.2. Morning and Evening

This section splits the results presented above into two: (1) for a morning peak-period, and (2) for an evening peak-period. This results in the sample size being half of the sample size of the previous section. The morning results used the arriving and corresponding departing traffic mix distribution at AAS during the morning. Likewise, the evening results were obtained using the arriving and corresponding departing traffic mix distribution during the morning. The number of heavies in the traffic mix for both arrivals and departures is higher in the morning compared to the evening.

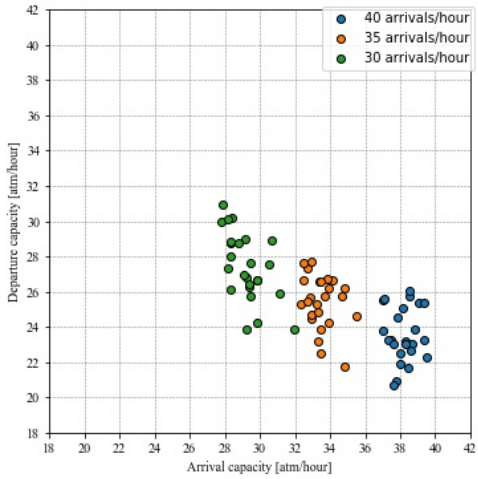

Figure 9.6: Departure capacity as a function of the arrival capacity in the morning

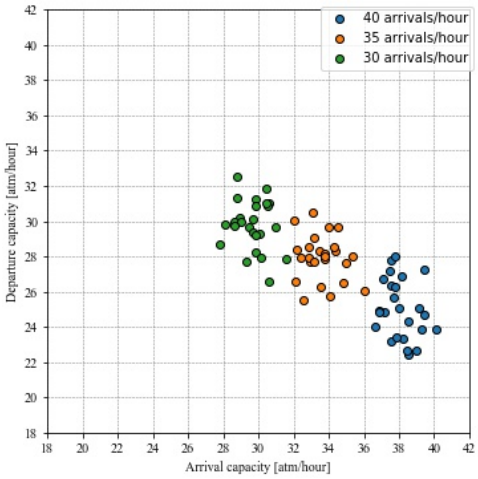

Figure 9.7: Departure capacity as a function of the arrival capacity in the evening

Figure 9.6 and 9.7 show the departure capacity as a function of the arrival capacity in respectively the morning and evening. The spread of the arrival capacity in the evening is higher compared to the morning. The range of the departure capacity in the morning and evening are similar to one another. Furthermore, Figure 9.6 and 9.7 show that the interaction between arrival and departure capacity is stronger in the morning than in the evening. Figure 9.8 and 9.9 support this. Here, the departure capacity is plotted as a function of the arrival load. The departure capacity is approximately 2 atm/hour lower for each of the arrival loads in the morning compared to the evening.

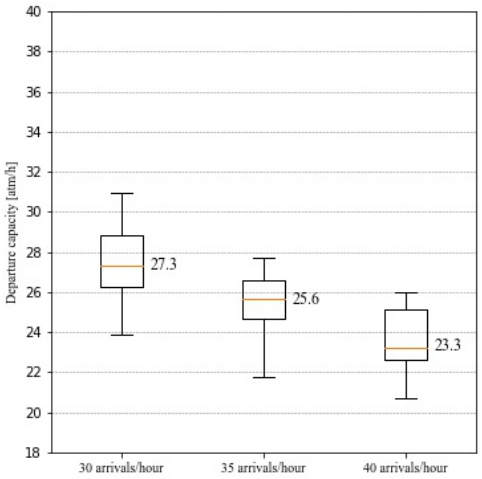

Figure 9.8: Departure capacity as a function of the arrival load in the morning

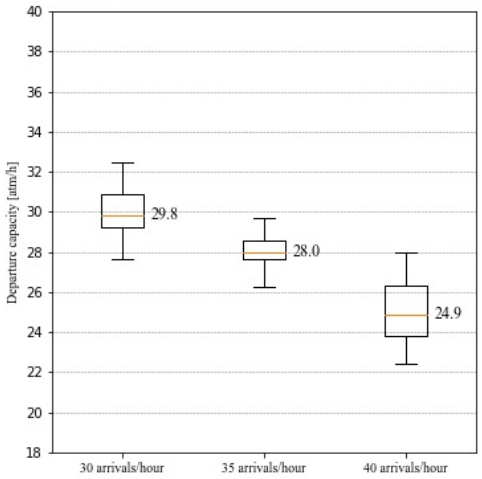

Figure 9.9: Departure capacity as a function of the arrival load in the evening

Figure 9.10 and 9.11 depict the departure delay as a function of the arrival delay for respectively the morning peak period and the evening peak period. Comparing the two figures shows that the range in arrival delay is larger in the morning than in the evening. The maximum average arrival delay is approximately 50 seconds higher in the morning than in the evening. Figure 9.12 and 9.13 show the departure delay as a function of the arrival load during respectively a morning and evening peak period. Here it is seen that the departure delay is higher in the morning for an arrival load of 30 and 35 atm/hour compared to the evening. The departure delay for an arrival load of 40 atm/hour in the evening is significantly higher than in the morning.

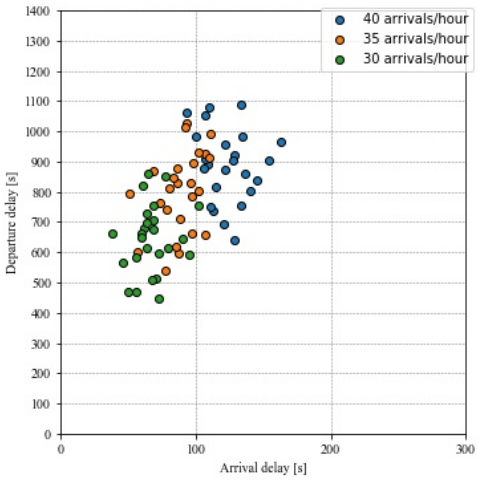

Figure 9.10: Departure delay as a function of the arrival delay in the morning

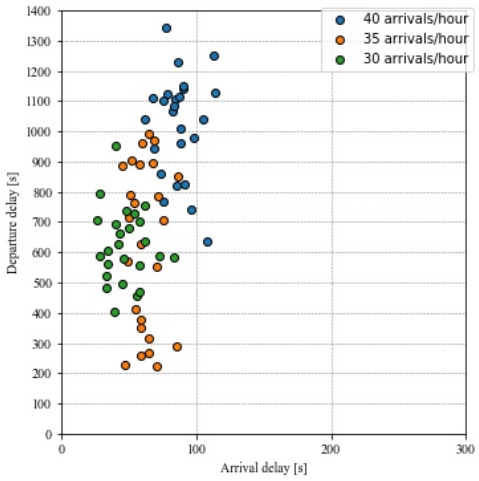

Figure 9.11: Departure delay as a function of the arrival delay in the evening

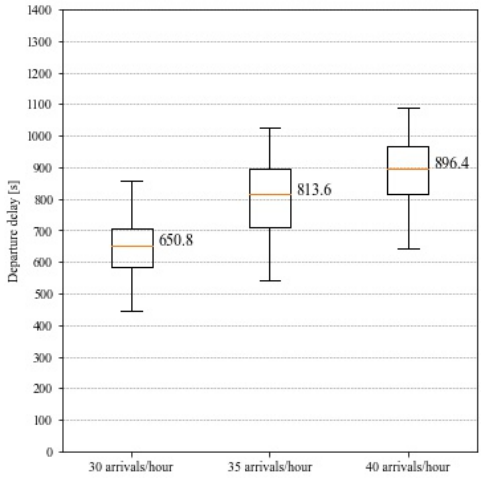

Figure 9.12: Departure delay as a function of the arrival load in the morning

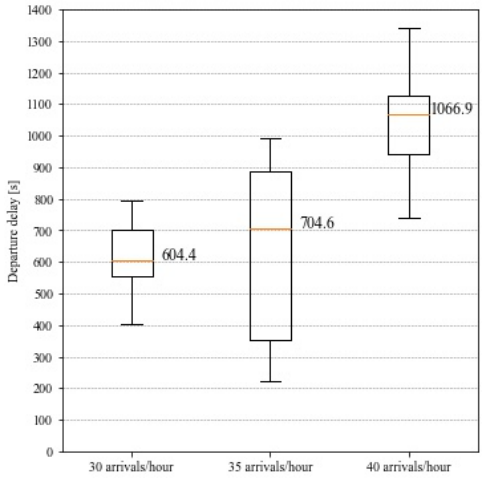

Figure 9.13: Departure delay as a function of the arrival load in the evening

9.3. Discussion

Experiment I was designed to give insight into the future magnitude of arrival and departure capacity interference. The dependency of arrival runway 18C and departure runway 24 at AAS was used to assess the interference. The experiment used the uncoordinated model for testing various conditions which distinguished between different levels of arriving and departure load and between arrival and departure traffic mix distribution in the morning and evening.

The ranges in departure capacity is probably a cause of a combination of two: (1) the scenario generator and, (2) the working principles of the AMAN and the ATCO module. The scenario generator determines the creation times of arriving aircraft semi-randomly. The AMAN in imposes delays solely. The AMAN will not schedule arriving aircraft such that they will need to be advanced. Furthermore, the ATCO module cannot perform the tactical actions executed by ATCOs in real life, like changing the arrival sequence and frontloading. The combination of these may cause the timings of the arriving aircraft at the eligibility horizon to be more advantageous for the departures for one scenario compared to the other.

The average arrival delay increases for higher arrival loads compared to lower arrival loads, as was expected. Considering that the pressure at the arrival runway increases for higher arrival loads, and the AMAN schedules maintaining at least the minimum required IAT, arriving aircraft delays will accumulate. The results showed as well that the average arrival delay is higher in the morning than in the evening. This is as expected since in the evening the percentage heavies in the traffic mix are low, arriving aircraft are allowed to land closer to one another, which increases the arrival capacity and lowers the delay.

The results showed that when the arrival load increases the departure capacity decreases as a result. This corresponds to the hypothesis, when the arrival load increases, the AMAN will generate tighter arrival streams. For the ATCO module, it will become more challenging to find an arrival interval that is large enough to fit a departure. Furthermore, the arrival and departure capacity interference is more substantial in the morning than in the evening at AAS. This means that, even though larger IATs are present due to high amount of heavies in the mix, the departure ground situation cannot take advantage of this because the number of heavies in departing aircraft traffic mix is also high.

Assuming a current arrival load of 35 atm/hour and assuming the arriving and departing aircraft traffic mix does not significantly change in the future, it can be concluded that the departure capacity at runway 24 will drop by 2.3 atm/hour and 3.1 atm/hour respectively during the morning arrival-peak period and evening arrival-peak period when the arrival load increases to 40 atm/hour.

10

Experiment II: Coordinated Arrival and Departure Management

Chapter 6 elaborated the working principles and algorithms of three coordination modules between the AMAN and DMAN. Each of the coordination modules aims to increase the throughput of dependent arrival and departure runway combinations. This experiment will assess the performance of each coordination module to answer research question X.

10.1. Experimental Set-Up

Like in experiment I, arrival runway 18C and departure runway 24 at AAS is used to assess the three coordination modules. Arrival runway 18C and departure runway 24 is the most frequently used arrival and departure runway combination at AAS, which is affected by the missed approach dependency, see Figure 10.1. Chapter 2 explained the interaction between arrivals and departures for this dependency. The single arrival and departure runway combination causes arriving aircraft from each IAF will all land on the same runway. Likewise, departing aircraft for all sectors will depart from the same runway.

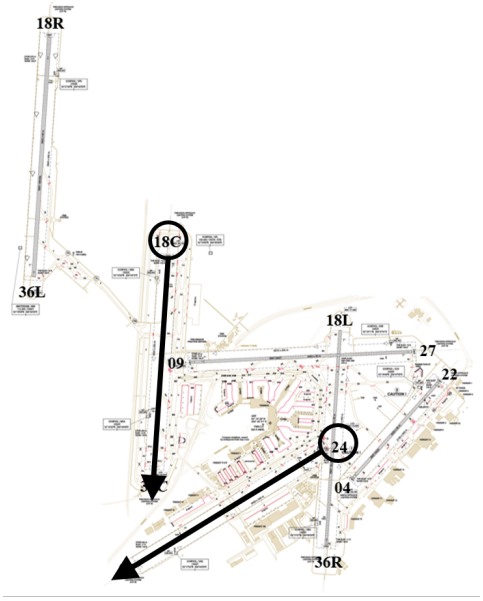

Figure 10.1: Arrival runway 18C in combination with departure runway 24 at AAS

10.1.1. Apparatus

For performing this experiment 4 models are used: (1) the uncoordinated ADMAN, (2) the coordinated ADMAN using coordination module I, (3) the coordinated ADMAN using coordination module II, and (4) the coordinated ADMAN using coordination module III. The uncoordinated ADMAN serves as a baseline model to which the coordination modules can be compared to. Chapter 6 explained that coordination module I calculates the number available departure slots assuming all departures as WTC M. In coordination module II, the number of heavies in the departing fleet mix is taken into account by incorporating a time margin over the minimum required IADT and IDAT. The last coordination module, coordination module III, distinguishes between departure slots that fit aircraft WTC M and departure slots that fit aircraft WTC H.

10.1.2. Independent Variables

The independent variables that are used in experiment 2 can be found in Table 10.1, 10.2, 10.3, and 10.4. Since the coordination modules will be evaluated using AAS as case, the performance module is filled with data from AAS as well.

Table 10.1: AMAN input variables

Variable	Input
Active arrival runway	18C
Eligibility horizon	30 min
Active Advisory horizon	15 min
Declared capacity	3 NM

Table 10.2: DMAN input variables

Variable	Input
Active departure runway	24
Declared capacity	30, or 40 atm/h

Table 10.3: Coordination module input variables

Variable	Input
Preferred departure-to-arrival ratio	1.0
Active coordination module	Module I, II or III

Table 10.4: Performance module input data

Variable	Input	Defined per
Average approach speed	EHAM runway 18C	Aircraft type
Average departure speed	EHAM runway 24	Aircraft type
Arrival completion time	SYSTEM X	Aircraft WTC
Departure completion time	LVNL Operational expert	aircraft WTC
Runway occupancy time	EHAM runway 24	Aircraft WTC
SID common departure path	AIP the Netherlands	SID combination
Distance-based separation minima	ICAO	Aircraft WTC
Time-based separation minima	ICAO	Aircraft WTC

10.1.3. Traffic Scenarios

In the conditional set-up of experiment 2, three levels of arrival load are chosen, (1) a low level of arrival load, 30 arrivals per hour, (1) an medium level of arrival load, 35 arrivals per hour, and (3) a high level of arrival load, 40 arrivals per hour. For the departing aircraft load, the experiment only uses levels to decrease the total number of experimental set-ups, (1) a low level of departure load, 30 departures per hour, and (2) a high level of departure load, 40 departures per hour. The declared capacity of the DMAN is equal to one of the two loads.

The scenario generator described in Chapter is used to generate scenarios according to the experimental set-ups presented in Table 9.4 and the independent variables. Each scenario performs 25 repeats. In total, 12 scenarios will be examined in this experiment and thus, 300 simulations.

Table 10.5: Traffic scenarios

Scenario	Arrivals	Departures	Traffic mix distribution	Duration	Repeats
1	30/hour	30/hour	Morning arrival peak	1.5 hour	25
2			Evening arrival peak	1.5 hour	25
3		40/hour	Evening arrival peak	1.5 hour	25
4			Morning arrival peak	1.5 hour	25
5	35/hour	30/hour	Morning arrival peak	1.5 hour	25
6			Evening arrival peak	1.5 hour	25
7		40/hour	Evening arrival peak	1.5 hour	25
8			Morning arrival peak	1.5 hour	25
9	40/hour	30/hour	Morning arrival peak	1.5 hour	25
10			Evening arrival peak	1.5 hour	25
11		40/hour	Evening arrival peak	1.5 hour	25
12			Morning arrival peak	1.5 hour	25

10.1.4. Measurements

To assess the performance of the three coordination modules, capacity will be used as the main Key Performance Area (KPA). Therefore, each repeat for every model will be evaluated using the following metrics:

1. Arrival capacity: the number of arrivals that landed per hour, which is equal to the total number of arrivals (n_{ar}) divided by the arrival time interval times the number of seconds in one hour, see Equation 10.1. The arrival time interval equals the Actual Time of Arrival of the last arriving aircraft ($ATA_{i=n}$) relative to the Actual Time of Arrival of the first arriving aircraft ($ATA_{i=0}$). The arrival capacity is calculated per repeat.

$$C_{ar} = \frac{n_{ar}}{ATA_{i=n_{ar}} - ATA_{i=0}} \cdot 3600 \tag{10.1}$$

2. Departure capacity: the number of departures that landed per hour, which is equal to the total number of departures (n_{ar}) that took off divided by the departure time interval times the number of seconds in one hour, see Equation 10.2. Since the time interval in which aircraft arrive and the time interval in which aircraft depart may not fully align, the departure time interval starts when the first departure takes off, the Actual Take-Off Time ($ATOT_{i=0}$). Considering that the AFI finder cannot give departure clearances anymore after the last arrival has landed, the end of the departure time interval is equal to the Actual Time of Arrival of the last arriving aircraft ($ATA_{i=n}$). As the latter may cause that not all departing aircraft take-off within the arrival time interval, the departure time interval is divided by the number of departures that took-off. The departure capacity is calculated per repeat.

$$C_{dep} = \frac{n_{dep}}{ATA_{i=n_{ar}} - ATOT_{i=0}} \cdot 3600 \tag{10.2}$$

3. Arrival delay: the time difference between the Actual Time of Arrival (ATA_i) and the Earliest Time of Arrival (ETA_i) summed over all arriving aircraft and divided by the total number of arriving aircraft (n_{ar}), see Equation 10.3. The latter is the average delay imposed by the AMAN to ensure the minimum required time between two arriving aircraft. The arrival delay is calculated per repeat.

$$D_{ar} = \frac{\sum_{i=0}^{n_{ar}} ATA_i - ETA_i}{n_{ar}} \tag{10.3}$$

4. Departure delay: the time difference between the Actual Take-Off Time ($ATOT_i$) and the Target Take-Off Time ($TTOT_i$) summed over all departing aircraft that took-off and divided by the total number of departing aircraft that took-off (n_{dep}), see Equation 10.4. This delay represents the delay that is due to the dependency between the arrival and departure runway. The departure delay is calculated per repeat.

$$D_{dep} = \frac{\sum_{i=0}^{n_{dep}} ATOT_i - TTOT_i}{n_{dep}} \tag{10.4}$$

5. Coordination module interventions: the number of times the coordination module had to adjust the scheduled arrivals by (1) slack advancing, (2) slack delaying and (3) aircraft delaying. Each coordination module could perform the latter three in one update, so the number does not represent the number of times the coordination module changes the arrival schedule.

6. Workload: the coordination modules changes the arrival schedule. This may result in more considerable delays for the arriving aircraft to absorb. ATCOs use information from the AMAN to guide aircraft in the TMA by either speed adjustments, vectoring or holding. As the type of delay adsorption depends on the size of the delay, the delay changes may cause a change in the distribution between the types of delay absorption. The workload metric categorizes each arrival delay as one of the delay adsorption types by Equation 10.5, 10.6 and 10.7.

$$\text{Speed:} \quad D_{ar_i} \leq 180 \text{ s} \tag{10.5}$$

$$\text{Vectoring:} \quad 180 \text{ s} < D_{ar_i} \leq 540 \text{ s} \tag{10.6}$$

$$\text{Holding:} \quad D_{ar_i} > 540 \text{ s} \tag{10.7}$$

10.1.5. Hypotheses

Experiment II evaluates the logic behind the coordination modules for the first time. Therefore, it is part of exploratory research. For this, no formal hypothesis testing will be performed. However, some probable outcomes have been formulated to help the thought process. All coordination modules use the departure situation as input for the metering of arriving aircraft in the TMA. Consequently, the departure capacity will become higher, and the departure delay will become lower, compared to when there is no coordination module present between the AMAN and DMAN. On the arrival side, the arrival capacity will decrease, and the arrival delay will be higher for the coordinated cases compared to the uncoordinated cases. No estimation of the magnitude of the increases and decreases of the delays and capacity can be made.

Since coordination module II uses a heavy time margin on top of the minimum required IADT and IDAT for a medium departure, AIs need to be larger before coordination module II assigns a departure slot to the AI compared to coordination module I. Coordination module II meters the inbound traffic using larger AIs, therefore, the expectation is that the resulting departure capacity of coordination module II will be larger, and the resulting departure delay lower compared to coordination module I.

Coordination module III meters the arriving aircraft as a function of the departure situation by distinguishing between departure slots that fit a departure of WTC M and WTC H. The coordination module creates AIs for departures of WTC M or H, only having knowledge on the number of heavies in the departing traffic, but without knowing the exact location of the planned departure in the arrival stream. It may be the case that a medium departure takes-off in an AI which is tailored for a heavy departure because no heavy departure is ready to take-off. To what extend this will or will not happen is unpredictable.

10.2. Results

The results of experiment 2 are presented for the different levels of arrival load: (1) low arrival load, (2) medium arrival load, and (3) high arrival load. Arrival and departure capacity interference becomes most apparent when the pressure at the departure runway is high; this section presents the results for a departure load of 40 atm/hour. Appendix C presents the same results for a departure load of 30 atm/hour. One should keep in mind that the coordination modules aim for a preferred departure-to-arrival ratio of 1.

10.2.1. Low Arrival Load

Figure 10.2 shows the arrival and departure capacity for an arrival load of 30 atm/hour. For the uncoordinated model, the arrival capacity is approximately 30 atm/hour. The departure capacity is slightly lower than the arrival capacity, 0.5 atm/hour lower. Coordination modules I, II and III raise the departure capacity by respectively 1.8, 3.2, and 2.7 atm/hour. The departure capacity of coordination module III is lower compared to coordination module II; however, the spread is slightly lower.

Figure 10.3 shows the average arrival and departure delay for an arrival load of 30 atm/hour. The average arrival delay hardly changes over the uncoordinated ADMAN and coordination mechanism I and II. The arrival

delay is even lower for coordination mechanism I and II compared to the uncoordinated case. For coordination module I the arrival delay increases with 23.4 % relative to the uncoordinated ADMAN. The departure delay decreases with 25.7%, 35.1% and 36.7% for respectively coordination modules I, II and III.

Figure 10.4 show the number of times the coordination module had to intervene in the arrival schedule by slack delaying, slack advancing or delaying for an arrival load of 30 atm/hour. The number of times coordination module I and II resolve the conflicts by delaying aircraft is almost zero. Coordination module II intervenes the arrival schedule more often than coordination module I as the number of times coordination module II adjusts the arrival schedule by slack advancing and slack delaying is higher. The total number of interventions of coordination module III is higher than the number of interventions of coordination module I and II. Specifically, the number of times coordination module III adjusts the arrival schedule by delaying arriving aircraft is high compared to coordination module I and II. The number interventions per minute for coordination module I, II, and III is respectively 0.5, 0.6 and 0.9.

Figure 10.5 shows that the distribution between the types of delay adsorption hardly changes for coordination module I and II. The number of arriving aircraft that absorbs its delay by vectoring is even lower than for the uncoordinated case. As the delays increase for coordination module III, the number of aircraft that absorb its delay by vectoring is also higher for coordination module III.

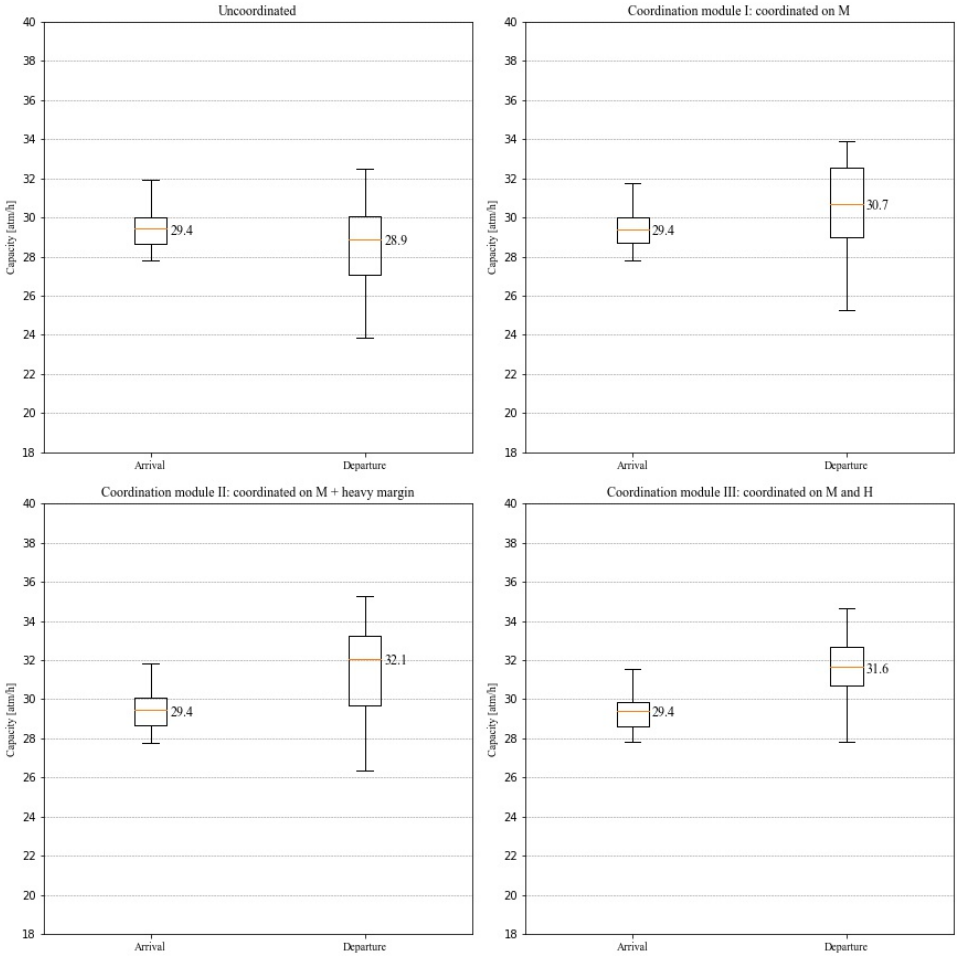

Figure 10.2: Arrival and departure capacity for the uncoordinated and coordinated ADMANs

10.2.2. Medium Arrival Load

Figure 10.6 shows the arrival and departure capacity for an arrival load of 35 atm/hour. For the uncoordinated model, the arrival capacity is approximately 33.5 atm/hour, which is less than the arrival load. Furthermore, the departure capacity is significantly lower than the arrival capacity, 6.9 atm/hour lower. Coordination mod-

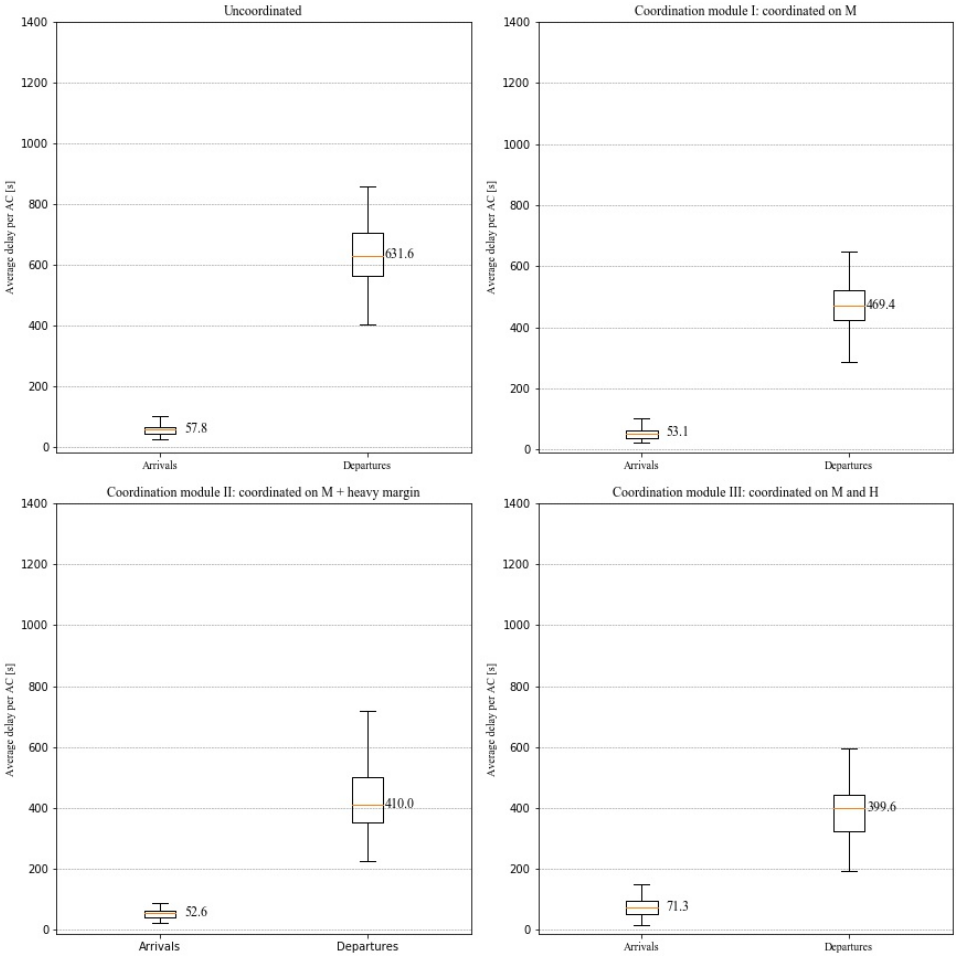

Figure 10.3: Arrival and departure delay for the uncoordinated and coordinated ADMANs

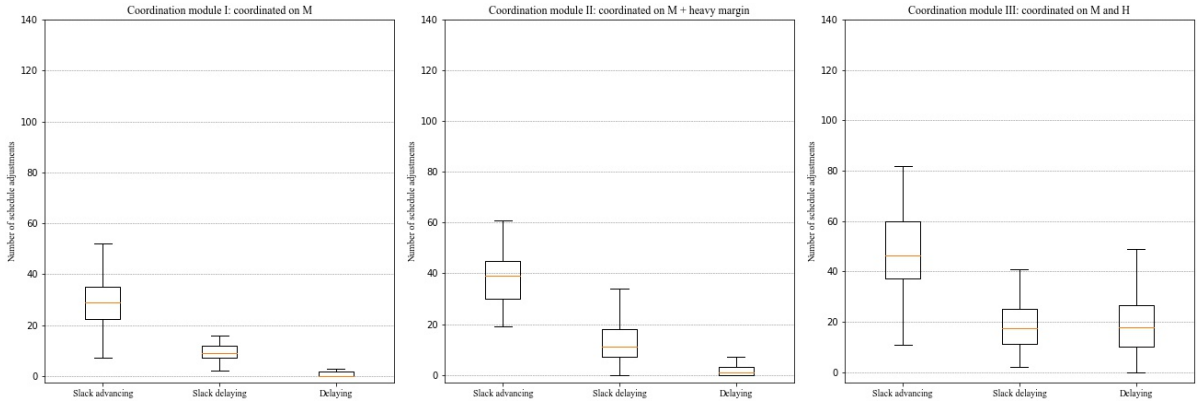

Figure 10.4: Coordination mechanism interventions

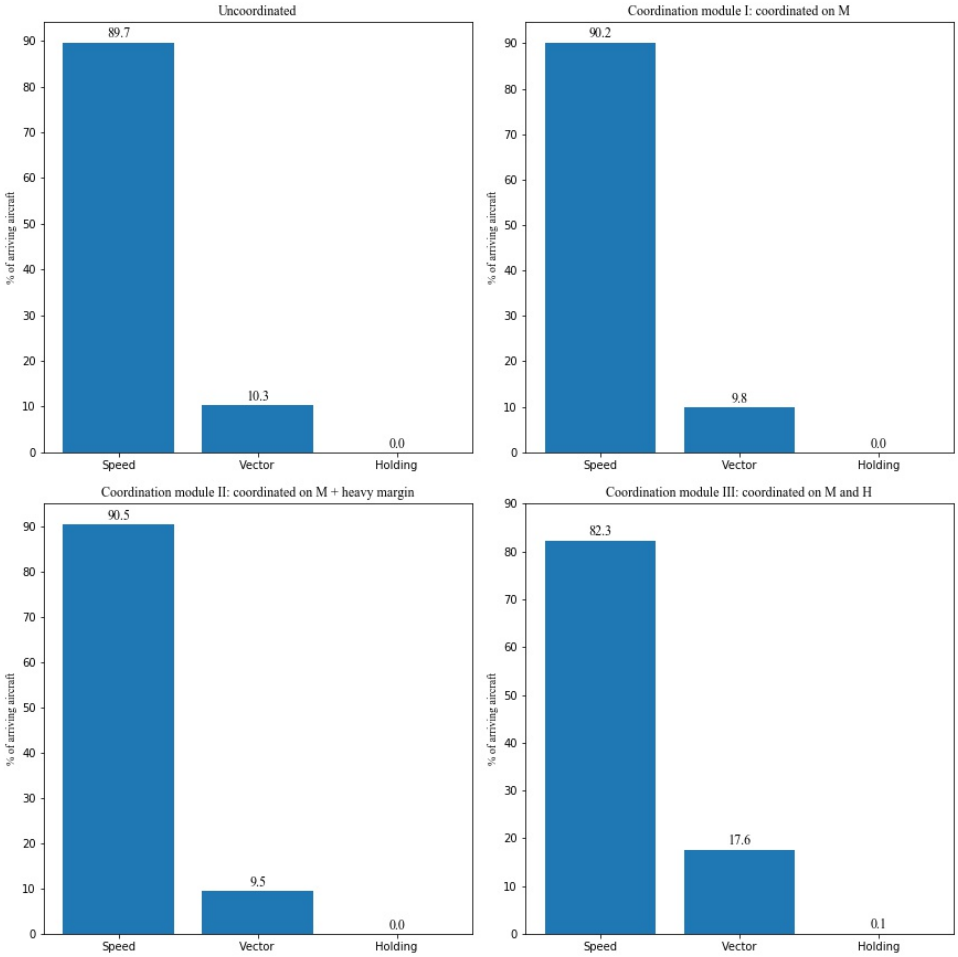

Figure 10.5: Workload

ules I, II and III raise the departure capacity by respectively 4.0, 4.5, and 5.2 atm/hour without losing noteworthy arrival capacity. The spread of the departure capacity for coordination module III is about half the spread of the departure capacity of coordination module I and II.

Figure 10.7 shows the average arrival and departure delay for an arrival load of 35 atm/hour. The average arrival delay hardly changes over the uncoordinated ADMAN and coordination mechanism I and II. The arrival delay is even lower for coordination mechanism I and II compared to the uncoordinated case. For coordination module III, the arrival delay increases significantly relative to the uncoordinated ADMAN. The departure delay decreases with 40.4%, 43.7% and 48.6% for respectively coordination modules I, II and III.

Figure 10.8 show the number of times the coordination module had to intervene in the arrival schedule by slack delaying, slack advancing or delaying for an arrival load of 35 atm/hour. The number of times coordination module I and II resolve the conflicts by delaying aircraft is approximately ten times. Coordination module II intervenes the arrival schedule more often than coordination module I as the number of times coordination module II adjusts the arrival schedule by slack advancing and slack delaying is higher. The total number of interventions of coordination module III is higher than the number of interventions of coordination module I and II. Specifically, the number of times coordination module III adjusts the arrival schedule by delaying arriving aircraft is high compared to coordination module I and II.

Figure 10.9 shows that the distribution between the types of delay adsorption hardly changes for coordination module I and II. The number of arriving aircraft that absorbs its delay by vectoring is even lower than for the uncoordinated case. For coordination module III the distribution between the types of delay absorption is turned around. The number of arriving aircraft that will be vectored into the TMA or stacked before entrance

increases respectively with 42.2 % and 8.8 %.

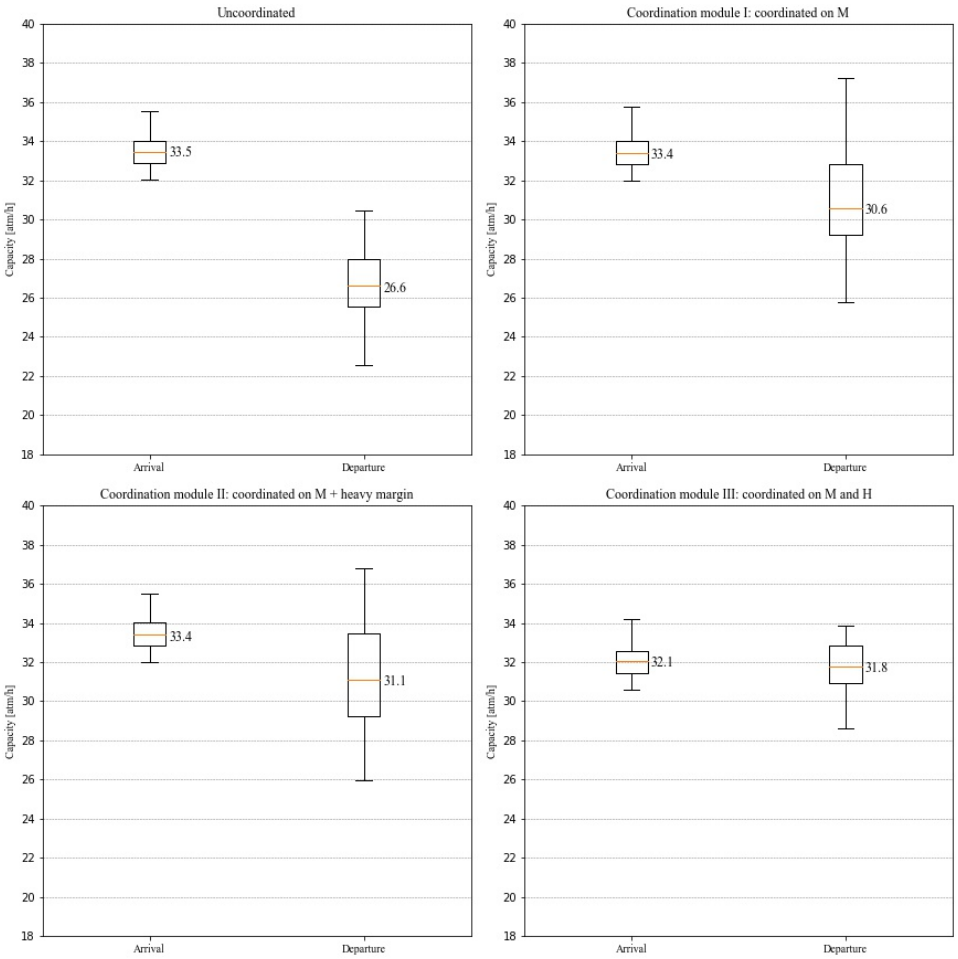

Figure 10.6: Arrival and departure capacity for the uncoordinated and coordinated ADMANs

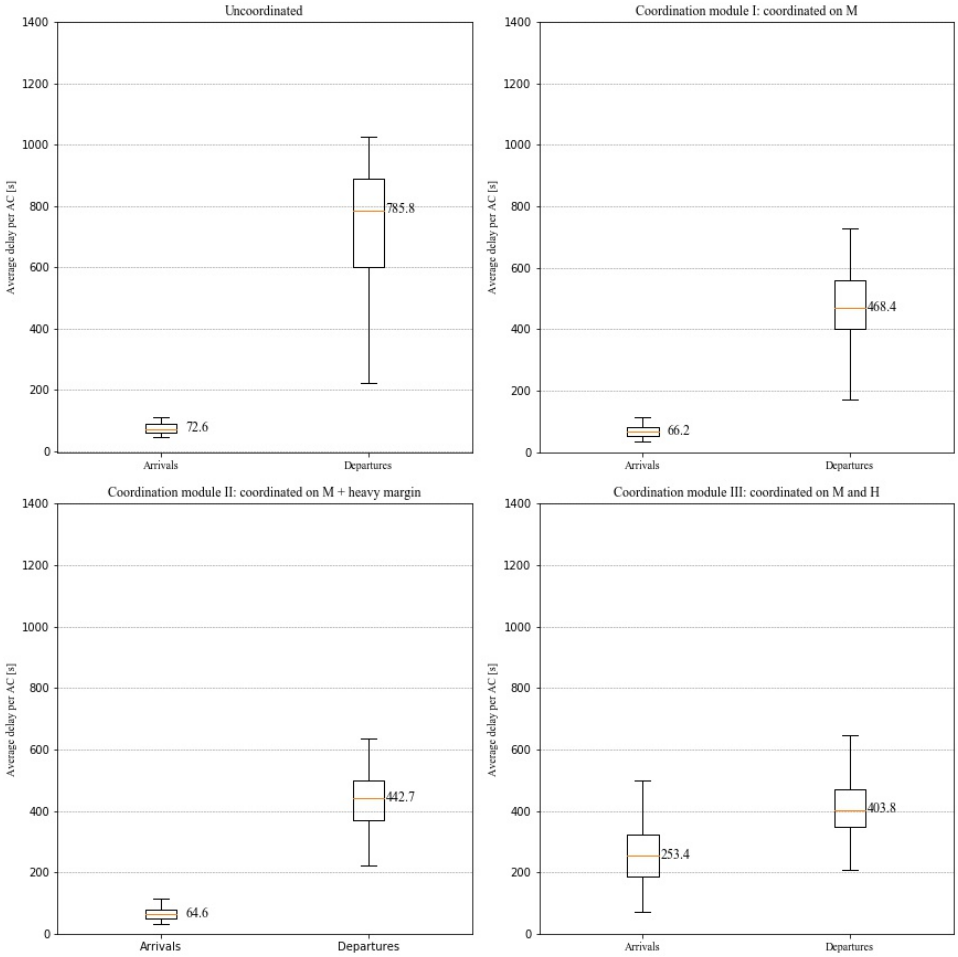

Figure 10.7: Arrival and departure delay for the uncoordinated and coordinated ADMANs

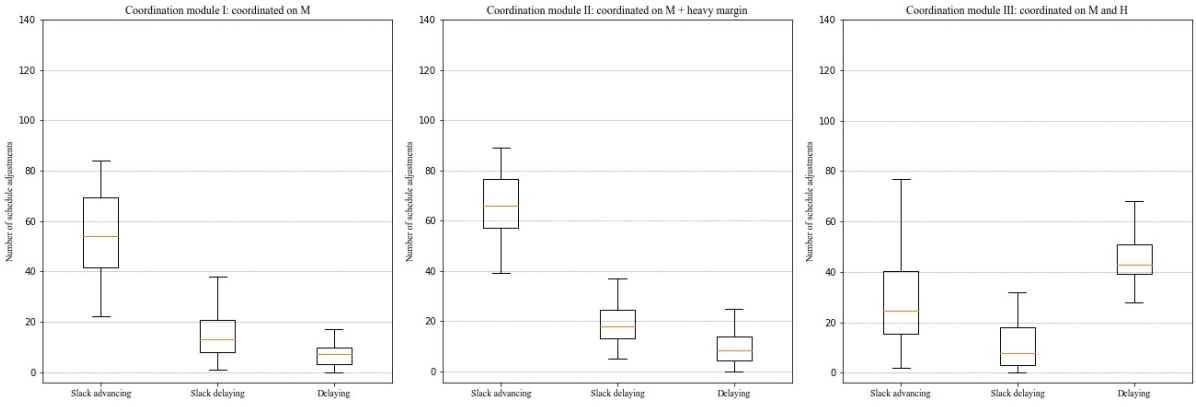

Figure 10.8: Coordination mechanism interventions

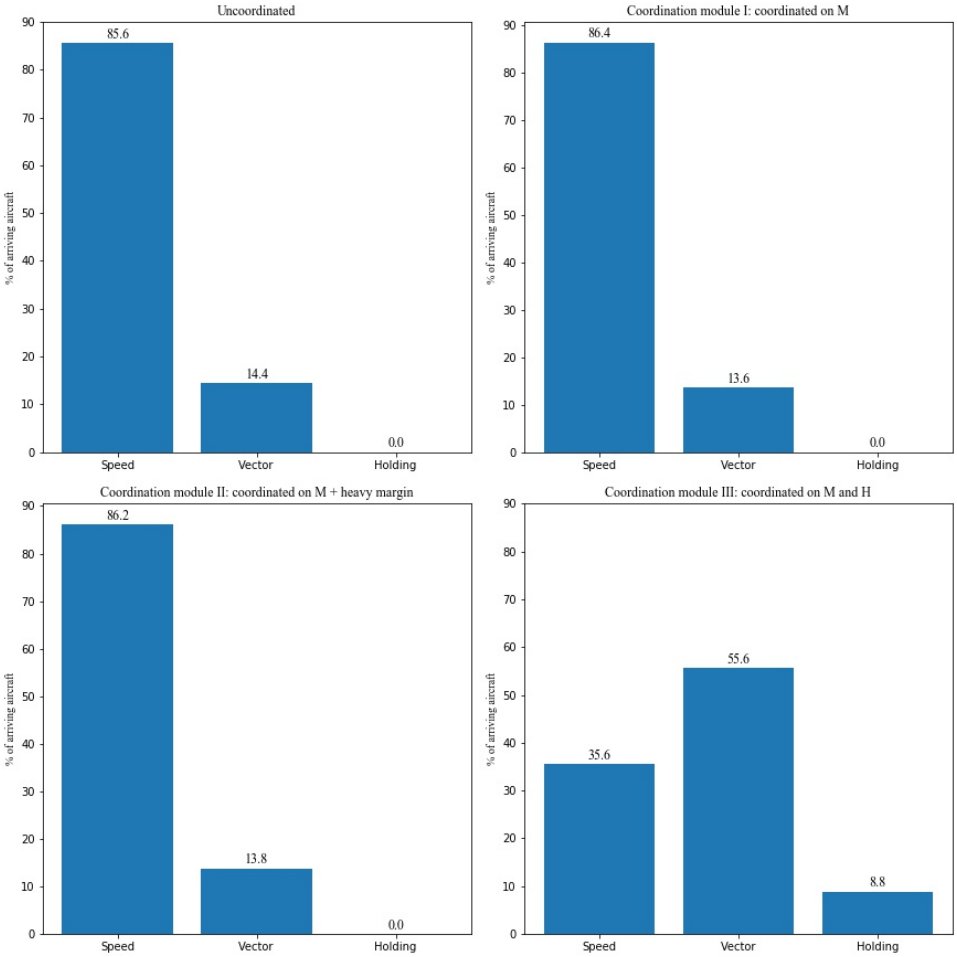

Figure 10.9: Workload

10.2.3. High Arrival Load

Figure 10.10 shows the arrival and departure capacity for an arrival load of 40 atm/hour. For the uncoordinated model, the arrival capacity is approximately 38.0 atm/hour, which is less than the arrival load. Furthermore, the departure capacity is significantly lower than the arrival capacity, 14.0 atm/hour lower. Coordination modules I, II and III raise the departure capacity by respectively 6.7, 7.0, and 7.6 atm/hour. The increase in departure capacity is hardly at the expense of arrival capacity for coordination module I and II.

Figure 10.11 shows the average arrival and departure delay for an arrival load of 40 atm/hour. The average arrival delay hardly changes between the uncoordinated ADMAN and coordination mechanism. For coordination module II and III, the arrival delay increases significantly relative to the uncoordinated ADMAN. The departure delay decreases with 49.9%, 53.3% and 56.4% for respectively coordination modules I, II and III.

Figure 10.12 shows the number of times the coordination module had to intervene in the arrival schedule by slack delaying, slack advancing or delaying for an arrival load of 40 atm/hour. The spread of the number of arrival schedule adjustments by slack delaying and aircraft delaying is significantly high for coordination module I and II. The number of schedule adjustments by slack delaying is low compared to the others for all three coordination modules. The number interventions per minute for coordination module I II and III are respectively 1.8, 1.4 and 0.9.

Figure 10.13 shows that the distribution between the types of delay adsorption hardly changes for coordination module I and II. The number of arriving aircraft that absorbs its delay by vectoring is even lower than for the uncoordinated case. For coordination module III the distribution between the types of delay absorption is turned around. The number of arriving aircraft that will be vectored into the TMA or stacked before

entrance increases respectively with 4.3% and 56.1 %.

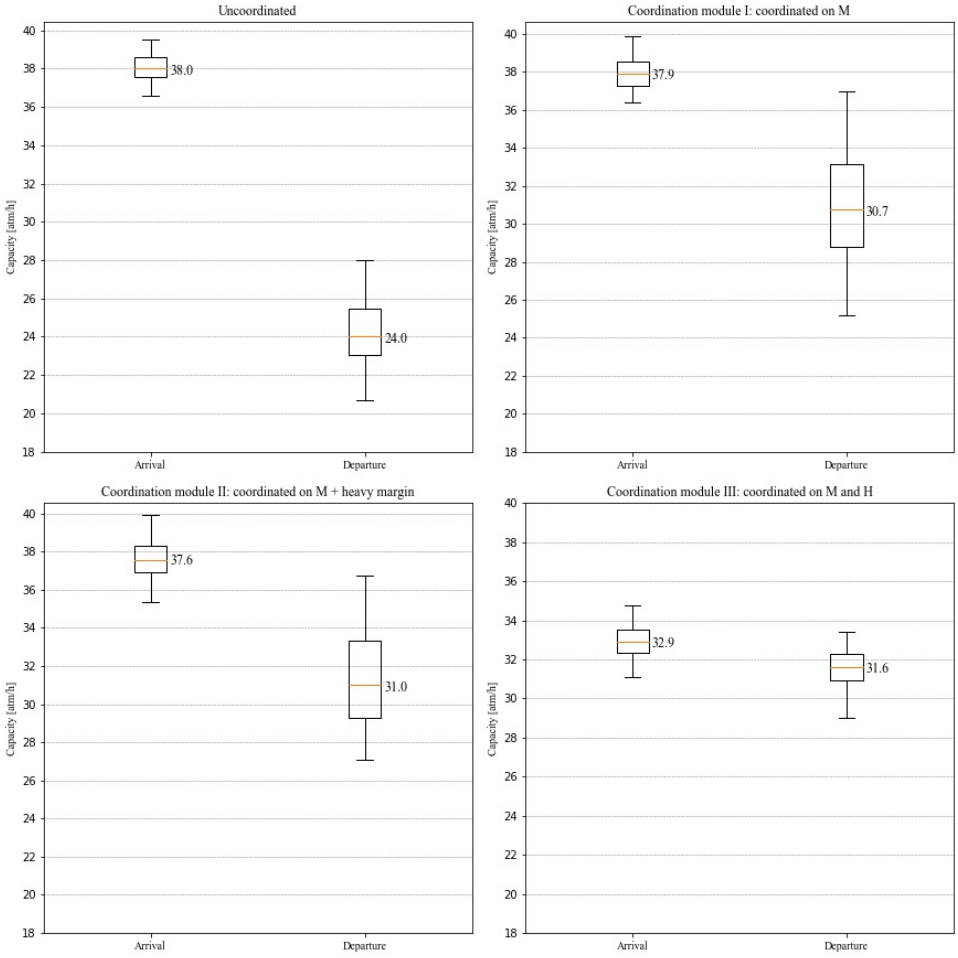

Figure 10.10: Arrival and departure capacity for the uncoordinated and coordinated ADMANs

10.3. Discussion

Experiment II was set-up to assess the performance of the coordination modules. The dependency of arrival runway 18C and departure runway 24 at AAS was used to assess the coordination modules. The experiment used the uncoordinated and coordinated models for testing various conditions in which distinguished between varying levels of arriving and departure loads.

10.3.1. Coordination Module I

The results for a low level and medium level of arrival load showed that the departure capacity could be raised without losing any arrival capacity. Furthermore, the results noted that the arrival delay is even lower for coordination module I compared the uncoordinated ADMAN. The logic behind this is that when an AMAN is metering a load of 30 atm/hour, the arrival load is lower than the arrival runway capacity resulting in a substantial amount of slack in the arrival stream. Coordination mechanisms I uses this slack to rearrange the STAs of the arrivals by slack advancing or slack delaying. However, since both coordination modules advanced slack more often than delayed slack and almost did not delay any aircraft, see Figure 10.4, it is plausible that the arrival delay decreases for coordination module I compared to the uncoordinated results.

The results of the medium arrival load and high arrival load for coordination module I showed that the preferred departure-to-arrival ratio of 1 is not achieved, the departure capacity is still lower than the arrival capacity. Coordination module I overestimates the number of departure slots that are available in the scheduled arrival stream. This is logical since it assumes all departing aircraft as WTC M, which is of course not the

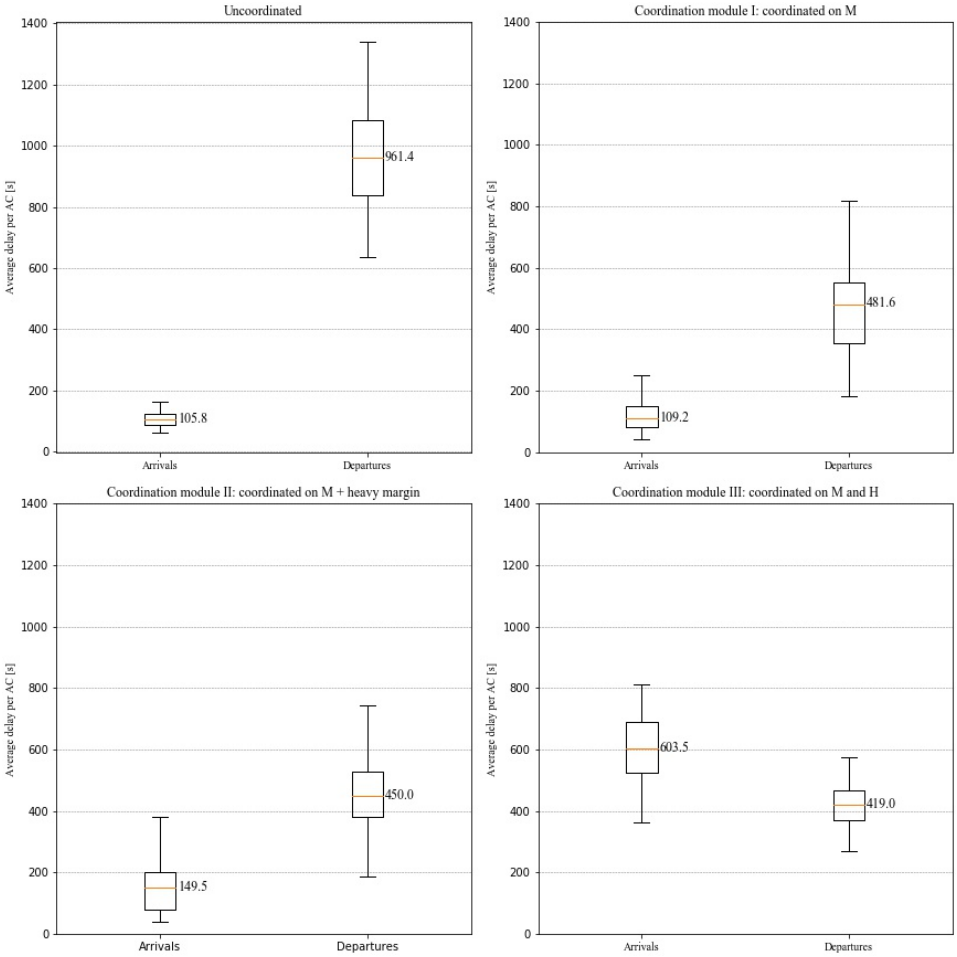

Figure 10.11: Arrival and departure delay for the uncoordinated and coordinated ADMANs

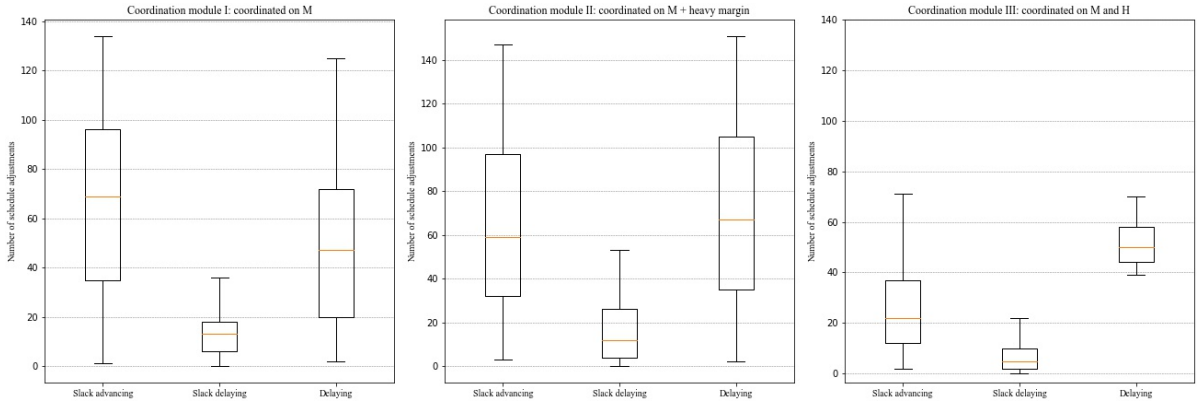

Figure 10.12: Coordination mechanism interventions

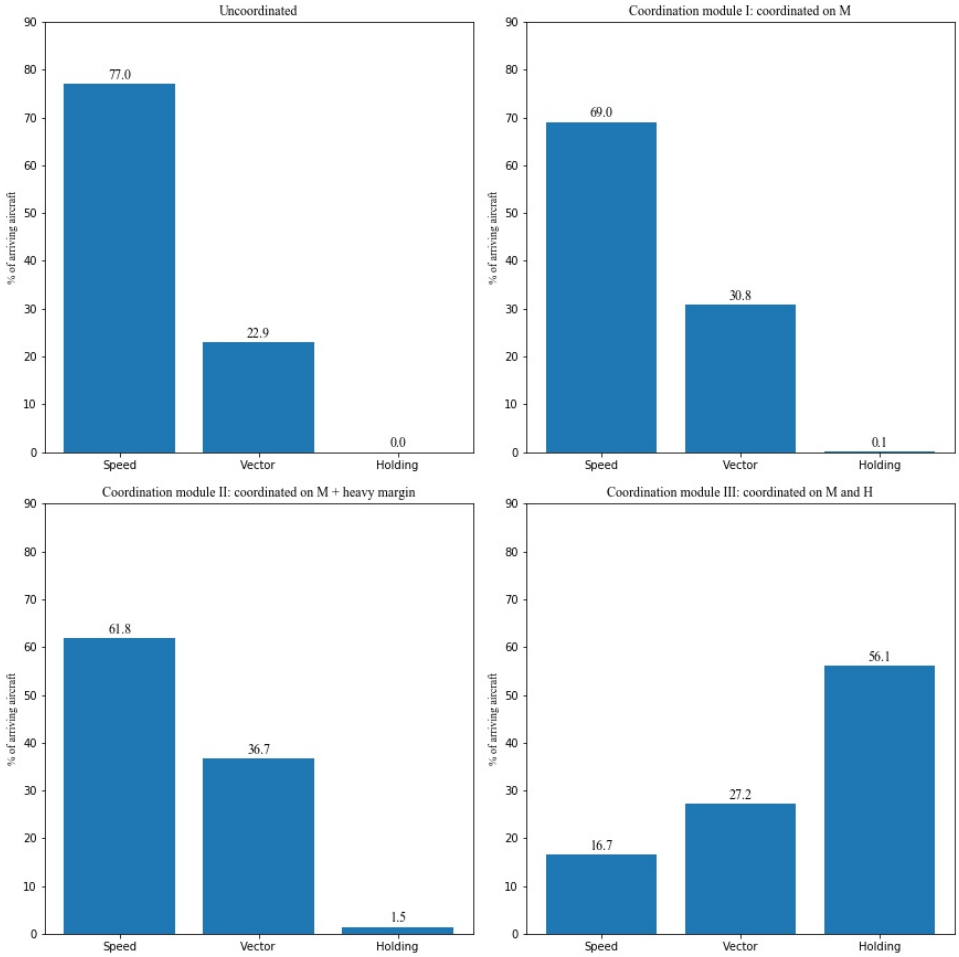

Figure 10.13: Workload

case.

10.3.2. Coordination Module II

The results of the medium arrival load and high arrival load for coordination module II showed that the preferred departure-to-arrival ratio of 1 is also not achieved. Coordination module II applies a heavy time margin. This time margin compensates for the difference in IADT and IDAT between a departure of WTC M and a departure of WTC H. However, it does not compensate for the difference in the minimum required IDT between a heavy and medium departure.

In coordination module II, the time that is required between two arrivals before a departure slot is assigned is larger than in coordination module I as it uses a heavy time margin. The extra time between arriving aircraft that is needed to accommodate the departing aircraft of WTC H is equally spread over all the SAIs, and the arriving aircraft are metered into the TMA accordingly. However, the ATCO module in this study cannot accumulate the extra time that is available in the TMA to specific AIs to create AAFIs that better match the departing traffic mix. In this implementation, the time is there for ATCOs to create AIs specifically aimed for heavy departures, but it is unused. Therefore, the results of this experiment may undervalue the potential of coordination module II.

For each level of arrival load, the resulting departure capacity of coordination module II is higher, and the resulting departure delay is lower compared to the results of coordination module I. This result agrees with the hypothesis: coordination module II outperforms coordination module I.

10.3.3. Coordination Module III

For low and medium arrival load coordination module III was able to increase the departure capacity and decrease the departure delay without imposing a considerable delay on the arriving aircraft or without losing significant arrival capacity. The latter appears for the same reason as was explained in the discussion of coordination module I. The small increase in arrival delay matches the fact that for a low level of arrival load coordination module III delayed arriving aircraft significantly more than coordination module I and II, see Figure 10.4 and 10.8.

The results for a high level of load showed that a significant increase in departure capacity could be achieved at the price of losing arrival capacity. Figure 10.10 showed that the difference in increase of departure capacity between coordination module III and the other two is relatively small. However, coordination module I and II do not lose as much arrival capacity as coordination module III does. The significant increase in arrival delay for coordination module III reflects the loss of arrival capacity. An explanation for this behaviour could be the one that was explained in the hypothesis. Here it was told that coordination module III meters the arriving aircraft as a function of the departure ground situation by distinguishing between departure slots that fit a departure of WTC M and departure slots that fit WTC H. The coordination module creates AIs for departures of WTC M or WTC H, only having knowledge on the number of heavies in the departing traffic, but without knowing the exact location of the planned departure in the arrival stream. It may be the case that the STAs of two arriving aircraft are planned as such that it can accommodate a heavy departure. Nonetheless, the departure slot, which was meant for a heavy departure, is taken by a medium departure because the heavy departure is sequenced later in the departure stream.

IV

Conclusions and Recommendations

11

Conclusions

This study focused on the interaction between arriving and departing aircraft for dependent arrival and departure runway combinations and the magnitude of the resulting arrival and departure capacity interference. With this knowledge, this research developed and assessed strategies for coordination between Arrival Management and Departure Management.

During the literature study, four types of dependencies between runways were distinguished: (1) parallel, (2) intersecting, (3) converging and diverging, and (4) mixed mode. The interaction between aircraft arrivals and departures for dependent arriving and departing runways composes of two parts: (1) the arrival-departure interaction and (2) the departure-arrival interaction. The quantification for the two interactions differs per arrival and departure runway dependency and depends on aircraft performance characteristics. ATC uses additional procedures for the use of dependent arrival and departure runways, such as extra limitations on the visibility and cloud base.

Additionally, during the literature study, an arrival and departure capacity interference assessment for Amsterdam Airport Schiphol was performed. Here it was found that arrival runway 18C in combination with departure runway 24 is the most frequently used dependent arrival and departure runway combination. Furthermore, the assessment demonstrated that the departure capacity of runway 24 is lower when it is in combination with a dependent arrival runway compared to an independent arrival runway.

Arrival and Departure Managers were developed and used at many airports independently from one another, which results in large differences among them. The complexity of the used algorithms, the system architecture, and the type of advisories differ from system to system. Along with this, research into strategic coordination between Arrival and Departure Management was found to be marginal. The studies that did focus on combined Arrival and Departure Management differed in the level of sophistication. None of them focused on developing a coordination mechanism between the AMAN and DMAN for airports that use converging or intersecting runways; instead, they were all aimed at mixed-mode operations.

The literature study concluded that any future coordination between the Arrival Manager and Departure Manager should not require advanced Arrival and Departure Managers. This also meant that the coordination mechanism should provoke at least as possible adjustments to the core working principles of the AMAN and DMAN. Additionally, the coordination mechanism cannot change the existing division of responsibilities between ATCOs.

The uncoordinated Arrival and Departure Management (ADMAN) simulator was developed for two purposes: (1) to assess the future magnitude of arrival and departure capacity interference at AAS, and (2) to serve as a baseline model to which any future coordinated ADMAN could be compared to. The uncoordinated ADMAN mimicked the current management of arriving and departing aircraft in which the AMAN and DMAN work independently from one another. To fulfil the first purpose, experiment I was executed by performing fast-time simulations. The first experiment used arrival runway 18C in combination with departure runway 24 to

test the capacity interference for different levels of arrival load during morning and evening arrival peaks.

Assuming a current arrival load of approximately 35 atm/hour and no significant change in traffic mix distribution, the results showed that the departure capacity of runway 24 in combination with arrival runway 18C will drop by by 2.3 atm/hour and 3.1 atm/hour respectively during the morning arrival-peak period and evening arrival-peak period when the arrival load increases to 40 atm/hour. Relatively speaking, the departure capacity drops with 9.0% and 11.1% respectively during the morning arrival-peak period and evening arrival-peak period when the arrival load increases to 40 atm/hour. These results demonstrated the need for coordination mechanism between the management of arriving and departing aircraft at AAS.

Subsequently, the coordinated ADMAN simulator was developed in which three types of coordination modules were implemented that operate between the AMAN and DMAN. Each of the implemented coordination modules checks the number of departure slots that are available in the scheduled arrival stream and intervene if necessary. They aim to increase the throughput of dependent arrival and departure runway combinations. Experiment II assessed the performance of the coordination modules in terms of capacity, delay, coordination module interventions and ATCO workload. Experiment II was executed by performing fast-time simulations. The experiment used arrival runway 18C in combination with departure runway 24 to test the modules for different levels of arrival load during morning and evening arrival peaks.

Experiment II showed that the departure capacity could be increased, and departure delay could be decreased, when the AMAN meters the arriving aircraft as a function of the departure ground situation. Coordination module I overestimated the number of departure slots and therefore failed to achieve the departure-to-arrival ratio of 1. Coordination module II outperformed coordination module I for all levels of arrival load. In coordination module II a heavy time margin was included. The heavy time margin added time on top of the minimum required IADT and IDAT for a medium departure to compensate for the number of heavies in the departing traffic mix. The concept proved to be beneficial. However, its performance was likely undervalued due to the limited performance of the ATCO module. Coordination module III outperformed module I and II for low and medium arrival load but showed significant arrival capacity loss compared to coordination module I and II when testing it for high arrival loads.

12

Recommendations

The research presented in this report set the first steps toward coordinated Arrival and Departure Management for dependent arrival and departure runway operations. However, new questions arose during the research process and still need answers. Therefore, within the scope of the project, several recommendations can be formulated to complement this research in the future.

First of all, during this research, all input variables were obtained from data concerning Amsterdam Airport Schiphol. Furthermore, the working principles of the AMAN were based on the AMAN operational at Amsterdam Airport Schiphol also. For other airports that suffer from arrival and departure capacity interference as well, the results of this research may not be valid for their use. However, by relatively simple changes to the model, results for other airports could be achieved.

In real life, arriving aircraft enter the TMA around their assigned EAT. Once they have entered the TMA, APP establishes that the arriving aircraft will be aligned with the runway before they are handed over to TWR and start their final approach. During this phase of the approach, APP may swap aircraft and change inter-arrival spacing if it is beneficial for the runway throughput. The ATCO module implemented in this study is not capable of changing the sequence and inter-arrival spacing between arriving aircraft that have entered the TMA. For assessing the performance of coordination module II, this lack may have undervalued its performance. To overcome this and, moreover, to improve the realism of the simulator, it is recommended to upgrade the ATCO module.

As coordination module I was outperformed on all aspects by coordination module II, it is recommended to not proceed any further with this concept. For coordination module II it is advised to revise the heavy time margin and find options to include the difference in the minimum required IDT between two medium departing aircraft and when one of the departures is heavy. As this research set the start for coordinated arrival and departure management for dependent runway operations, other concepts could be developed to mitigate the effect of arrival and departure capacity interference.

Each coordination module used an optimizer function to select the SAIs that were to be enlarged to generate extra departure slots. The current drawback of the optimizer function is that it selects SAIs to accommodate one extra departure only, not two or more departures. This means that when the preferred arrival-to-departure ratio was to be larger than one, the optimization algorithm could potentially give errors. Therefore the SAI selector still needs to be adjusted such it can facilitate the latter. In this research, the coordination modules were tested using a preferred arrival-to-departure ratio of 1. The functionality of the coordination modules with different values for the preferred arrival-to-departure ratio still needs to be tested. Also, studies testing other types of steering mechanisms to control the arriving and departing are recommended.

V

Appendix

A

Case Study: Arrival and Departure Capacity Interference Assessment

This appendix shows the arrival and departure capacity interference results for departure runway 18L, 18C and 36C at AAS. The figures depict the departure capacity in combination with different arrival runways during good and marginal weather conditions.

Departures from runway 18L

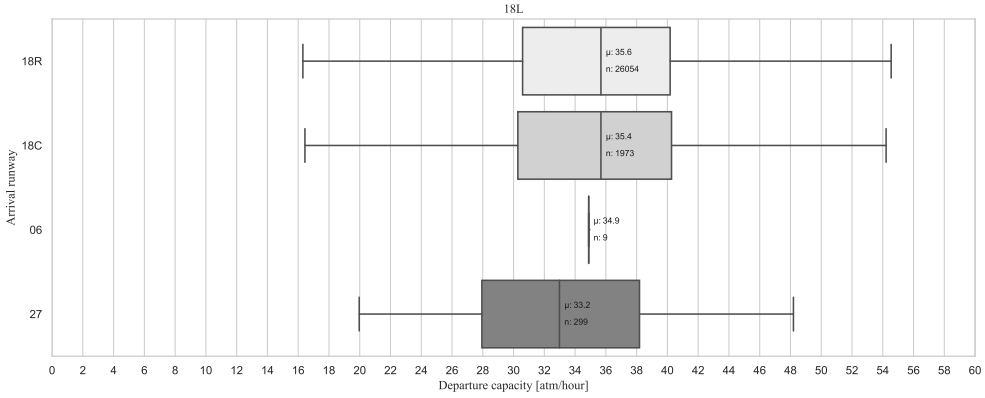

(a)

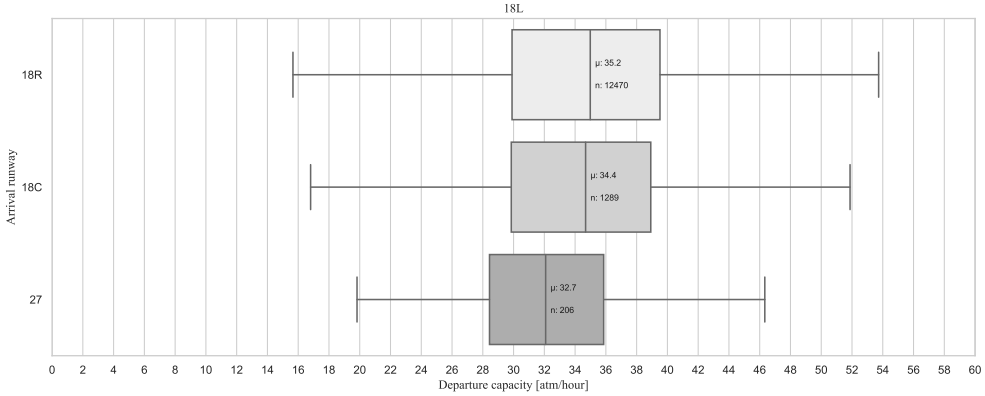

(b)

Figure A.1: Departure capacity of 18L in combination with different arrival runways for (a) good, and (b) marginal weather conditions

Departures from runway 18C

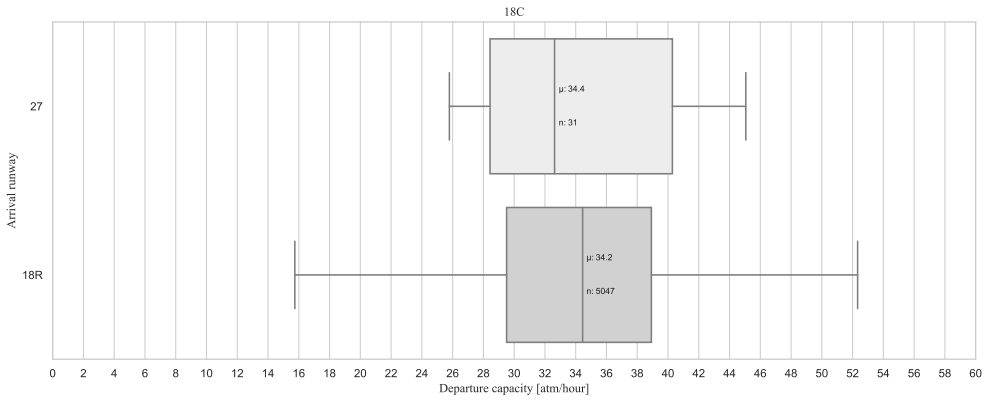

(a)

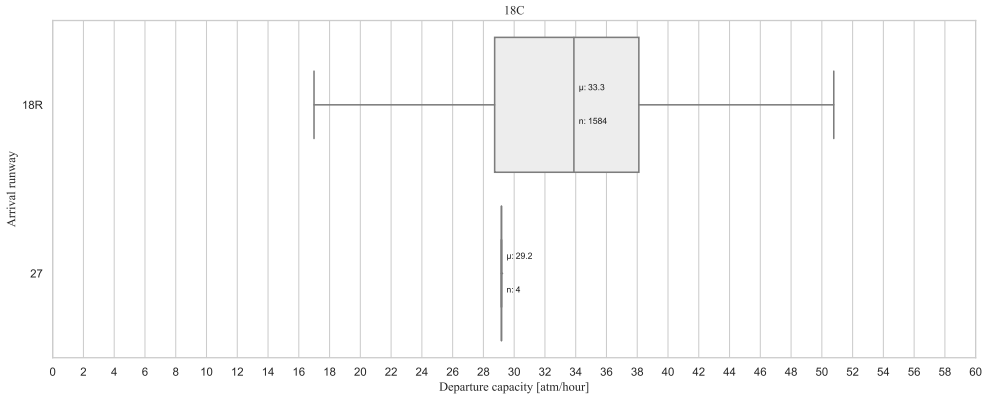

(b)

Figure A.2: Departure capacity of 18C in combination with different arrival runways for (a) good, and (b) marginal weather conditions

Departures from runway 36C

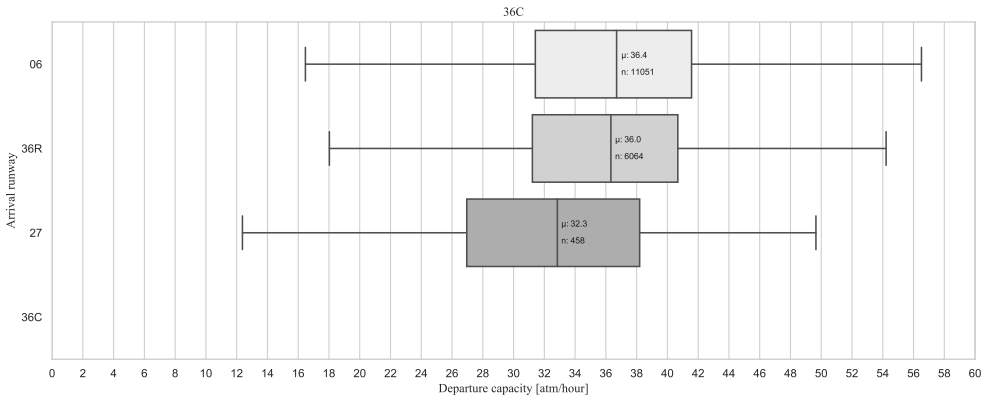

(a)

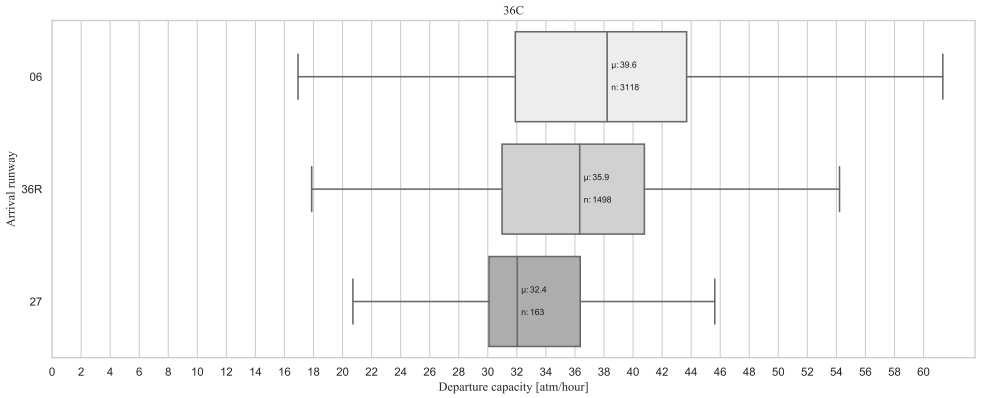

(b)

Figure A.3: Departure capacity of 36C in combination with different arrival runways for (a) good, and (b) marginal weather conditions

B

Experiment I: Arrival and Departure Capacity Interference

This appendix shows the results of Experiment I when there is a departure demand of 30 atm/hour. The results of experiment 1 are presented for: (1) when no distinction is made in the time of the day, and (2) when a distinction is made between morning and evening.

Total

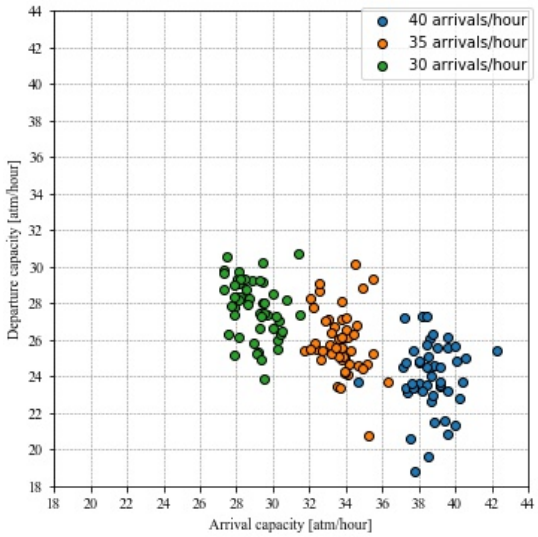

Figure B.1: Departure capacity as a function of the arrival capacity

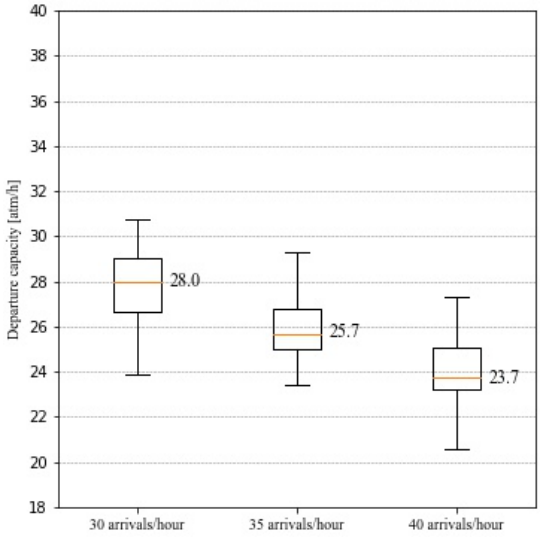

Figure B.2: Departure capacity as function of the arrival demand

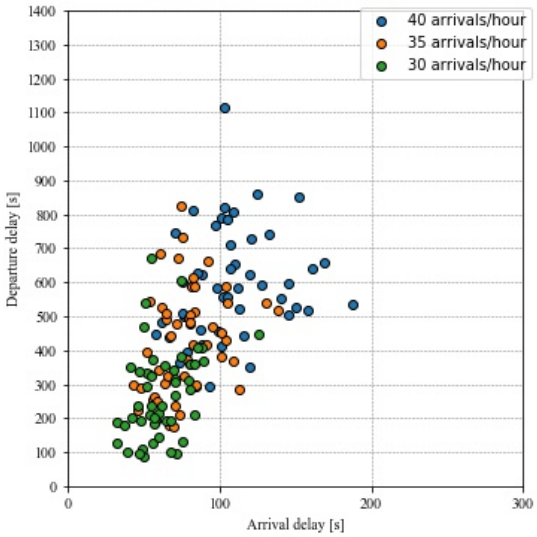

Figure B.3: Departure delay as a function of the arrival delay

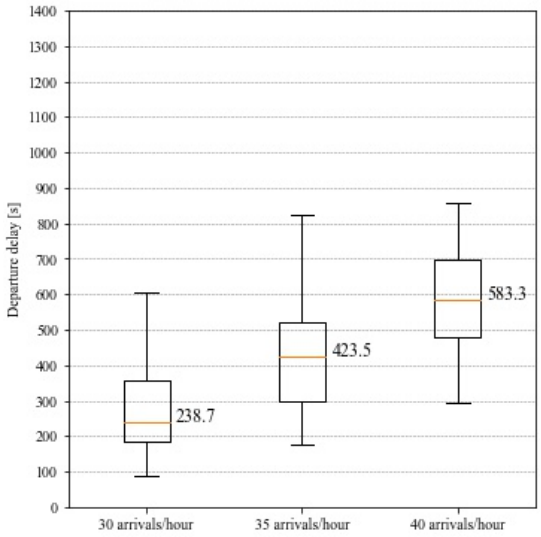

Figure B.4: Departure delay as a function of the arrival demand

Morning and Evening

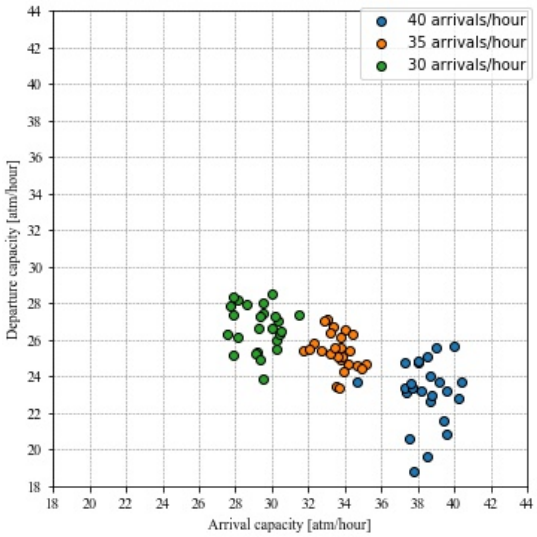

Figure B.5: Departure capacity as a function of the arrival capacity in the morning

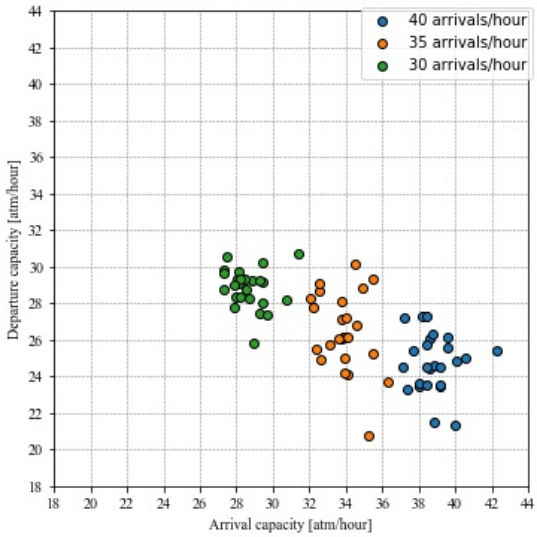

Figure B.6: Departure capacity as a function of the arrival capacity in the evening

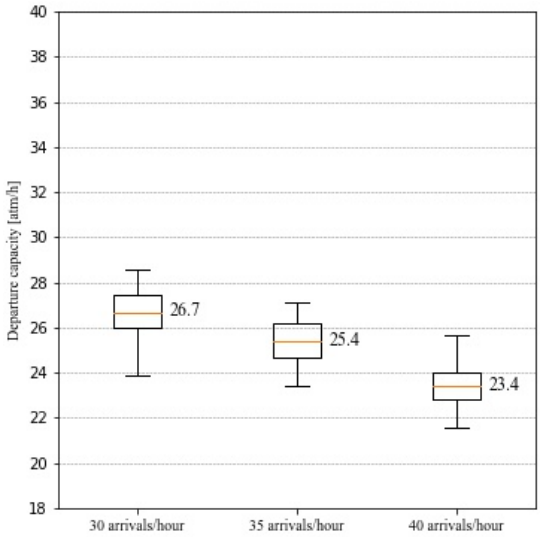

Figure B.7: Departure capacity as a function of the arrival demand in the morning

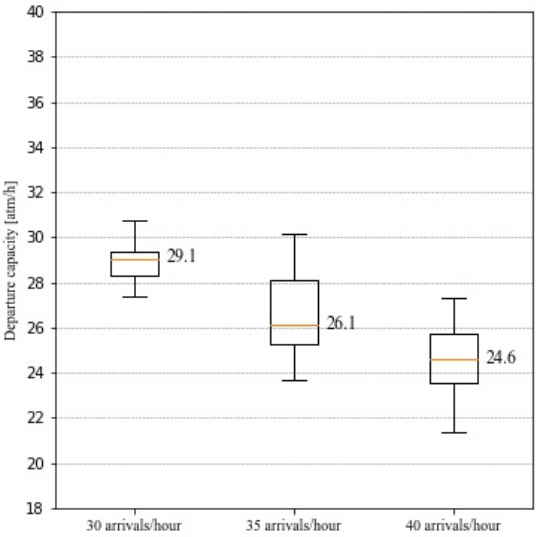

Figure B.8: Departure capacity as a function of the arrival demand in the evening

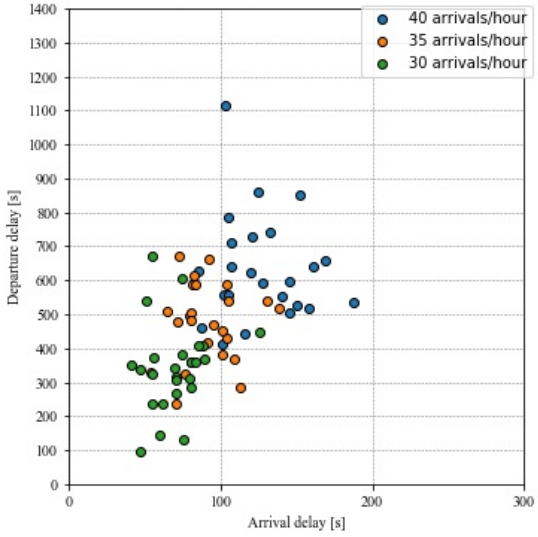

Figure B.9: Departure delay as a function of the arrival delay in the morning

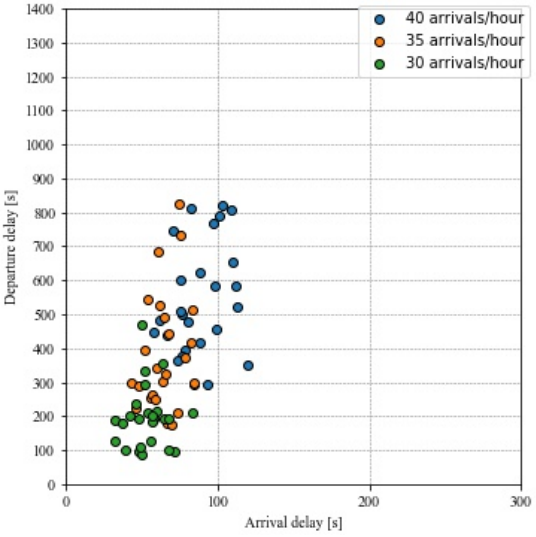

Figure B.10: Departure delay as a function of the arrival delay in the evening

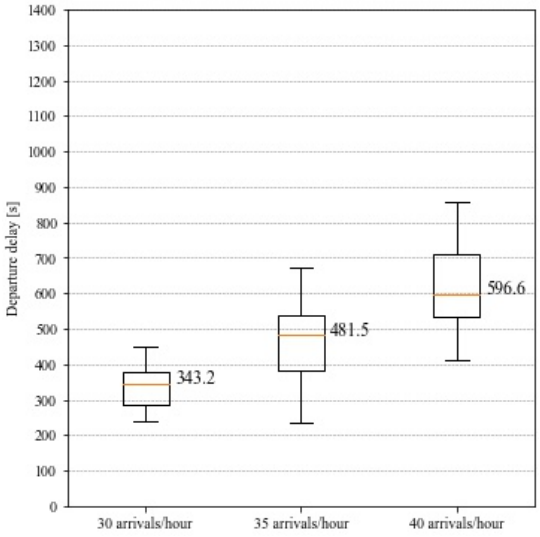

Figure B.11: Departure delay as a function of the arrival demand in the morning

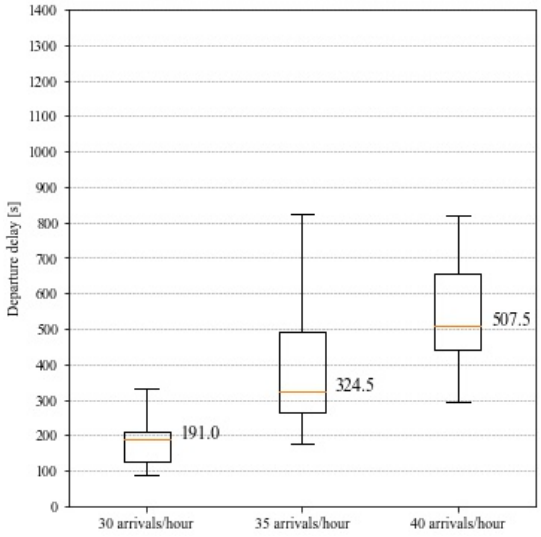

Figure B.12: Departure delay as a function of the arrival demand in the evening

C

Experiment II: Coordinated Arrival and Departure Management

This appendix shows the results of Experiment II when there is a departure load of 30 atm/hour. The results of experiment 2 are presented for the different levels of arrival load: (1) low arrival load, (2)medium arrival load, and (3) high arrival load.

Low Arrival Load

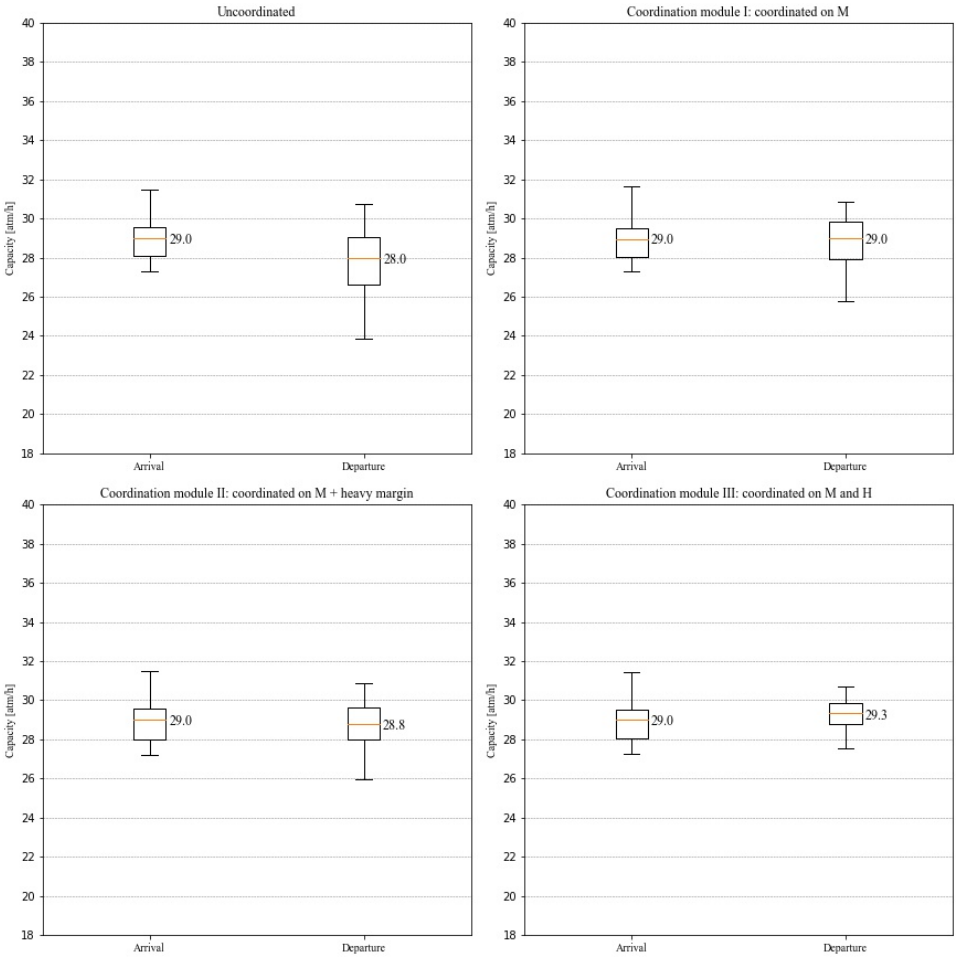

Figure C.1: Arrival and departure capacity for the uncoordinated and coordinated ADMANs

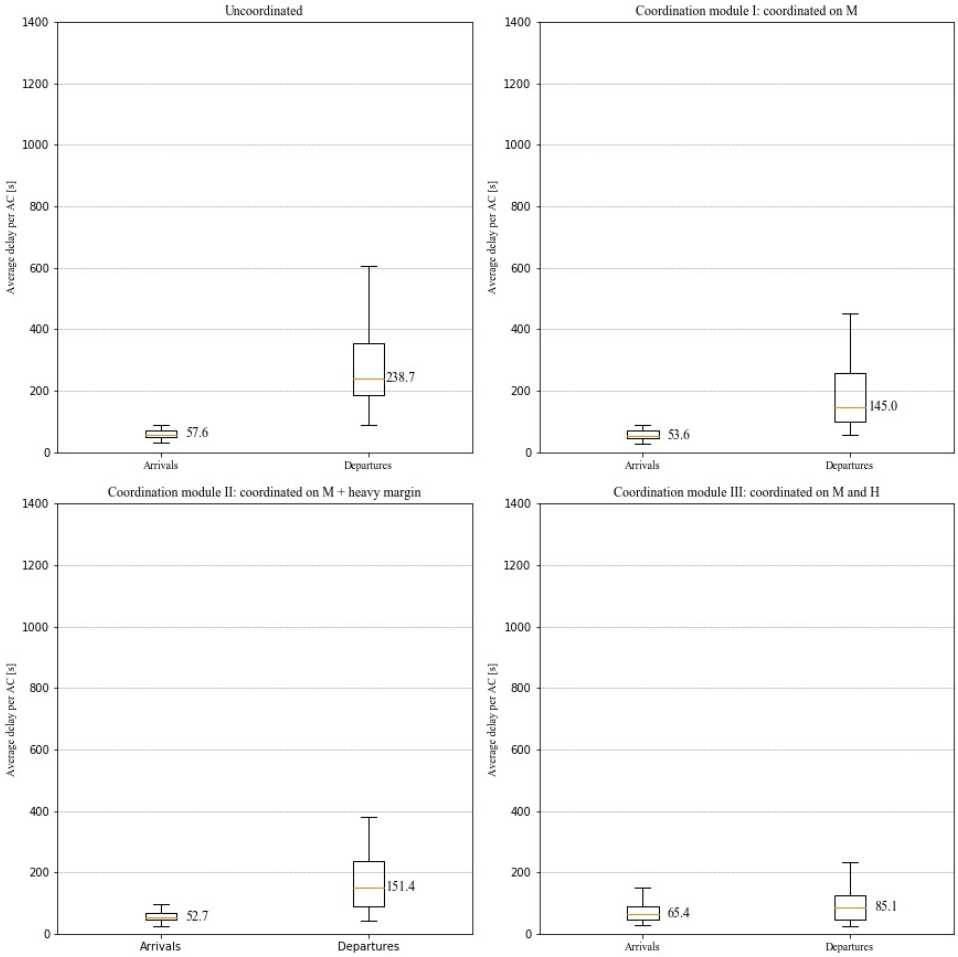

Figure C.2: Arrival and departure delay for the uncoordinated and coordinated ADMANs

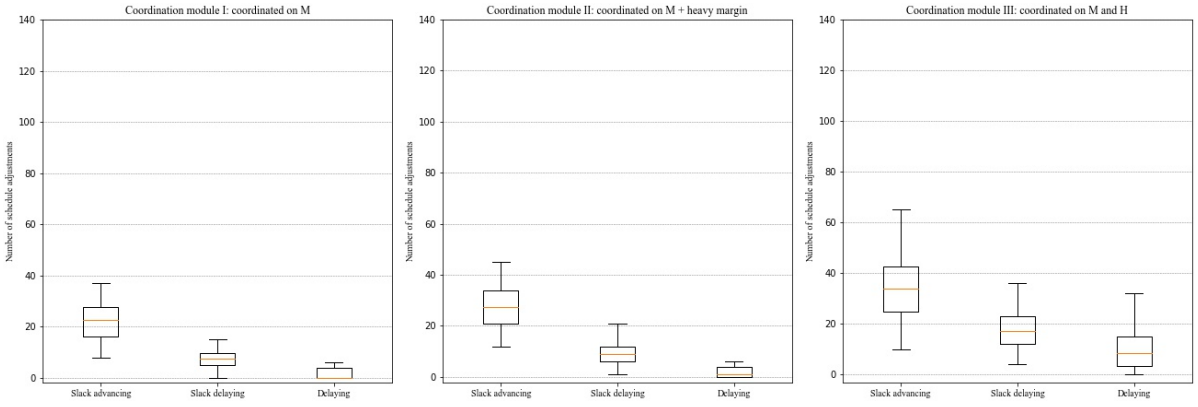

Figure C.3: Coordination mechanism interventions

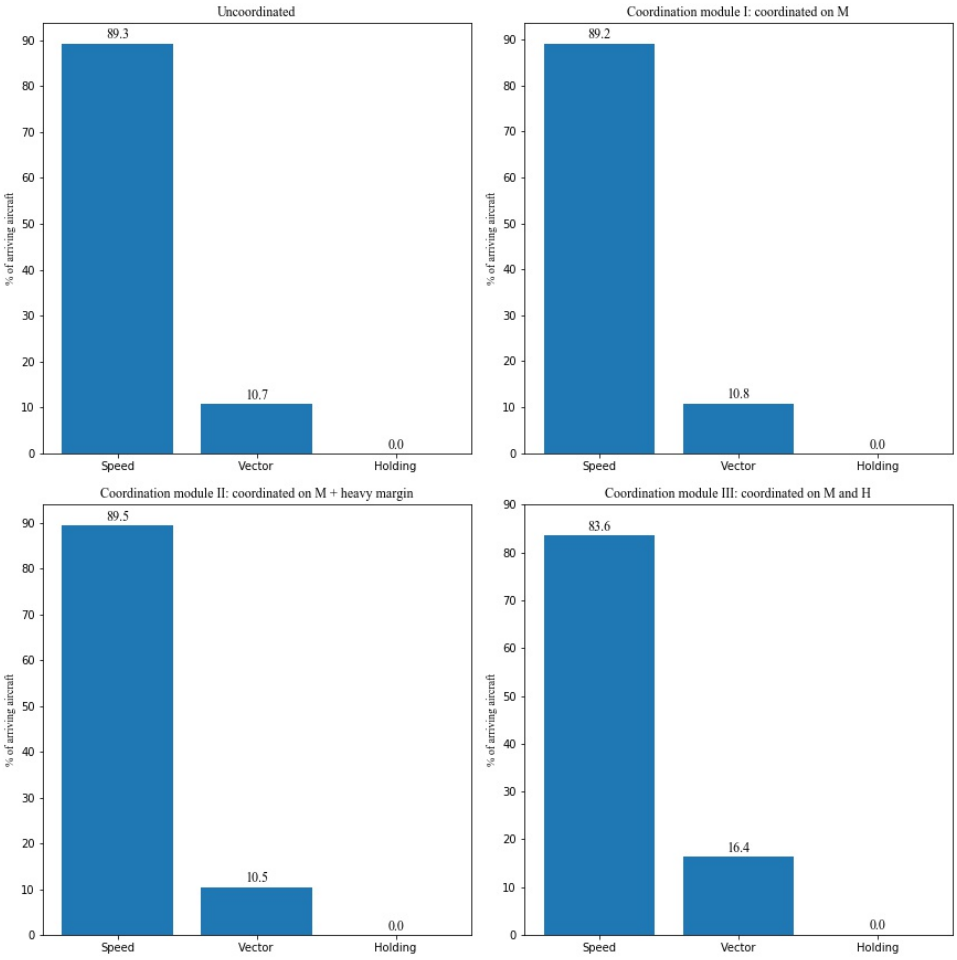

Figure C.4: Workload

Medium Arrival Load

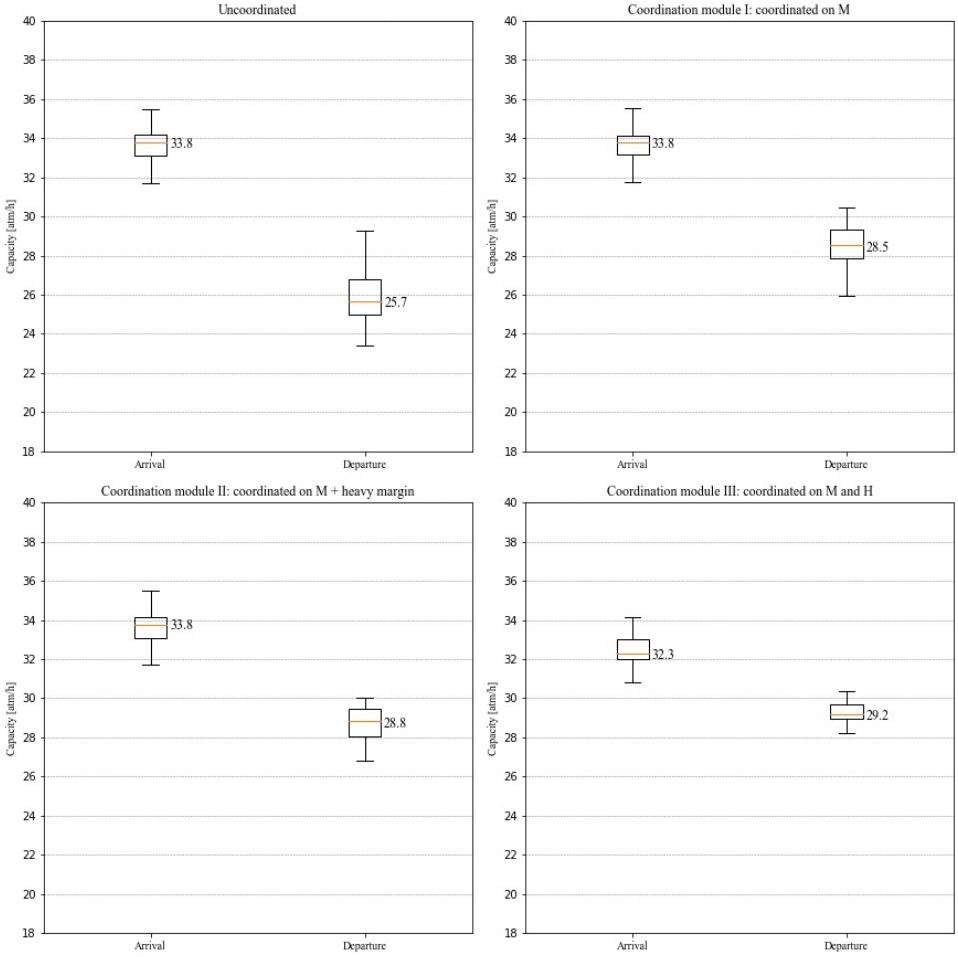

Figure C.5: Arrival and departure capacity for the uncoordinated and coordinated ADMANs

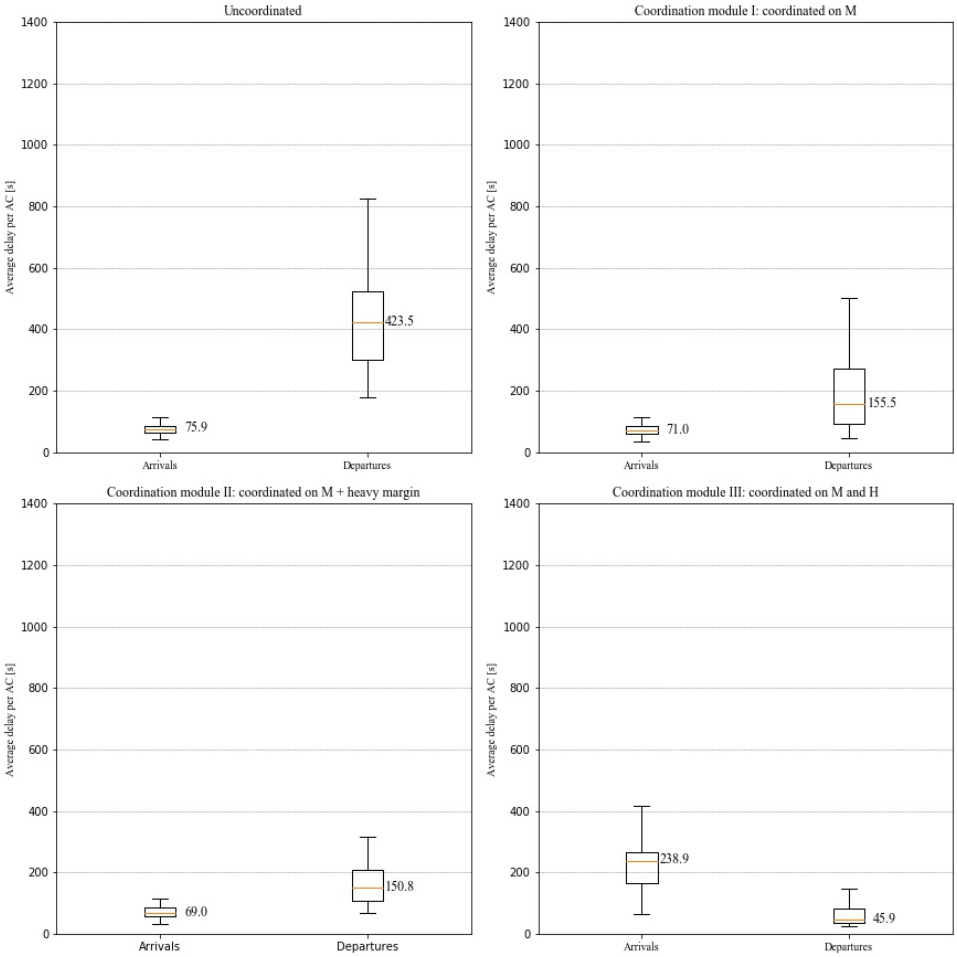

Figure C.6: Arrival and departure delay for the uncoordinated and coordinated ADMANs

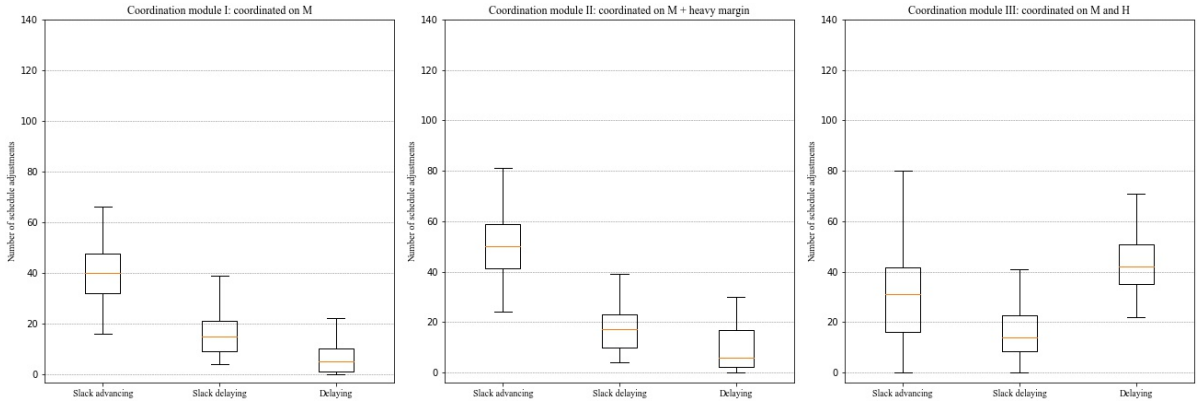

Figure C.7: Coordination mechanism interventions

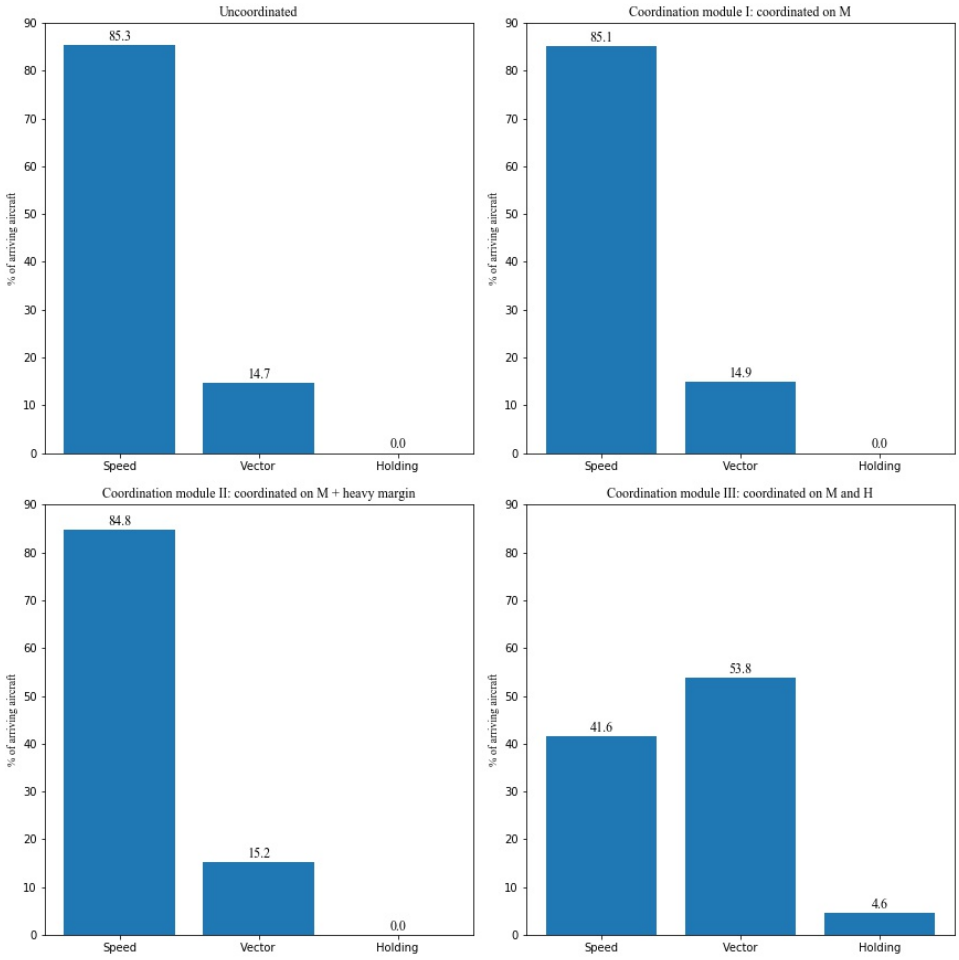

Figure C.8: Workload

High Arrival Load

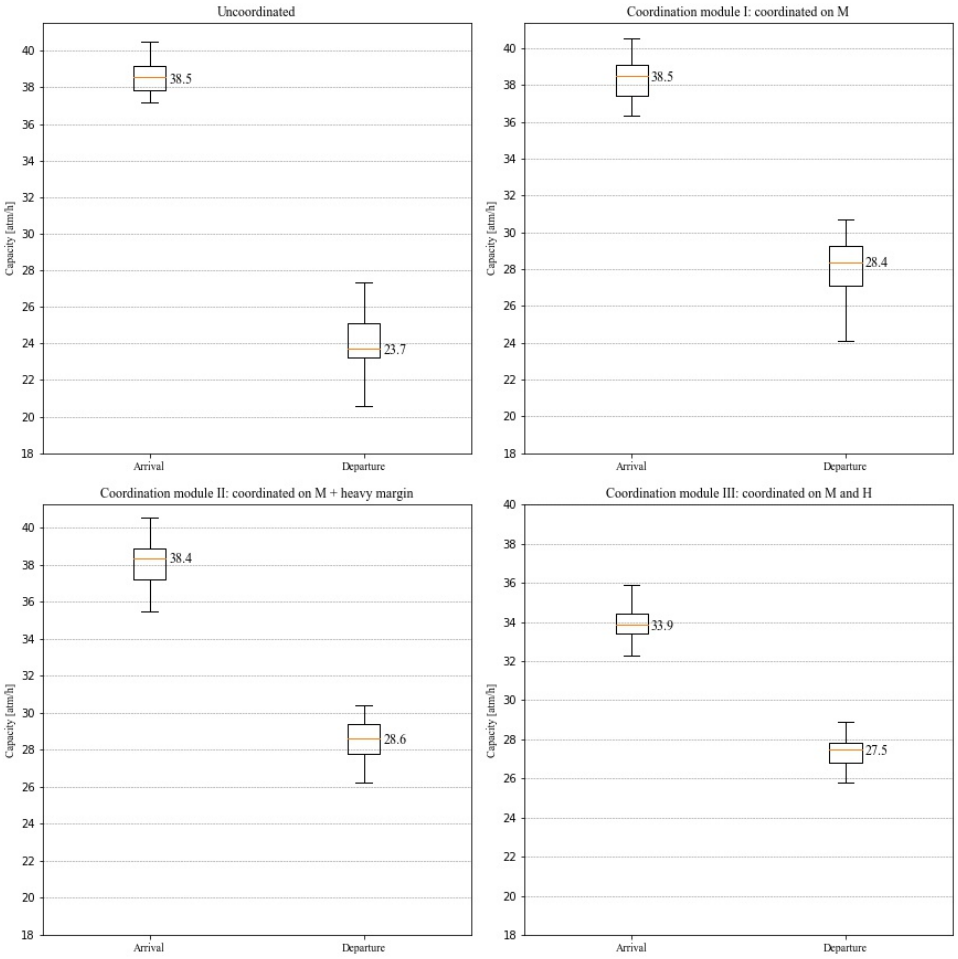

Figure C.9: Arrival and departure capacity for the uncoordinated and coordinated ADMANs

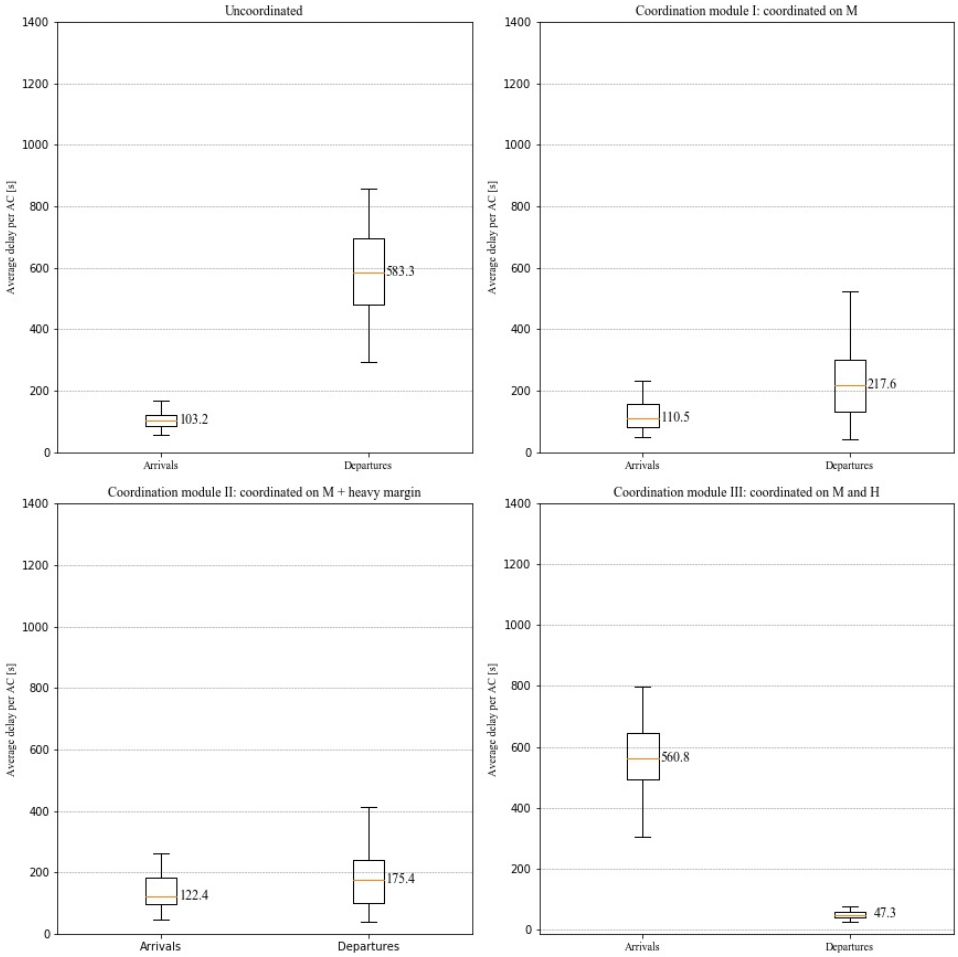

Figure C.10: Arrival and departure delay for the uncoordinated and coordinated ADMANs

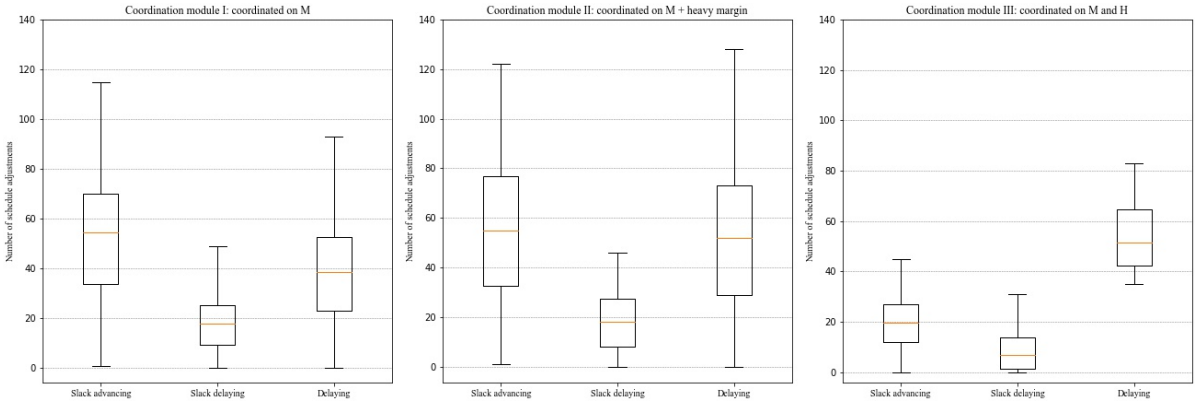

Figure C.11: Coordination mechanism interventions

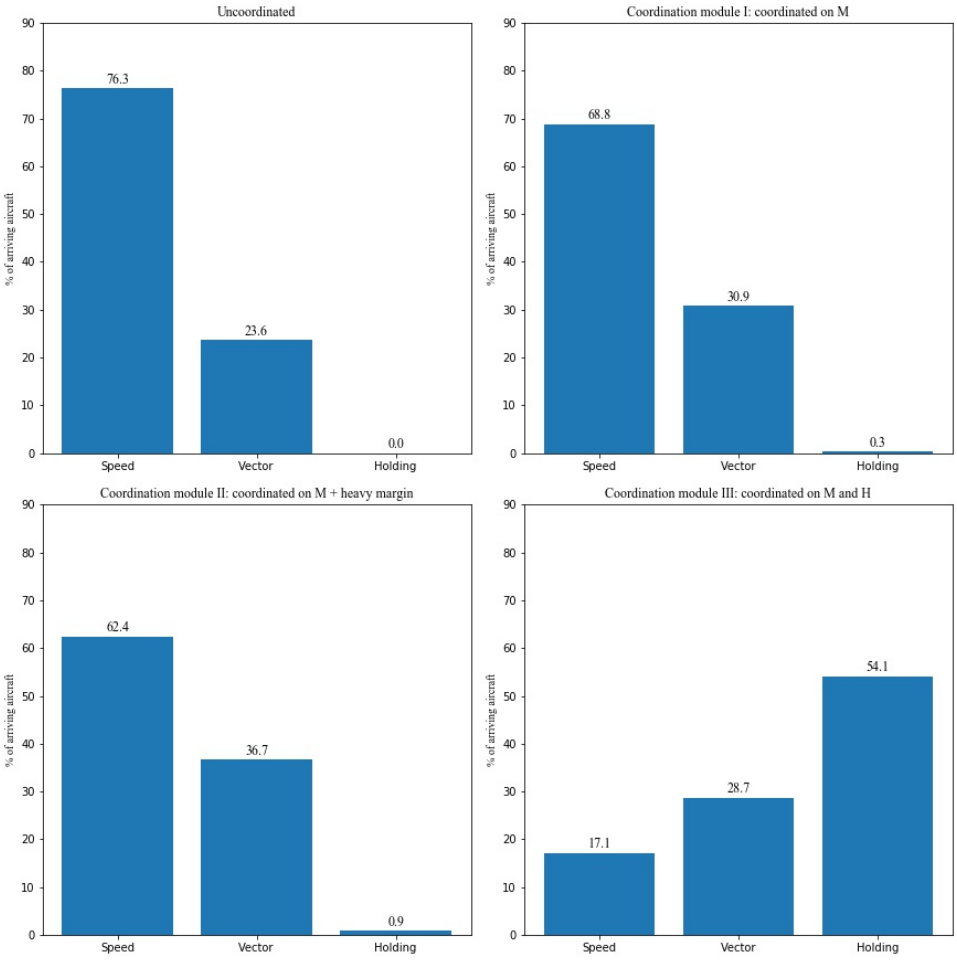

Figure C.12: Workload

D

Planning

The planning and workflow logic of this thesis can be found in the Gantt Chart presented below.

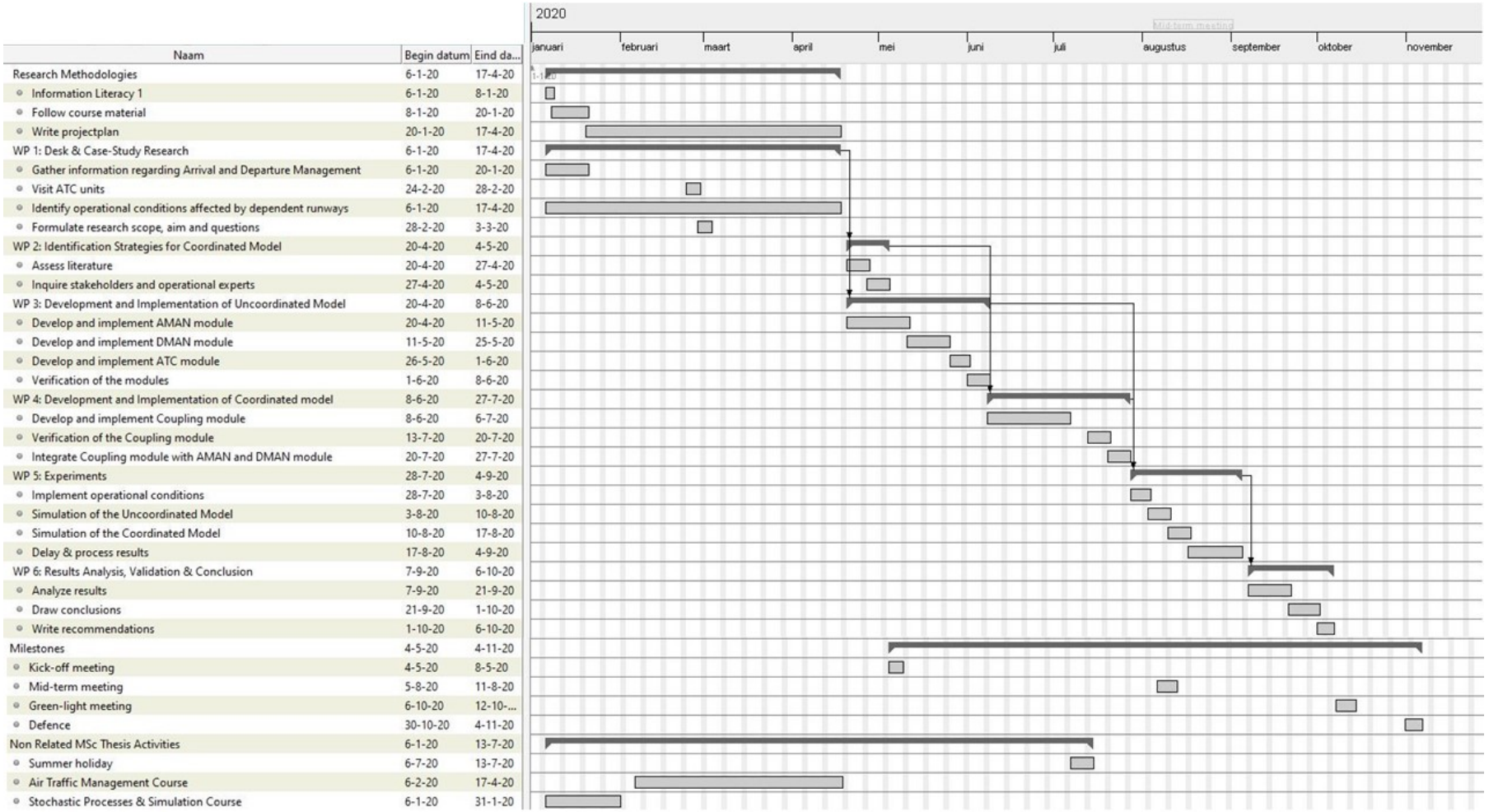

Naam	Begin datum	Eind da...
Research Methodologies	6-1-20	17-4-20
Information Literacy 1	6-1-20	8-1-20
Follow course material	8-1-20	20-1-20
Write projectplan	20-1-20	17-4-20
WP 1: Desk & Case-Study Research	6-1-20	17-4-20
Gather information regarding Arrival and Departure Management	6-1-20	20-1-20
Visit ATC units	24-2-20	28-2-20
Identify operational conditions affected by dependent runways	6-1-20	17-4-20
Formulate research scope, aim and questions	28-2-20	3-3-20
WP 2: Identification Strategies for Coordinated Model	20-4-20	4-5-20
Assess literature	20-4-20	27-4-20
Inquire stakeholders and operational experts	27-4-20	4-5-20
WP 3: Development and Implementation of Uncoordinated Model	20-4-20	8-6-20
Develop and implement AMAN module	20-4-20	11-5-20
Develop and implement DMAN module	11-5-20	25-5-20
Develop and implement ATC module	26-5-20	1-6-20
Verification of the modules	1-6-20	8-6-20
WP 4: Development and Implementation of Coordinated model	8-6-20	27-7-20
Develop and implement Coupling module	8-6-20	6-7-20
Verification of the Coupling module	13-7-20	20-7-20
Integrate Coupling module with AMAN and DMAN module	20-7-20	27-7-20
WP 5: Experiments	28-7-20	4-9-20
Implement operational conditions	28-7-20	3-8-20
Simulation of the Uncoordinated Model	3-8-20	10-8-20
Simulation of the Coordinated Model	10-8-20	17-8-20
Delay & process results	17-8-20	4-9-20
WP 6: Results Analysis, Validation & Conclusion	7-9-20	6-10-20
Analyze results	7-9-20	21-9-20
Draw conclusions	21-9-20	1-10-20
Write recommendations	1-10-20	6-10-20
Milestones	4-5-20	4-11-20
Kick-off meeting	4-5-20	8-5-20
Mid-term meeting	5-8-20	11-8-20
Green-light meeting	6-10-20	12-10-...
Defence	30-10-20	4-11-20
Non Related MSc Thesis Activities	6-1-20	13-7-20
Summer holiday	6-7-20	13-7-20
Air Traffic Management Course	6-2-20	17-4-20
Stochastic Processes & Simulation Course	6-1-20	31-1-20

Figure D.1: Thesis planning

References

[1] Air Traffic Control the Netherlands. Six interesting facts about air traffic control. https://en.lvnl.nl/news/news-items/six-interesting-facts-about-air-traffic-contro, 2018. Accessed: 2020-01-29.

[2] Air Traffic Control the Netherlands. Dependent runway use. https://en.lvnl.nl/environment/runway-use/dependent-runway-use, 2019. Accessed: 2019-11-27.

[3] Air Traffic Control the Netherlands. Route gebruik. https://www.lvnl.nl/omgeving/routegebruik, 2019. Accessed: 2020-01-29.

[4] Air Traffic Control the Netherlands. Runway use. https://en.lvnl.nl/environment/runway-use, 2019. Accessed: 2019-11-26.

[5] I. Anagnostakis, J.P. Clarke, D. Bohme, and U. Volckers. Runway operations planning and control sequencing and scheduling. In *Proceedings of the 34th Annual Hawaii International Conference on System Sciences*, pages 12–pp. IEEE, 2001.

[6] D. Böhme. Tactical departure management with the eurocontrol/dlr dman. In *6th USA/Europe Air Traffic Management Research and Development Seminar, Baltimore, MD*, 2005.

[7] D. Bohme, R. Brucherseifer, and L. Christoffels. Coordinated arrival departure management. In *7th USA/Europe ATM 2007 R&D Seminar.—2007*, 2007.

[8] M. Dame. Flow based integration of arrival and departure management. Technical Report 54/Release 4, SESAR, 12 2015.

[9] J. de Wit, M. Tielrooij, C. Borst, M.M. van Paassen, and M. Mulder. Supporting runway planning by visualizing capacity balances of arriving aircraft streams. In *2014 IEEE International Conference on Systems, Man, and Cybernetics (SMC)*, pages 2989–2994. IEEE, 2014.

[10] P. Diffenderfer, Z. Tao, and G. Payton. Automated integration of arrival/departure schedules. In *Proceedings of the Tenth USA/Europe Air Traffic Management Seminar, Chicago, Illinois*, 2013.

[11] F. Dijkstra and E. Westerveld. Opdracht atm-aman-dman-koppeling luchtverkeersleiding nederland. unpublished, 2019.

[12] E.P. Gilbo. Optimizing airport capacity utilization in air traffic flow management subject to constraints at arrival and departure fixes. *IEEE Transactions on Control Systems Technology*, 5(5):490–503, 1997.

[13] N. Hasevoets and P. Conroy. Arrival manager: Implementation guidelines and lessons learned. *EUROCONTROL, Brussels, Tech. Rep*, 2010.

[14] International Civil Aviation Organisation. Wake turbulence separation in rvsm airspace. https://www.icao.int/MID/Documents/2017/ATM%20SG3/WP27.pdf, 2017. Accessed: 2020-01-12.

[15] A. Jacquillat, A.R. Odoni, and M.D. Webster. Airport congestion mitigation through dynamic control of runway configurations and of arrival and departure service rates under stochastic operating conditions. 2014.

[16] M. Kupfer, T. Callantine, L. Martin, J. Mercer, and E. Palmer. Controller support tools for schedule-based terminal-area operations. In *Proceedings of the Ninth USA/Europe Air Traffic Management Research and Development Seminar*, 2011.

[17] M. F. Lamers. Enhanced runway capacity at airports with complex runway layouts. Master's thesis, Delft University of Technology, 6 2016.

[18] G.W. Lohr and D.M. Williams. Current practices in runway configuration management (rcm) and arrival/departure runway balancing (adrb). 2008.

[19] Air Traffic Control the Netherlands LVNL. *OPS Manual*, 4 2020.

[20] Ministry. Airspace vision preliminary policy document. 2011.

[21] National Air Traffic Services. Introduction to airspace. https://www.nats.aero/ae-home/introduction-to-airspace/, 2019. Accessed: 2019-11-21.

[22] T. Thoreson B. Neufville, R. De Reynolds. *Airport Systems. Planning, Design and Management.* 2003.

[23] F. Rooseleer and V. Treve. Recat-eu european wake turbulence categorisation and separation minima on approach and departure. *EUROCONTROL Headquarters, Brussels*, 2015.

[24] Royal Schiphol Group. Netwerk van bestemmingen. https://www.jaarverslagschiphol.nl/onze-resultaten/netwerk-capaciteit-en-beveiliging/netwerk-van-bestemmingen, 2019. Accessed: 2020-01-31.

[25] M.A. Stamatopoulos, K.G. Zografos, and A.R. Odoni. A decision support system for airport strategic planning. *Transportation Research Part C: Emerging Technologies*, 12(2):91–117, 2004.

[26] Unknown. Centre of excellence. https://kdc-mainport.nl/centre-of-excellence/, 2020. Accessed: 2020-03-17.

[27] J. van der Klugt. Calculating capacity of dependent runway configurations. Master's thesis, Delft University of Technology, 11 2012.

[28] A. Van Welsenaere, J. Ellerbroek, J.M. Hoekstra, and E. Westerveld. Analysis on the impact of pop-up flight occurrence when extending the arrival management horizon. In *Proceedings of the 12th USA/Europe Air Traffic Management Rechearch and Development Seminar, Seattle*, 2017.

[29] H.S. Yoo, P. Lee, and E. Palmer. Improving departure throughput by dynamically adjusting inter-arrival spacing. In *2014 IEEE/AIAA 33rd Digital Avionics Systems Conference (DASC)*, pages 1A4–1. IEEE, 2014.